Stony Brook University

Recovery of Trabecular Bone from Disuse Induced Deterioration in Cellular, Morphological and Biomechanical Properties

A Dissertation Presented

by

Engin Ozcivici

to

The Graduate School

in Partial fulfillment of the

Requirements

for the Degree of

Doctor of Philosophy

in

Biomedical Engineering

Stony Brook University

May 2009

Stony Brook University

The Graduate School

Engin Ozcivici

We, the dissertation committee for the above candidate for the

Doctor of Philosophy degree,
hereby recommend acceptance of this dissertation.

Stefan Judex, Ph.D., Advisor
Associate Professor
Department of Biomedical Engineering

Clinton T. Rubin, Ph.D, Committee Chair
Distinguished Professor and Chair
Department of Biomedical Engineering

Yi-Xian Qin, Ph.D.
Professor
Department of Biomedical Engineering

Balaji Sitharaman, Ph.D.
Assistant Professor
Department of Biomedical Engineering

Karl J. Jepsen, Ph.D., External Member
Associate Professor
Mount Sinai School of Medicine

This dissertation is accepted by the Graduate School

Lawrence Martin

Dean of the Graduate School

Abstract of the Dissertation

Recovery of Trabecular Bone from Disuse Induced Deterioration in Cellular, Morphological and Biomechanical Properties

by

Engin Ozcivici

Doctor of Philosophy

in

Biomedical Engineering
Stony Brook University

2009

Bone tissue adapts to loads that are placed on it. For that reason, loss of functional weight-bearing and mobility (disuse) induces deterioration in weight-bearing skeletal sites, by disruption of the balance of bone formation and resorption towards net tissue loss. Ultimately, individuals that experience disuse (e.g. bedrest patients, spaceship crews) are threatened by increased risk of mechanical failure upon returning to regular weight bearing activities (reambulation) under traumatic or atraumatic loading. Furthermore, reambulation facilitates bone regain in smaller magnitude compared to tissue deterioration during disuse, and often individuals may not regain the entire bone tissue that was wasted during disuse. On the other hand, exogenous mechanical loading is anabolic to bone tissue. For example, organisms that are subjected to mechanical loading in vibratory form with low magnitude and high frequencies show increased bone formation that ultimately increases bone quantity and quality. As a non-invasive and non-pharmaceutical intervention, vibratory stimulus also induces very small

deformations to bone tissue; therefore its applications are safe in mechanical perspective to bones of any size and shape, including those that suffer from extensive bone loss.

The overall objective of this dissertation was to determine: 1) the extent of coupling between morphological and micro-mechanical parameters during disuse and reambulation. Also if any of the parameters pertaining to either morphology or micro-mechanical properties can be used as a predictor of tissue response to upcoming disuse or reambulation 2) tissue- and cellular-level deterioration during disuse and if that could be prevented using high frequency low magnitude vibratory stimulus.

Results showed that disuse induced deterioration in bone morphology and micro-mechanical properties were not recovered for the similar duration of reambulation. Also, it was found that neither morphological nor micro-mechanical properties can fully predict bone's upcoming response to changes in mechanical environment. On the other hand, vibratory stimulus applied during disuse was found to be affecting bone marrow cells to maintain their osteogenic potential. Upon reambulation, the maintenance of osteogenic potential in bone marrow cells increased the bone mass that was regenerated.

Overall, results imply the importance of preventing disuse induced bone loss since regeneration of lost bone tissue may not always possible. However, in the absence of preventive measures, daily application of vibratory stimulus can increase bone tissue's capabilities of regeneration, offering a non-invasive and non-pharmaceutical remedy for disuse induced bone loss.

Table of Contents

List of Symbols and Abbreviations

ANOVA – analysis of variance

B6 – C57BL/6J

BALB – BALB/cByJ

BFR/BS – bone formation rate per bone surface

BMD – bone mineral density

Bmp – bone morphogenetic protein

BS – bone surface

BS/BV – bone surface to volume ratio

BV – bone volume

BV/TV – bone volume fraction

C3H – C3H/HeJ

Conn.D – trabecular connectedness

Ct.Ar – cortical bone area

DA – degree of anisotrophy

E – elastic modulus

Ec.En – endocortical envelope area

F1 – first generation cross

F2 – second generation cross

FITC – fluorescein isothiocyanate

I_{max} – principal moment of inertia

I_{min} - principal moment of inertia

i.p. – intraperitoneal

I_p – polar moment of inertia

MAR – mineral apposition rate

mRNA – messenger ribonucleic acid

microCT or µCT – micro-computed tomography

µε – micro-strain

MS/BS – mineralizing surface per bone surface

MSC – mesenchymal stem cell

N – Newton

υ – Poisson's ratio

NF-kappaB – nuclear factor kappa-light-chain-enhancer of activated B cells

Ob.S/BS – osteoblast surface per bone surface

OC– osteocalcin

Oc.S/BS – osteoclast surface per bone surface

OP – osteopontin

OVX – ovaryectomized

QTL – quantitative trait loci

PBS – phosphatase buffered saline

PE – Phycoerythrin

PTH – parathyroid hormone

PVM – peak Von-Mises

RNA – ribonucleic acid

SCA-1 – stem cell antigen -1

SNK – Student-Newman-Keuls

SVM – skewness of Von-Mises stresses

Tb – trabecular

Tb.N – trabecular number

Tb.Th – trabecular thickness

Tb.TMD – trabecular tissue mineral density

TRAP – tartrate resistant acid phosphatase

TV – tissue volume

List of Figures

Difference in letters denominate significant ($p<0.05$) differences between groups (ANOVA and SNK).

Figure 4.5. (a) Cell size (FSC) and complexity (SSC) of bone marrow cells subjected to flow cytometry. Regions in which cells accumulated are denoted by R1, R2, and R3. Fluorescence of cells that were positive for SCA-1 and CD90.2 surface antigens resided (b) in R2 or (c) R3. Ratio of SCA-1 and CD90.2 positive cells to total marrow cells (d) in R2 after 3w, (e) in R3 after 3w, (d) in R2 after 6w, (g) in R3 after 6w. Difference in letters denominate significant ($p<0.05$) differences between groups (ANOVA and SNK).

Figure 4.6. Longitudinal changes in (a) endocortical envelope area, (b) trabecular bone volume, and (c) trabecular bone volume fraction of the tibial metaphysis in mice that either received vibrations only during the disuse period (VIB-D, n=6) or during reambulation (VIB-R, n=6). Open triangles correspond to-cross-sectional data of age-matched control mice (n=12).

List of Tables

ACKNOWLEDGEMENTS

The success of this dissertation belongs to a number of individuals as their contributions were non-trivial during the entire process. For that I am extremely lucky and grateful.

Dr. Stefan Judex played the biggest role. He accepted me into his lab, nurtured and guided me, advised swiftly when I wasn't getting it and I am pretty sure he will continue this role to the end of my career in science. Thank you sir for believing in me, and I am sorry if I couldn't meet all of your expectations.

Dr. Raman P. Singh, my Master's advisor, encouraged and supported me on my decision to pursue my ambitions in the field of Biomedical Engineering. He was, also, a great mentor.

Members of my dissertation committee should also be mentioned. Their guidance, feedback and support altered my general understanding and interpretations of the data greatly. For that thank you to Drs. Yi-Xian Qin and Balaji Sitharaman. Further, Dr. Karl J. Jepsen agreed to serve as the external member of my committee, came to Stony Brook all the way from NYC and broke me into pieces during the examination. I am extremely lucky, since he didn't forget to mend me into novel ways of interpreting my data.

Academic environment in Psych A 3rd floor is extremely rich and nurturing. Many individuals, world class in research, guided and helped me in every single step during the dissertation. Drs. Suzanne Ferreri, Russell Garman and Hoyan Lam were there from the day one helping the new fish from Mechanical Engineering fresh out of water. Dr.

Liqin Xie, Ali Torab Parhiz and Shiyun Xu share the glory of F2 data. Svetlana Lublinsky helped with the mass phenotyping expedition. Dr. Yen K. Luu and Benjamin Adler provided insight, support and advice for the crusade to the Holy Grail: Bone marrow stem cells. A final acknowledgement goes to a special BME student: Dr. Evren U. Azeloglu, an old friend who piqued my interest in biomedical sciences in the first place.

I realized later that progress of my dissertation was monitored closely by a mastermind, the chair of my committee: Dr. Clinton T. Rubin. I felt his presence directly and indirectly, guiding my research as well as the decisions I make for my career in science. He made me believe that understanding how biological systems work is a remarkable talent, but the real glory lies in controlling those systems externally. It just has to be in high frequency domain! I owe you a lot sir, thank you.

My family was great. Although they thought I was in USA for a Master's in mechanical engineering they were supportive and understanding. If I am never agitated and always taking things easy that is because of my brother, Emre Ozcivici, and our lengthy conversations about nothing and everything.

Finally, I would like to acknowledge my lovely wife, Dr. Gulistan Mese for her support, patience and guidance. She shared her *in depth* biology knowledge with me, and without it I couldn't survive in Biomedical Engineering a single day, no doubt. I am honored to dedicate this dissertation to her.

PUBLICATIONS

This is a list of peer-reviewed publications, book chapters and conference proceedings that were produced during the course of the dissertation.

PEER REVIEWED JOURNAL PUBLICATIONS

1. **Ozcivici, E.**, Garman, R., Judex, S. (2007) High-frequency Oscillatory Motions Enhance the Simulated Mechanical Properties of Non-weight Bearing Trabecular Bone. ***Journal of Biomechanics*** 40(15), 3404-3011.
2. Lublinsky, S., **Ozcivici, E.**, Judex, S. (2007) An Automated Algorithm to Detect the Trabecular-cortical Bone Interface in MicroCT Images. ***Calcified Tissue International*** 81(4):285-93.
3. Luu, Y. K., Lublinsky, S., **Ozcivici, E.**, Capilla, E., Pessin J. E., Rubin, C. T., Judex, S. (2009) In Vivo Quantification of Subcutaneous and Visceral Adiposity by Micro Computed Tomography in a Small Animal Model. ***Medical Engineering & Physics*** 31(1):34-41.

BOOK CHAPTERS

1. **Ozcivici, E.**, Ferreri, S., Qin, Y.X., Judex, S., (2008) Determination of bone's mechanical matrix properties by nanoindentation. In: ***Methods in Molecular Biology: Osteoporosis***. Westendorf, J. (ed.). The Humana Press, Totowa, NJ.
2. **Ozcivici, E.**, Luu, Y.K., Rubin, C., Judex, S., (2008) High resolution imaging of murine organs and tissues by in vivo micro-computed tomography. In: ***The Protocols of Musculoskeletal Research: A Practical Manual for Laboratory Techniques***. Qin, Y.X. (ed.). World Scientific, Hackensack, NJ.

CONFERENCE PROCEEDINGS AND PRESENTATIONS

1. **Ozcivici, E.**, Garman, R., Xu, S., Chung, H., Judex, S. (2006) High-frequency oscillations attenuate the decline in bone's loading characteristics during disuse. Transactions of the Orthopaedic Research Society, Chicago, IL.
2. Judex, S., Gambino, C., Xu, S., Torab-Parhiz, A., Xie, L., Rubin, C., Donahue, L.R., **Ozcivici, E.** (2006) Genetic variations define muscle's susceptibility to disuse and subsequent reambulation. 5th World Congress of Biomechanics, Munich, Germany. Journal of Biomechanics 39(Sl), p. S42.
3. **Ozcivici, E.**, Garman, R., Chung, H., Xu, S., Judex, S. (2006) High-frequency oscillatory motions applied to the tibia during disuse normalize trabecular stress distributions. 5th World Congress of Biomechanics, Munich, Germany. Journal of Biomechanics 39(Sl), p. S471.
4. **Ozcivici, E.**, Garman, R., Rubin, C., Judex, S. (2006) Micro-mechanical adaptations of trabecular bone to small amplitude oscillations. Journal of Bone and Mineral Research 21: S48-S48 Suppl. 1, SEP 2006
5. **Ozcivici, E.**, Gambino, C., Xu, S., Torab-Parhiz, A., Xie, L., Rubin, C., Judex, S. (2007) Is mechanosensitivity similar for muscle and bone? Transactions of the Orthopaedic Research Society, San Diego, CA.

6. **Ozcivici, E.**, Xu, S., Torab-Parhiz, A., Chung, H., Gambino, C., Li, A., Donahue, L.R., Rubin, C., Judex, S. (2007) Cortical bone morphology and mechanosensitivity are modulated by genetic variations. 33rd Northeast Bioengineering Conference, Stony Brook, NY.

7. Bosch, C., Lublinsky, S., Xu., S., **Ozcivici E.**, Judex, S. (2007) Bone's mechanical properties, as determined by microCT, are dependent on precise contour lines. 33rd Northeast Bioengineering Conference, Stony Brook, NY.

8. **Ozcivici, E.**, Lublinsky, S., Rubin, C., Donahue, L., Judex, S. (2007) Musculoskeletal response to altered mechanical demand is tissue specific and influenced by genetic make-up. Journal of Bone and Mineral Research 22: S490-S490 Suppl. 1, SEP 2007

9. Keng, Y., **Ozcivici, E.**, Lublinsky, S., Squire, M., Judex, S. (2007) Modulation of trabecular bone's micromechanical properties by genetic background. Biomedical Engineering Society.

10. **Ozcivici, E.**, Luu, Y.K., Rubin, C.T., Judex, S. (2008) The osteogenic potential of bone marrow, compromised by disuse, is normalized by brief exposure to a low-level mechanical signal**.** Journal of Bone and Mineral Research 23: S499-S499 Suppl. 1, SEP 2008

11. **Ozcivici, E.**, and Judex, S. (2008) Trabecular risk of fracture, caused by disuse, is strongly influenced by baseline morphology. Journal of Bone and Mineral Research 23: S82-S82 Suppl. 1, SEP 2008

12. Adler, B., Luu, Y.K., **Ozcivici, E.**, Judex, S., Rubin, C. (2009) Mechanically Biasing the Bone and Fat Phenotype: Long Term (6 month) Exposure to Low Magnitude Mechanical Stimulation Suppresses Adiposity and Promotes Osteogenesis ASBMR New Frontiers in Skeletal Research: Bone, Fat and Brain Connection.

13. **Ozcivici, E.**, Rubin, C., Judex, S. (2009) Mechanical signals increase the pool of osteoprogenitor cells during disuse, suppress bone marrow adiposity and accelerate bone recovery during reambulation**.** ASBMR New Frontiers in Skeletal Research: Bone, Fat and Brain Connection.

Chapter 1

INTRODUCTION

INTRODUCTION TO BONE BIOLOGY

Osseous tissue (bone) is the primary member of skeletal system with the vital functions for the organism such as mechanical support, mineral homeostasis, blood cell production, protection of delicate tissues and leverage for motion. Even though it is often perceived as inert, in fact bone is a very dynamic organ. For example, bone cells are sensitive to the changes in hormone levels in circulation (e.g. PTH or calcitonin) and in response they can change the circulatory levels of metabolic ions[1]. Similarly, bone can sense its mechanical environment and adapt its structure and geometry to withstand external loads. For bone to respond rapidly to new mechanical settings (or hormonal fluctuations), bone cells contribute to a dynamic process called remodeling, by actively forming and resorbing mineralized tissue. For a healthy individual, these cells that are responsible for the formation of new calcified tissue (Osteoblasts) and cells that are responsible for resorbing existing calcified tissue (Osteoclasts) work cooperatively [1, 2]. Once activated, osteoclasts perforate existing bone surface and osteoblasts follow the resorption cavity to deposit new bone matrix. Rapid structural response in skeleton as an adaptive response to the external mechanical loads is accomplished by the orchestrated work of specialized cells that reside in the bone marrow, on the surface of the bone or within the bone tissue.

Osteoblasts are the cell population that is responsible for the new bone formation. These cells come from the mesenchymal lineage and position themselves on the surface of calcified tissue. With the appropriate biophysical and/or biochemical

signals, osteoblasts secrete osteocalcin, a molecule that calcium ions home and begin mineralization [3]. Upon full mineralization, osteoblasts become trapped in the osteoid lacunae.

Upon the entrapment in osteoid lacunae surrounded by mineral matrix, osteoblasts transform to **osteocytes**, a cell type that has a distinct phenotype with cytoplasmic tendrils that braches within the micron-level channels of bones (lacuna-canaliculi). Osteocytes are able to receive nutrients and remove byproducts through the canalicular network. They also perceive mechanical signals from the changes in shear stresses in the fluid environment and in turn secrete biochemical signals to neighboring osteocytes or other cells.

Perhaps one of the most vital components of bone adaptation is the bone turnover, and sole bone formation is not enough to accomplish this task by itself. Unnecessary or damaged tissue is continuously perforated by tissue resorbing cells, for osteoblasts to induce new bone formation. Cells that are responsible for this maintenance are called **osteoclasts**. Unlike osteoblasts that come from mesenchymal origin, osteoclasts come from hematopoetic lineage and recruited in bone marrow as well as spleen and liver. These cells are large (>20μm diameter), multi nucleated and they can produce acidic lysosomes [4]. Osteoclasts target bone surface and create a local drop in the pH that dissolves the organic and inorganic phases in bone tissue. Resorbed bone surface attract bone lining osteoblasts for novel bone formation. Coupled formative and resorptive activity balances the bone turnover in healthy adults. However, altered physiological or pathological conditions such as loss of functional

weight bearing or menopause may disturb this balanced coupling in the favor of net bone loss, by suppressing new bone formation, increasing bone resorption or both.

MECHANOTRANSDUCTION IN BONE

Balance between bone formation and bone resorption can be disturbed by exogenous mechanical stimuli either to the favor of formation or resorption depending on the nature of the stimulus (exercise or disuse), resulting in net gain or loss in bone tissue. This adaptive mechanism includes distinct and complementary phases such as transforming the presence or deprivation of the external mechanical force to a local mechanical signal (mechanocoupling); a biochemical response to the mechanical signal by gene expression and protein activation (biochemical coupling); cell-to-cell signaling (signal transmission) and appropriate tissue level response (effector response) [5].

Mechanosensitivity of bone tissue

It is still not entirely clear how the mechanical forces are sensed by the bone tissue. It is known that mechanical signals should be dynamic in nature to be perceived for adaptive response [6] and static loads were shown to induce resorptive effects on bone tissue similar to disuse [7]. Other than being dynamic, different aspects of mechanical deformation was suggested to be important in bone formation, such as strain magnitude, strain gradients, strain rate and strain history [8-13]. Also bone can readily

sense and respond to mechanical loading over a broad spectrum of loading frequencies [14-16].

Effects of fluid flow

In addition to magnitude and characteristics of the strains, effects of strains on the fluid environment of bone were also thought to be important in new bone formation. Mechanical loads on bone matrix cause interstitial fluid flow in a dose dependent manner [17]. Osteocytes may sense the fluid shear and trigger a response that can initiate biochemical signaling to other bone cells [18]. For example, compared to axial loads, torsional loads were found to create smaller interstitial fluid flow and induce less osteogenesis in turkey ulna model [19]. Furthermore, oscillating fluid flow was shown to be anabolic in bone without actual matrix deformations [20].

On the level of the cell, byproducts of dynamic strains such as matrix deformations, fluid flow or streaming potentials may be mediators of anabolic response. Several cell culture studies showed the increased growth and maturation of osteoblast (or osteoblast like) cells under fluid shear stresses [21, 22] or matrix deformations [23].

EFFECTS OF EXERCISE ON BONE

Consistent with the evidence that bone cells respond to mechanical loads, long-term physical exercise is shown to increase skeletal mass in general [24, 25]. Specifically,

repetitive external loading of the weight-bearing skeleton results in increased peak bone mass [26], increased bone formation [11, 27], decreased bone resorption and ultimately enhanced bone strength [28]. Although the exact mechanisms are still unclear, strain magnitudes that are caused by external loads and/or the byproduct of these strains, such as strain gradients, strain rates or interstitial fluid flow may be associated with the changes in bone's morphology [8, 10, 15, 29]. Bone's adaptive potential to exercise can also be employed for a non-pharmaceutical alternative to prevent or treat osteopenia related to disuse or aging. However, using strenuous exercise in order to treat or prevent disuse related bone loss was never shown to be successful against detrimental effects of disuse. For example, daily exercise may be effective in preserving muscle mass, but not bone mass during spaceflight [30]. Also the applicability of strenuous exercise may not be ideal for the osteopenic bones after disuse, because the strain profile that is generated by the axial loading and bending moments during vigorous physical exercise (1000-3000 με) may not be safe for already frail bone micro-architecture [31, 32].

MECHANICAL UNLOADING

Effects of mechanical unloading on the level of tissue

Physiological conditions that are referred as "disuse" indicate reduced or lost mechanical loading in the weight-bearing sites of skeletal segments, temporarily or

permanently. Disuse is ultimately catabolic for musculoskeleton, deteriorating its quality and quantity [33, 34]. This deterioration is not surprising because the quantity and morphology of an individual's musculoskeleton is greatly influenced by the loads that it is subjected to[35]. The removal of these loads, disrupts the balance between bone formation and resorption in favor of catabolism [36]. Patients that are confined to bedrest lose their trabecular bone mineral density on the order of 0.3%-2.3% over 17wks period [36], mostly in the trabecular bone of their lower extremities. Similarly astronauts lose 0.4%-23.4% of their trabecular bone mineral density over 6 months of space missions, at an average rate of close to 2% per month [30, 37]. Reambulation after the removal of the catabolic signal recovers site specific bone tissue but full recovery of bone tissue to pre-disuse levels has not been observed[38, 39].

The exact mechanism of bone loss during disuse is currently unclear, given that reduced bone formation [40], increased bone resorption [41] or both [42] were shown to be important during spaceflight. However, these studies covered different flight durations and examined different systemic markers of formation and resorption. Irrespective of the involved mechanism, spaceship crew show sustained negative calcium balance during the flight [43].

Effects of mechanical unloading on the level of cell

Even though it is clear that during disuse, the balance between bone formation and bone resorption is disturbed towards net bone loss, it is not entirely clear how bone turnover balance is disturbed at the level of the cell. It was suggested that disuse limits

the differentiation of osteoblasts to osteocytes, hence arresting the bone formation [44, 45]. Also, there was evidence that apoptotic pathways may be triggered during disuse causing osteblasts to commit suicide [46, 47].

Reduced viability and apoptosis was also suggested for osteocytes during disuse, due to the reduced transport of nutrients and toxic waste buildup in canalicular network [48]. Recent evidence showed in vivo, that disuse induces osteocyte apoptosis, followed by increase in osteoclast recruitment in mice[49].

Another hypothesis is that osteoblasts secrete growth factors during disuse that increase osteoclast recruitment, thereby increasing the bone resorption [50]. Supporting this hypothesis, in vivo evidence suggested increase in osteoclastic activity during disuse [51]. Furthermore, bone resorption during disuse was found to increase in a age- and sex-specific manner [52, 53]. However, contradicting evidence in several rodent models suggests that osteoclastic activity may not differ during disuse [54, 55].

Recently, it was also suggested that mesenchymal stem cells in the bone marrow lose their commitment to osteogenic lineage and instead commit to adipogenesis once they are exposed to disuse [56].

ANIMAL MODELS OF DISUSE

Simulating bone's adaptive response to loss of mechanical loading is possible through several established animal models. Cast immobilization, sciatic neurectomy, spinal cord

injury and botulinum toxin injections were all showed to affect bone morphology [57-60]. However, these models are either invasive, do not allow for simulation of recovery or are not cost-effective. Suspension of rodent hindlimbs by elevating the tail on the other hand is a well established and recognized model for chronic unloading [61]. Hindlimb unloading model does not require surgery and it does not constrain limbs from free movement. It is used to simulate bone's temporal and site-specific response to weightlessness through molecular, cellular and structural level adaptations [62-65].

In female adult (6 mo old) Fischer rats it was displayed that 2 weeks of hindlimb unloading affects bone morphology (volume fraction, trabecular number), bone formation related gene expressions (Collogen type I, osteonectin, osteocalcin) and dynamic bone parameters (mineral apposition rate, bone formation rate) [53]. Compared to shorter periods of disuse, extended exposure to disuse (1 month) results in suppression of anabolic activity even more dramatic in bone formation rates[66]. Bone formation is consistently shown to be reduced during disuse [53, 66, 67]. Bone resorption on the other hand, is shown to be either not affected from disuse [54, 68] or increased [69].

Unlike rat model, in which hindlimb unloading induces deterioration in trabecular and cortical bone morphology, mouse models of hindlimb unloading cause strain- and sex-specific response, providing the opportunity to account for the genetic background in the unloading model [65, 70, 71].

MOLECULAR REGULATION ON BONE

Effects of genetic background on bone mass

Differences in genetic background influence bone mass and geometry of individuals. More than 60% of the variations in peak bone mass have documented to be heritable [72] and the remaining variability depend on environmental factors, including activity levels, and nutrition[73]. Recent data suggests that heritability influences 75% and 83% of variance in femoral and lumbar bone mineral density among man, respectively and remaining variability is explained by environmental factors [74]. Gender is also found to be an important factor in determining peak bone mass across individuals [75, 76].

Further evidence on how distinct genetic backgrounds affect bone quantity and micro-architecture was also shown in inbred mouse strains. For example, female C3H mice at skeletal maturity showed 9% smaller trabecular bone volume fraction, yet 30% larger trabecular thickness compared to adult female BALB mice [77].

Effects of genetic background on susceptibility to bone loss

Similar to peak bone mass, susceptibility to bone loss and related mechanical failure is also influenced by genetic background across individuals [78]. For example, women of Caucasian descent are 10% more susceptible to osteoporotic fractures compared to women from African American descent [79]. Further, on the level of the cell, number of

osteocytes in bones from African American women may be less prone to decline related to aging compared to women of Caucasian descent[80].

Effects of genetic background are important in bone's response to disuse as well. Bone loss in skeletal extremities during disuse occurs because of the lack of weight-bearing, but interestingly the magnitude of bone loss is also quite variable across individuals that are exposed to disuse. For example, bedrest patients lose 0.1-0.6% bone mass per month and astronauts lose 0.1-4% per month. [36] [30, 37]. Given that disuse induced bone loss may not be correlated with age, weight and height of the individual [30], genetic background becomes an important parameter in determination of the bone's response to disuse.

Further evidence of how individual genetic background affects bone's mechanosensitivity was shown in the disuse studies with inbred strains of mice. For example, female BALB/cByJ (BALB) mice were highly responsive to 3wks of simulated disuse by losing 60% of their trabecular bone mass and 10% of their cortical area. Female C3H/HeJ (C3H) inbred strain on the other hand, which is genetically distinct from BALB, remained comparatively unresponsive to disuse [65].Moreover, sexual bimorphism was found to be another important variant in determining disuse induced response in trabecular bone, given that male C3H mice was shown to lose more bone during 3wks of hindlimb unloading, while male BALB mice showed less compared to their female counterparts [71].

Determination of genes that contribute to bone mass and mechanosensitivity

Until now, some candidate genes were identified that can contribute to bone quantity and geometry [81-83], however only recently a genomic loci on chromosome 20 were associated with BMP2 gene that may modulate bone morphology with enough statistical power [84]. Because of the diverse environmental variables it is generally more complex to address skeletal phenotypes (geometry, quantity, mechanosensitivity) in human studies. Studies based on inbred animal strains on the other hand, offer the advantage of controlled environment, where the only variable can be reduced to differences in genome.

Inbred animal strains have homozygous alleles for a given gene locus (either dominant or recessive), except the sex chromosomes. Intercrosses between inbred animal strains, result in heterozygous alleles in first generation (F1). Further crossing F1 strains result in a genetically heterogeneous population (F2), containing both homozygous and heterozygous alleles. Phenotypes that are controlled with multiple genes (polygenic traits, e.g. skin color or bone mass) thereby causes a continuous phenotype distribution in the second generation, as opposed to traits that are controlled with single genes (e.g. eye color). Theoretically, extreme ends of this distribution should include animals that possess the required alleles for that specific phenotype. This methodology enabled the determination of hundreds of chromosomal regions that are statistically likely to modulate a given phenotype (QTLs) leading to identification of more than 30 genes in mammalian, covering complex traits like body size, diabetes, tumor susceptibility or asthma [85]. Understanding the contribution of

specific genes to given phenotypes might lead to identification of drug targets as well as determination of group of individuals that have the high risk for experiencing that specific phenotype.

Animal studies that were concentrated on skeletal morphology and mechanosensitivity described possible genomic regions for contributing skeletal phenotypes. For example, it was shown that the differences in bone's response to exercise were not similar in C57BL/6J (BL6) mice and C3H/HeJ (C3H) mice and a certain region on chromosome 4 is highly associated with these differences [86, 87]. In addition to mechanosensitivity, specific chromosomal regions were also associated with morphology, site specificity and mechanical properties of bone [86, 88-90]. However, in contrast with all the reported significant genomic loci, no single gene was showed to determine bone's mechanosensitivity.

PHARMACEUTICAL INTERVENTIONS TO TREAT BONE LOSS

Even without the identification of underlying genetic mechanisms of mechanosensitivity that would ultimately allow for small molecule drug targets, several pharmaceutical strategies were developed over time to enhance bone strength and reverse the effects of physiologic or pathologic bone loss. Bisphosphonate treatment is the current gold standard for the prevention of bone loss associated with menopause. Bisphosphonates suppress osteoclastic activity and therefore reduce bone resorption[91], however they are

not as effective for preventing disuse related osteopenia [57, 92]. Also, using bisphosphanates over extended periods of times causes microcrack accumulation due to the inhibition of bone turnover, possibly reducing quality of bone [93, 94]. High-dose bisphosphonate injections, a treatment regime that is required in some cancer patients, has been associated with osteonecrosis in jaw [95].

Resorptive activity can also be suppressed using NF-kappaB ligand protein osteoprotegerin, but initial studies showed that molecule may have suppressive effects on formative activity as well as the resorptive activity [96]. Another strategy for the treatment of disuse related bone loss is to increase bone formation rather than suppressing bone resorption. Pharmaceutical approaches to enable this include parathyroid hormone[67], fluoride[97] or strontium ranelate[98] treatment. Nevertheless, those approaches may have side-effects, including hypercalcaemia, hypercalciuria and side-effects related to gastrointestinal, vascular or neurological processes [99-102].

OSTEOGENIC POTENTIAL OF MECHANICAL VIBRATIONS

An alternative strategy to utilize bone's mechanosensitivity for enhancing quality and quantity of bone is to use low magnitude, high frequency mechanical signals. Short duration application of mechanical stimuli that induce extremely small strains (<20με) in the bone matrix can become anabolic when applied at high frequencies (>20Hz) [103]. These stimuli are transmitted into the weight bearing skeleton via whole body vibrations

where they can enhance bone quantity and quality [104] with a preference for trabecular compartments [103, 105]. Daily exposure to high frequency oscillations is found to be anabolic for bone and muscle mass in axial skeleton for humans with different physical conditions [106-108] as well as mice [109, 110]. Most studies indicate the efficiency of whole body vibrations in increasing bone formation rather than suppression of bone resorption [62, 111-113], while some others reported reduced resorption as well [109]. Ultimately, micro-mechanical outcome of the adaptive response to vibrations on the level of tissue are stiffer trabecular bone with a more uniform stress distribution that is less prone to failure [114].

Even though it is not known how bone cells detect high frequency low magnitude mechanical signals and respond to them, certain mechanisms might be involved in the process. For example, lacuna-canaliculi, a complex network of channels that are filled with interstitial fluid and bone cells might be actively detecting and amplifying high frequency signals by the changes in pressure gradients [20] to initiate anabolic response [115]. An alternative theorem was also postulated recently indicating a possible sensing mechanism through cytoskeletal coupling by membrane and cell nucleus [112]. Also it is known that matrix deformations can be sensed by mesenchymal stem cells (MSCs) by integrin mediated extracellular matrix signaling, resulting in the potential decision of MSC for committing osteogenic lineage [116-118]. Recent evidence indicate that mechanical loading affect physical environment of bone marrow and increase osteogenic potential of the MSCs [119].

MESENCHYMAL STEM CELLS

MSCs are osteoprogenitors, meaning with intrinsic and/or extrinsic signals they can drive bone formation by transforming to osteoblasts, cells responsible for growth, maintenance and repair of bone tissue [120, 121]. Alternatively, with appropriate physical or chemical signals, they can commit to the lineages of other mesenchymal tissues such as liver, kidney, muscle, skin, cartilage, fat, marrow stromal, and neural[122-129] cells. Within the last decade, emerging research about function and applicability of adult MSCs in disease treatments and tissue engineering applications, revealed significant potential of this cell line for musculoskeletal tissue regeneration [130-132].

MSCs originate during embryologic development from stem cells of mesodermal layer, which give rise to mesenchymal tissue (e.g. bone, cartilage, fat, muscle, etc.). These stem cells are also present in postnatal organisms in various tissues in low abundance (e.g. bone periosteum, bone marrow, adipose tissue, liver, etc.)[121, 133]. Studies that utilized injection of MSC into target locations of critical size bone defects (e.g. skeletal trauma, skeletal augmentation)[134-137], or degenerative bone conditions (e.g. osteogenesis imperfecta, osteoporosis)[138, 139] showed promising anabolic potential of MSCs especially if they are already committed to bone lineage.

Furthermore, it is also suggested that aging [140], patalogical conditions (e.g. menopause [141] or osteogenesis imperfecta [142]) or altered physiological conditions (e.g. weightlessness [55]) reduce number and osteogenic potential of MSCs that are committed to bone lineage. A mouse model of aging, senesce accelerated mice prone 6 (SAMP6),

which spontaneously experiences osteoporosis when it is skeletally mature [143], were shown to have rescued phenotype (restored bone quantities) once it receives bone marrow transplants from wild type C57BL/6J, indicating that bone remodeling is highly dependent osteogenic potential MSCs and once their potential is restored from a possible debilitating condition, they can independently function towards forming healthy bone morphology.

OBJECTIVE AND HYPOTHESES

The overall objective of this dissertation was to identify cellular, morphological and micro-mechanical response of trabecular bone to altered weight-bearing conditions. This objective was addressed using following hypothesis and research questions.

Hypothesis 1. Variations in genetic background modulate trabecular bone's response to disuse and subsequent reambulation.

Research Questions

(1) How does a genetically heterogeneous population recover from a disuse-induced deterioration in trabecular bone mass, micro-architecture and micro-mechanical properties?

(2) Is the recovery of morphological and micro-mechanical parameters coupled during reambulation?

Hypothesis 2. Baseline morphology is a determinant of bone's response to disuse and subsequent reambulation.

Research Questions

(1) Are bone morphology and micro-mechanical properties at baseline correlated with longitudinal changes during disuse and reambulation?

(2) Do the most- and least-susceptible sub-populations to disuse differ in morphology at baseline?

(3) Do the sub-populations that show most- and least-recovery during reambulation differ in morphology at baseline?

Hypothesis 3. Disuse induced bone loss can be prevented by using high-frequency low-magnitude mechanical vibrations as a countermeasure.

Research Questions

(1) Can daily vibrations maintain the osteogenic potential of bone marrow cells during disuse?

(2) Can daily vibrations augment bone regeneration upon reambulation?

Chapter 2

TRABECULAR BONE RECOVERS FROM DISUSE PRIMARILY BY RESTORING ITS MECHANICAL PROPERTIES RATHER THAN ITS MASS

ABSTRACT

Disuse induced loss in trabecular bone tissue often shows limited recovery upon returning to ambulatory settings. Here, it was asked whether the recovery of tissue amount during reambulation is correlated to recovery in micro-mechanical properties. Female adult (4 mo old) mice from F2 cross of BALB and C3H (high- and low mechanosensitivity) strains were (n=359) subjected to disuse for 3wks and subsequently released for 3wks of reambulation, while 30 F2 mice were used as normal controls. As expected from a genetically heterogeneous population, high variability was observed in response to disuse, as evidenced by an average loss of 43% (range -12%-84%) in bone volume fraction (BV/TV) as indicated by in vivo microCT. On average, disuse caused a 27% increase in trabecular peak Von-Mises (PVM) stresses, and a 104% increase in the skewness of the VM stress distributions (SVM) as determined by finite element modeling. For those mice in which the loss of bone morphology during disuse was greater than in normal age-matched controls (97% of the population), 3wks of reambulation resulted in 14%±36%, 54%±61%, 52%±56% recovery for BV/TV, PVM and SVM. During reambulation, 66%, 89% and 87% of the population showed recovery in BV/TV, PVM and SVM, while the remainders continued to deteriorate. Complete recovery to baseline BV/TV, PVM and SVM levels was found in 2%, 10%, and 16% of the entire population for while 50% recovery occurred in 8%, 50%, and 49% of the population. These data suggest that genetic variations not only produce a remarkable range in the deterioration of bone's mechanical properties during disuse but also define whether a recovery of bone's mechanical properties will be initiated during

reambulation and the extent of it. The preferential recovery of trabecular micromechanical properties over bone volume also demonstrates that, in spite of the large genetic variability, the process of tissue recovery is modulated by mechanical loading and that bone quantity may be an inappropriate measure of assessing skeletal integrity during disuse and reambulation.

INTRODUCTION

Loss of weight-bearing in skeletal extremities, as experienced by crews of space missions or bedrest patients, is catabolic to musculoskeletal tissue. Specifically, this deterioration reduces bone quality and quantity [37] as well as its biomechanical properties [28, 144]. Reduced structural integrity of bone, combined with decreased skeletal muscle mass and postural stability [145], threatens individuals with traumatic or atraumatic fractures upon returning to regular weight-bearing activities [146, 147].

Even though loss of function is the apparent reason for the deterioration in the bone quantity and quality, the magnitude of the response were shown to be highly variable among individuals such as astronauts or bedrest patients (0.1-5% loss/month) [30, 37]. Given that those individuals were exposed to similar mechanical environments, importance of genetic background becomes clear in determination of bone's mechanosensitivity. [72]. Further evidence of how individual genetic background affects bone's mechanosensitivity was shown in the disuse studies with inbred strains of mice. For example, BALB/cByJ (BALB) mice were highly responsive to 3wks of simulated disuse by losing 60% of their trabecular bone mass, while C3H/HeJ (C3H) inbred strain remained comparatively unresponsive [65].

On the level of the cell, simulated disuse is shown to be modulating a decrease in size and function of the osteoprogenitor population outbred rats, thereby adversely affecting bone's ability to regenerate itself [55]. The implication of this becomes important once the individual return to regular weight-bearing conditions. Because of impaired bone formation, regeneration of tissue that was lost during disuse is often slow and

incomplete [36,148, 149]. At this point, it is not clear how bone regulates its tissue recovery upon reambulation and whether genetic background is a determinant of this process. It is entirely possible that variability in genetic structure may modulate tissue recovery, just as it is a strong determinant for development of bone quantity and morphology in healthy bones [77, 110].

On the other hand, given the bone's micro-mechanical properties are related to its geometry, quantity and micro-architecture [150-152], mechanical stresses in disuse bones should be experienced higher than physiological levels [153]. Perhaps morphological adaptations to the new mechanical demand are the leading factor for recovery in disuse bones. Here, using a 2nd generation heterogeneous mice population of BALB and C3H mice (high and low mechanosensitivity), the following research questions were addressed: (1) How does a genetically heterogeneous population recover from a disuse-induced deterioration in trabecular bone mass, micro-architecture and micro-mechanical properties? (2) Is the recovery of morphological and micro-mechanical parameters coupled during reambulation?

MATERIALS AND METHODS

Experimental design

All procedures were reviewed and approved by the Institutional Animal Care and Use Committee (IACUC). A total of 466 female adult (16 wks old) mice were selected from a second generation (F2) cross of BALB/cByJ (BALB) and C3H/HeJ (C3H) inbred strains were used for all experiments. At baseline, all mice were scanned in vivo by

microCT at distal femoral metaphysis and immediately after scans hindlimbs of F2 mice were unloaded (n=359) for 3 weeks by tail suspension method [154]. After 3 weeks (19 wks old), mice were scanned in vivo and then released for regular cage activity (reambulation) for 3 more weeks. Upon 3 weeks of reambulation (22 wks old) mice were scanned in vivo for a final time. Additional F2 mice (n=30) were assigned as age-matched controls and they were allowed for regular cage activity through 6 weeks experimental period and received in vivo scans at identical time points with identical scan parameters. Trabecular and cortical bone morphology of distal femoral metaphysis was quantified using in vivo micro-computed tomography (vivaCT40, Scanco Medical, Switzerland). Reconstructed 3D images from the scans were translated to finite element (FE) models and simulated under uniaxial compression for the evaluation of micro-mechanical properties of trabecular and the cortical bone.

Micro-computed tomography

Trabecular and cortical bone morphology was assessed from the in vivo microCT scans using an isometric voxel size of 17.5 μm for distal femoral metaphysis. Region of interest was defined as 600μm (35 slices) proximal from growth plate and spanned 1500 μm (85 slices) [65, 71]. Trabecular bone was separated from cortical bone using an image processing language algorithm [155] followed by a noise suppression using a 3D Gaussian filter which “sigma” and “support” values were set at 0.3 and 1. Threshold value that was used to contrast calcified tissue from background was set at 29.5% of the maximum voxel intensity and strictly controlled for all subjects. For trabecular bone, bone volume

fraction (BV/TV), trabecular connectedness (Conn.D), number (Tb.N) and thickness (Tb.Th) were determined.

Finite element modeling

Disuse induced changes in the micro-mechanical properties were evaluated by the simulation of uniaxial compression that is applied to the metaphyseal segments consisting both cortical and trabecular bone. Proximal and distal surfaces of the samples that were transverse to longitudinal loading, were subjected to 1 N of a uniformly distributed force to simulate a frictionless compression test [153]. Linear elastic properties were assigned to trabecular and cortical bone with an elastic modulus (E) of 25 GPa and Poisson's ratio (υ) of 0.3 [156-158]. FE solutions were completed via an iterative FE-solver [159] with a force (N) and displacement (mm) tolerance of 1×10^{-4} (ScancoFE, Scanco Medical, Switzerland). In the post-processing, voxels pertaining to trabecular and cortical bone were analyzed separately. Apparent stiffness values for trabecular bone were calculated as the ratio of input force to resultant displacement. Von-Mises (VM) stresses were calculated for all elements and represented with peak VM (PVM) stress values (Fig.2.1). In an effort to prevent local artifacts and singularities, instead of maximum stress value 95^{th}% was presented [153]. Because of the lack of normality in stress distributions [160], skewness of the VM stresses (SVM) was also reported as an indicator of trabecular efficiency in load bearing [114].

Statistics

All data were presented as mean (± standard deviation) and statistical significance was set at 5%. Unpaired t-tests were used to contrast morphological and micro-mechanical values between experimental and age-match control mice. Linear regressions were used to determine associations between longitudinal (%) changes in bone volume fraction and micro-mechanical parameters during disuse and recovery.

RESULTS

Longitudinal changes in bone morphology

Three weeks of hindlimb unloading caused significant losses in trabecular bone morphology at the distal femoral metaphysis. Compared to baseline values, mice that were subjected to disuse lost, on average, 43% of their trabecular BV/TV (Fig.2.2a), accompanied by means losses of 38% in Conn.D, 17% in Tb.N and 18% in Tb.Th (Table 2.1). As expected from a heterogeneous population, trabecular response to disuse was highly variable, ranging from 84% tissue loss to 12% gain (Fig.2.3a). Upon reambulation, BV/TV increased 10% compared to disuse levels, accompanied by 16% increase in Tb.Th. During reambulation, Conn.D and Tb.N showed continued deterioration (-18% and -8%, respectively) instead of any recovery. Age-matched controls showed 9% reduction in BV/TV, accompanied by 18% and 8% reduction in Conn.D and Tb.N. in the first 3wks. During the second 3wks, control mice differed in 1%, -11%, -2% and 3% in BV/TV, Conn.D, Tb.N, Tb.Th compared to previous time point (Fig.2.2a and Table 2.1).

Longitudinal changes in trabecular micro-mechanical properties

Reflecting the disuse induced changes in bone morphology, stiffness values and Von-Mises (VM) stress distributions was also altered for unloaded F2 bones. Disuse decreased trabecular stiffness by 34%, which increased 11% upon reambulation (Fig.2.2b). Results also showed 27% increase in peak VM (PVM) stress and 104% increase in skewness (SVM) values (Fig.2.2c,d). Upon reambulation, PVM and SVM decreased 10% and 22% (Fig.2.2c,d). Similar to BV/TV, micro-mechanical response to disuse was also extremely variable (Fig.2.3b-d). During first 3wks of the experiment, controls showed -8%, 2% and 8% change in stiffness, PVM and SVM. In the second 3wks controls showed 1%, -3% and -7% difference in stiffness, PVM and SVM.

Recovery of disuse induced deterioration during reambulation

Recovery in morphology and micro-mechanical properties, as calculated by % of the disuse induced change was calculated for all mice that showed deterioration during disuse period more than the age-matched controls. Reambulation for 3wks resulted in 14% recovery of disuse induced losses in BV/TV (Fig.2.4a) marked with high variations indicating that some mice continued to lose trabecular bone mass. Confirming this, during reambulation Conn.D and Tb.N showed further deterioration accounting to 35% and 37%, while Tb.Th recovered 87% of the losses. Furthermore, F2 mice recovered 14%, 54% and 52% of the deterioration in stiffness, PVM and SVM upon reambulation (Fig.2.4b-d).

Mice that showed positive recovery (>0%) in BV/TV was 65% of the entire population, while 89% and 85% of the population showed recovery in PVM and SVM (Table 2.2). Complete recovery (>100%) were experienced by only 2% of the population for BV/TV, while 10% and 16% of the population recovered PVM and SVM completely (Table 2.2).

Linear regressions showed longitudinal (%) changes BV/TV showed significant ($p<0.05$) correlations to stiffness ($R^2=0.78$), PVM ($R^2=0.46$) and SVM ($R^2=0.20$) during disuse (Fig.2.5a-c). During recovery period correlations between BV/TV and stiffness ($R^2=0.59$), PVM ($R^2=0.25$) and SVM ($R^2=0.08$) remained significant, however weakened extensively (Fig.2.5d-f).

DISCUSSION

Effects of disuse and subsequent reambulation on morphological and micro-mechanical properties in a skeletally mature genetically heterogeneous F2 population were documented. On average, trabecular bone quality and quantity were deteriorated in the femoral distal metaphysis while surrounding cortical bone appeared non-responsive to 3 wks of mechanical unloading. Trabecular micro-mechanical properties also reflected the deterioration in trabecular architecture, indicated by reduced quality in stress distribution (increased skewness of stress distribution) and increased peak stresses. Entire population was subjected to a 3 wks of subsequent reambulation following disuse where mice were allowed for habitual cage activity. Upon reambulation trabecular architecture showed continued deterioration except trabecular thickness, in

which disuse induced losses were mostly recovered. Trabecular bone volume fraction (BV/TV) and stiffness did not improve upon reambulation. Conversely, most of the F2 population recovered the deterioration in peak stresses and stress distributions. Furthermore, during disuse changes in BV/TV appeared to be highly correlated with stiffness and peak stress but not stress distributions. However, these correlations were weakened during the recovery period, indicating an uncoupling between morphology and micro-mechanical properties. Overall, results demonstrated poor recovery of morphological parameters except trabecular thickness, while trabecular bone more readily recovered its micro-mechanical properties.

Finite element simulation that was aimed to evaluate biomechanical properties of trabecular bone was selected as uniaxial compression in proximal to distal (longitudinal) anatomic direction and results were calculated as Von Mises (VM) stresses. The reason for this was (a) it provided a loading mode with physiological relevance and (b) complex shape of metaphyseal segment (lack of parallel surfaces) did not allow for simulations in other directions. However, due to the inherently complex structure of trabecular bone, longitudinal compressive loads can also result in stresses and strains in all normal and shear directions [153, 161]. In order to simplify the representation and account for all those stress components, Von-Mises (VM) stress values were evaluated, a derived stress value that is closely related to failure in trabecular bone [160].

As expected from the parental strains, F2 mice showed highly variable losses in trabecular structure but those losses averaged to a magnitude less than BALB and more

than C3H strains [65]. Changes in micro-mechanical properties reflected the response in morphology as decreased stiffness and increased peak stress levels, indicating an increase in risk of mechanical failure [162, 163]. Age-matched controls on the other hand showed minor differences during this period both in architectural and micro-mechanical properties, possibly because of aging. Furthermore, associations between trabecular BV/TV and stiffness as well as PVM stresses were very strong, indicating a coupled response to disuse induced deterioration[164-166].

At the point of reambulation, trabecular bones that were deprived of weight-bearing started to bear loads again. However, due to the extensive bone loss load bearing characteristics of the trabecular bone changed significantly, as expressed by the skewness values of the stress distributions. Increased peak stress and skewness compared to baseline values indicate that trabecular bone start the recovery in the presence of several overloaded and underloaded trabecular struts.

Overloaded structures are under the threat of mechanical failure or microdamage once the bone starts experiencing regular loads again [167, 168]. Microdamage accumulation was shown to be a potent modulator of bone remodeling in cortical and trabecular bone [169, 170]. Increased remodeling may lead to thickening of struts to reduce further damage. Underloaded trabecular struts on the other hand may be resorbed after returning to regular weight-bearing activity and in turn leading to apparent deterioration of the trabecular structure (e.g. decrease in trabecular number). Even though this study is limited in the sense that it lacks bone formation and resorption assays, longitudinal morphology and FE models indicate that remaining

trabecular bone adapted to loads placed upon it and increased its thickness upon reambulation. Number of trabecular struts on the other hand continued to decrease indicating the removal of underloaded tissue. Taken together, these adaptations upon subsequent reambulation resulted in slight increase in trabecular bone mass but net reduction in peak stresses and skewness values.

During recovery associations between morphology and micro-mechanical properties weakened indicating the reduced coupling between morphology and micro-mechanical properties. Possible reason for this loss in coupling was again may be related to the change of the way trabecular bone mass was adapting to reambulation (losing underconnected trabecular struts while increasing thickness of remaining ones). It is not surprising that addition of trabecular bone mass can increase the stiffness of the structure and reduce peak VM stresses. But increased bone mass by itself apparently cannot determine the structure's efficiency in load bearing. Even though only 2% of the entire population showed full recovery in bone mass, several times higher mice were able to restore their stress characteristics, confirming the importance of trabecular morphology over the mass. Given that bone quantity is not necessarily a good determinant of fracture risk [171], perhaps trabecular bone is primarily trying to adapt to mechanical loads in order to prevent risk of mechanical failure.

Trabecular adaptations to altered physiological conditions through losing individual struts and thickening (or fusing) the remaining ones was also shown in the weight-bearing bones of mice [172] and rats [173] under catabolic signal (OVX or aging). Furthermore, coronal sections revealed that thick trabecular bones in the OVX rats tend

to align parallel to the longitudinal direction where primary loading for weight-bearing occurs [173]. Results in this study confirmed the overadaptation of trabecular struts in the loading direction, in order to have a more uniform load distribution with smaller peak stresses in the longitudinal direction. Although this mechanical response was apparently beneficial for trabecular bone's regular weight-bearing, it is not clear whether trabecular bone is similarly protected in transverse direction or from torsional loads. Previous evidence showed that individuals that experience osteoporotic fractures had weaker trabecular structures in transverse direction compared to controls [174]. Further evidence showed that, trabecular bone of the vertebra that suffers from osteopenia may be similar in load bearing in longitudinal direction compared to control; however it was less protected from the off-axis loads [175]. Taken together, these results also indicate the importance of measuring structural information of the trabecular bone as well as the tissue quantity, which by itself is not necessarily sufficient to establish risk of mechanical failure of an individual.

Although it is clear that the duration of reambulation in this study may not be enough to facilitate a complete recovery, it is unlikely that trabecular architecture will return to baseline levels. Studies on human exposure to weightlessness can predict the time course of recovery in trabecular bone quantity during reambulation [176]. However lack of volumetric assessment of trabecular bone structure prevents the understanding of the nature of this regeneration. If it is true that reambulation response in human trabecular bone is similar to that of F2 mice, then exposed individuals will always be under the risk of fracture from off-axis loads, even though clinically (via DXA scans) their

bone mass shows apparent recovery of bone mass. Given that the trabecular response to the reintroduction of mechanical loads is quite similar to the trabecular response to catabolic stimulus such as menopause or aging, perhaps bone marrow environment never recovers from diminished osteogenic capabilities induced by disuse. If this is correct, it highlights the importance of the prophylactic measures to prevent catabolic effects of disuse on bone and marrow environment.

In summary, disuse induced deterioration in trabecular bone quantity and micro-mechanical properties were highly variable in genetically heterogeneous mice. Recovery of the tissue level losses during reambulation were extremely limited on the apparent level and also marked with high variations. On the other hand, regenerative response of the trabecular bone seems to prefer reducing stress magnitudes and making the load distributions more uniform over simple addition of bone mass. This process involves the thickening of trabecular struts to reduce peak stresses and resorption of underconnected struts, which sometimes may give the impression of reduced bone mass but in micro-mechanical terms, indicates a more uniform load distribution. Regardless of the differences in genetic background, most F2 mice showed similar response during recovery with less variability compared to tissue level changes. This indicates that tissue recovery may be modulated simply by mechanical demands in adult skeleton rather than pre-defined values dictated by the individual genetic background.

ACKNOWLEDGEMENTS

Financial support by NASA NAG 9-1499 is gratefully acknowledged.

Tables

Table 2.1. Trabecular and cortical bone morphology of F2 population at baseline (16wks), after 3 wks of hindlimb unloading (19wks), or upon 3 wks of reambulation (22wks) as well as age-matched control F2 mice at 19wks and 22wks. All parameters belonging to age-matched controls were not significantly different than baseline group.

*: significant differences between hindlimb unloaded and age-matched group ($p<0.05$).

†: no significant difference at baseline and at the end of hindlimb unloading.

	Conn.D [1/mm^3]		**Tb.N [1/mm]**		**Tb.Th [μm]**	
	Experimental	**Control**	**Experimental**	**Control**	**Experimental**	**Control**
Baseline	87±32		4.37±0.84		65.3±8.3	
Week 3	58±35*****	78±25*****	3.62±0.81*****	4.24±0.70*****	53.6±9.7*****	66.7±11.1*****
Week 6	45±28*****	69±24*****	3.35±0.87*****	4.15±0.79*****	61.9±9.5*****	68.6±11.2*****

Table 2.2. Proportion of the sub-population of F2 mice that recovered disuse induced deterioration. >0%: Positive recovery, >50%: mice recovered half of their losses, >100%: mice that showed complete recovery.

	>0%	**>50%**	**>100%**
BV/TV	65%	8%	2%
Conn.D	15%	1%	0%
Tb.N	11%	1%	0%
Tb.Th	95%	75%	18%
Tb.Stiff	59%	14%	3%
PVM	89%	50%	10%
SVM	85%	49%	16%

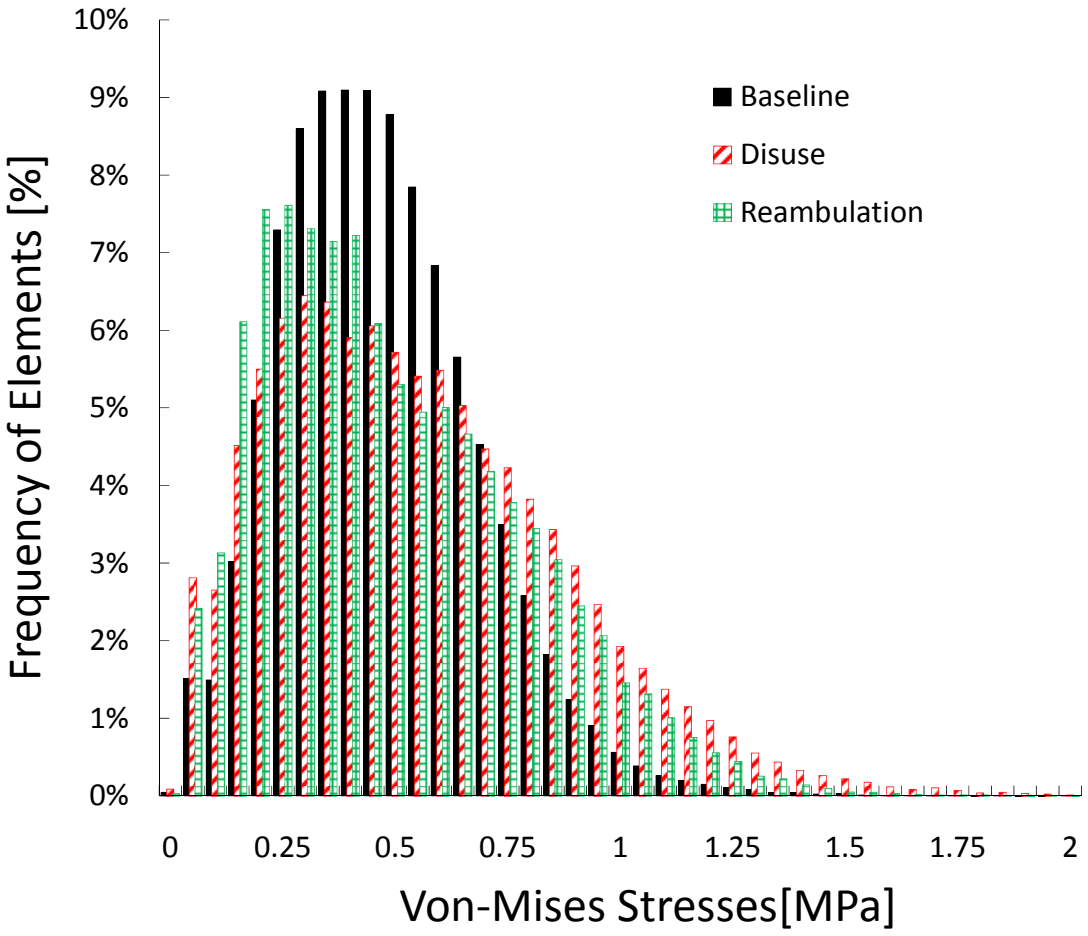

Figure 2.1. Von-Mises stress distributions in trabecular bone from a representative experimental F2 mouse. Micro-CT scans at baseline, at the end of hindlimb unloading (wk3) and reambulation (wk6) was translated to finite element models and simulated compression was applied in longitudinal direction with a uniform force of 1N. At baseline, stress values had a normal distribution (black bars) but the disuse induced deterioration in trabecular bone increased peak loads as well as the skewness of distribution (red bars). Reambulation mitigated stress values partially towards baseline values (green bars).

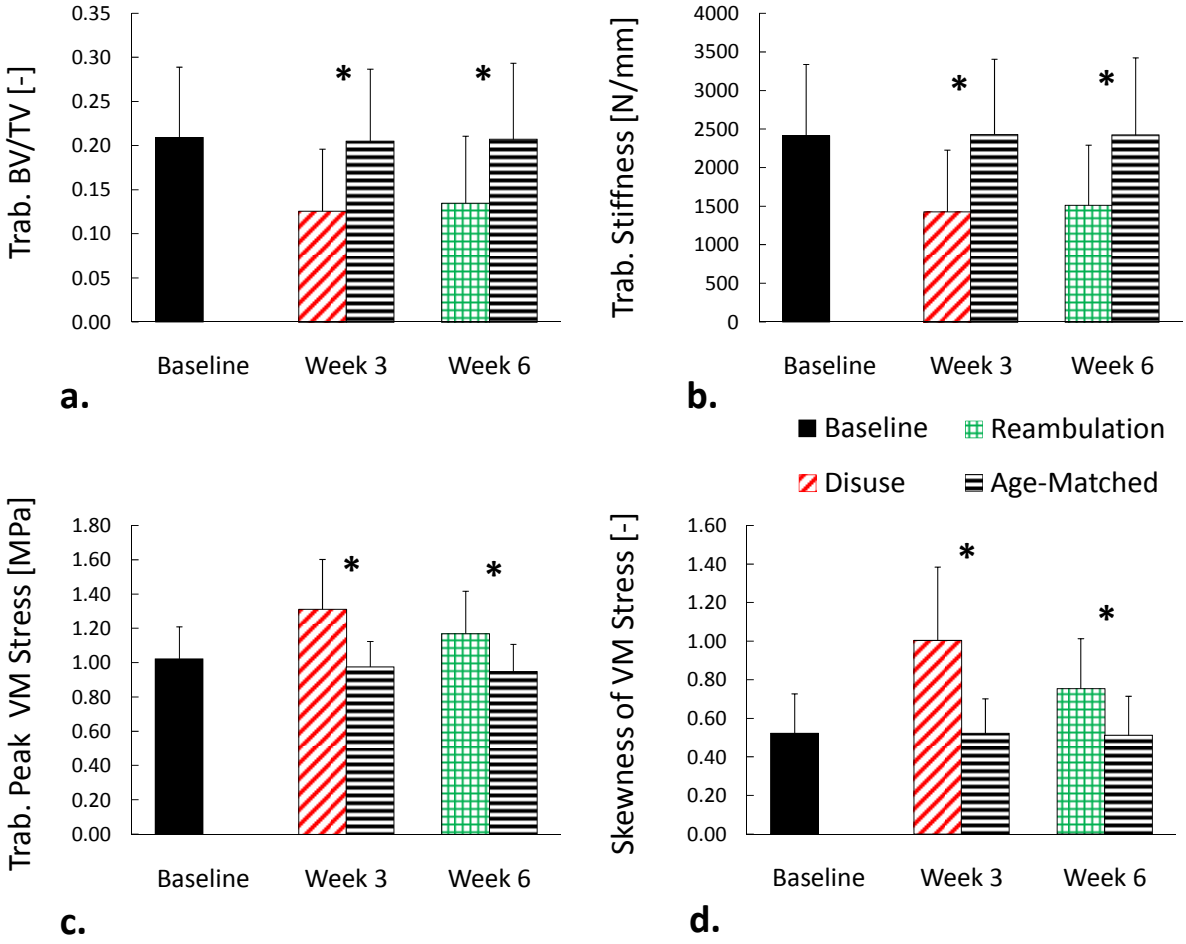

Figure 2.2. Selected morphological and micro-mechanical properties from femoral metaphysis of F2 mice at baseline, after disuse and upon reambulation. **a.** Trabecular bone volume fraction **b.** Trabecular stiffness **c.** Trabecular peak VM stresses, **d.** Skewness of trabecular VM stress distribution. *: significant differences between experimental and corresponding age-matched group ($p<0.05$)

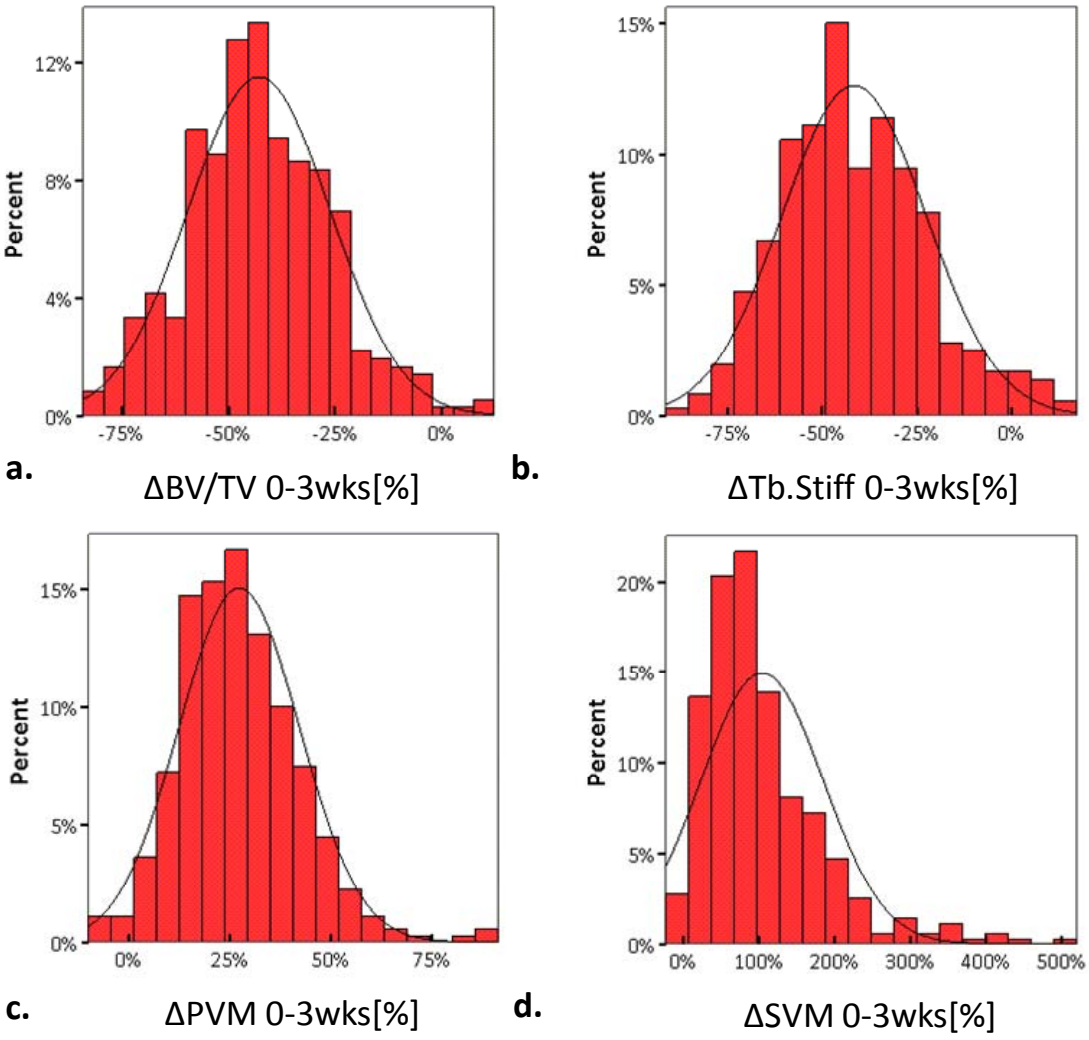

Figure 2.3. Distribution graphs of changes in selected morphological and micro-mechanical properties of trabecular bone during disuse. **a.** Trabecular bone volume fraction **b.** Trabecular stiffness **c.** Trabecular peak VM stresses, **d.** Skewness of trabecular VM stress distribution.

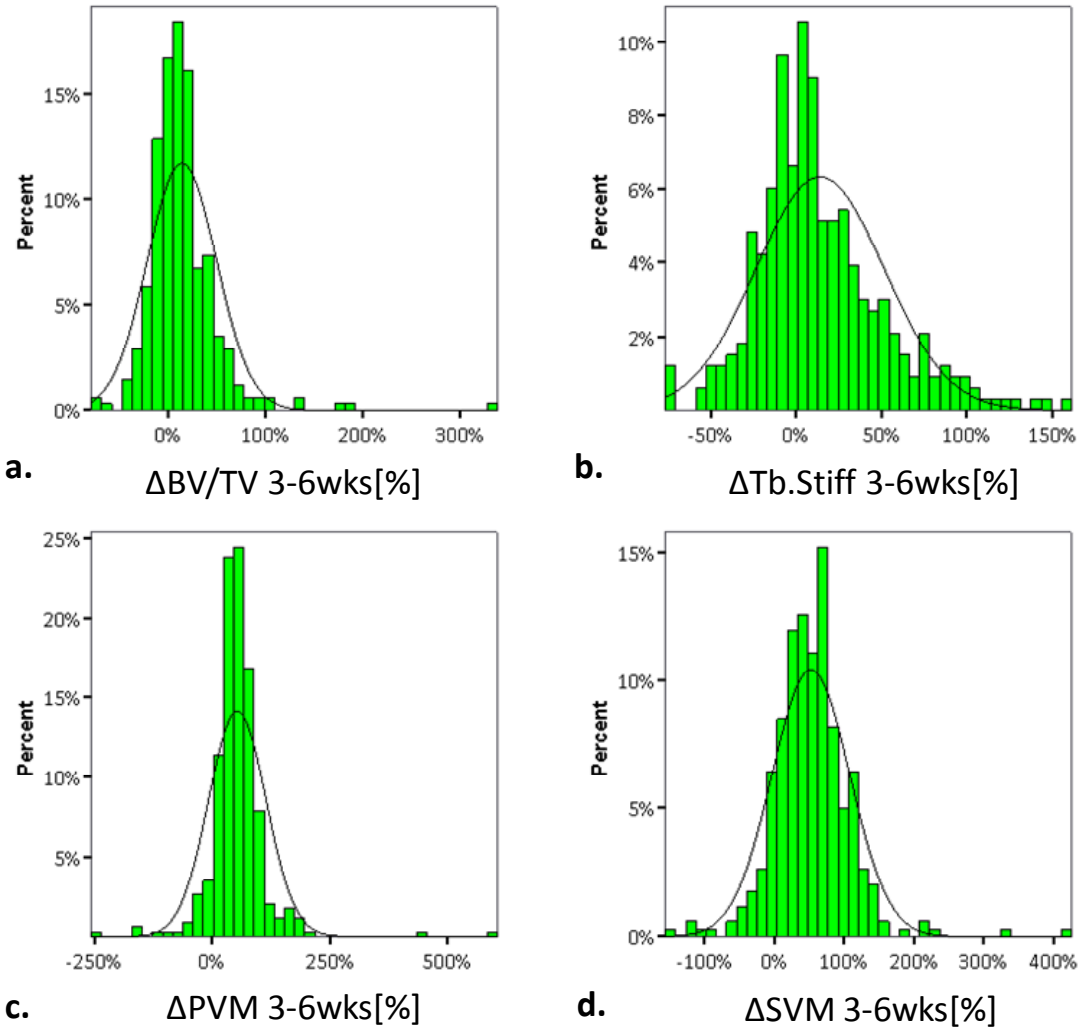

Figure 2.4. Distribution graphs of recovery of disuse induced losses in selected morphological and micro-mechanical properties of trabecular bone. **a.** Trabecular bone volume fraction **b.** Trabecular stiffness **c.** Trabecular peak VM stresses, **d.** Skewness of trabecular VM stress distribution.

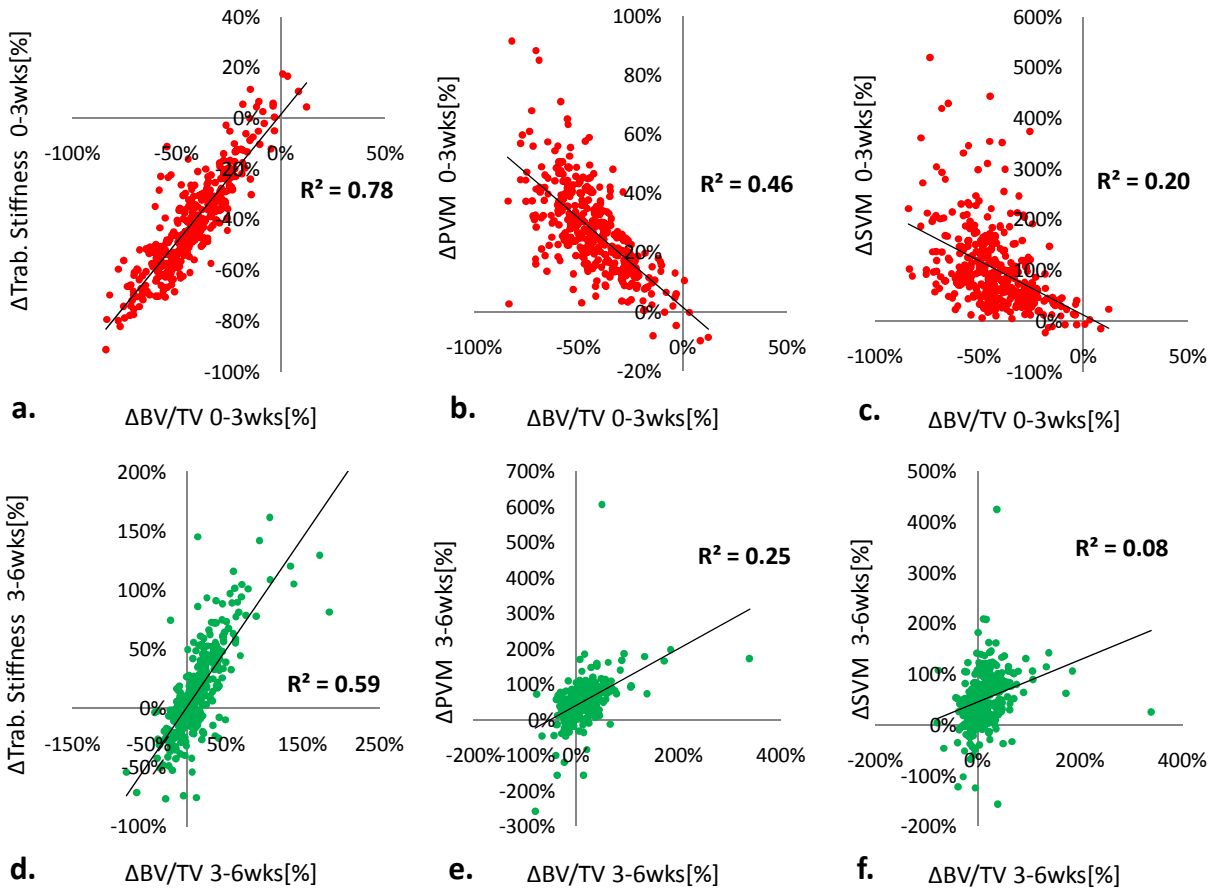

Figure 2.5 Linear regressions of trabecular bone volume fraction (BV/TV) to micro-mechanical properties during disuse (red dots) or during recovery (green dots) **a-d.** Trabecular stiffness **b-e.** Trabecular peak Von-Mises stresses, **c-f.** Skewness of trabecular VM stress distribution.

Chapter 3

CHANGES IN BONE'S MECHANICAL PROPERTIES DURING DISUSE AND REAMBULATION ARE LINKED TO TRABECULAR BASELINE ARCHITECTURE

ABSTRACT

Alterations in bone's mechanical environment affect bone's morphology and its mechanical properties. These changes are marked with high variations across individuals, indicating the importance of genetic background on bone's mechanosensitivity. Here, we attempted to identify baseline predictors of longitudinal response to altered weight-bearing in a genetically heterogeneous population. Female adult mice from 2nd generation cross of BALB and C3H strains (n=359) were subjected to 3wks of disuse and subsequently released for 3wks for reambulation. Baseline BV/TV, as measured by in vivo microCT, was found to be moderately correlated to disuse induced losses (R^2=0.27) however increments in peak stresses, as calculated by finite element simulations, were not correlated (R^2=0.01) to baseline values. Also baseline BV/TV and peak stresses were not correlated to changes upon reambulation. Once the entire cohort of F2 mice were stratified based on most (H.Ris) or least (L.Ris) risk of disuse induced increase in stress, H.Ris mice had 14% ($p<0.05$) smaller BV/TV at baseline than L.Res, but they had similar peak stresses. Once the F2 mice were stratified based on most (H.Rec) or least (L.Rec) recovery of disuse induced increase of peak stress upon reambulation, H.Rec and L.Rec mice had similar BV/TV at baseline, however peak stresses were 5% ($p=0.05$) higher in H.Rec mice. Data showed that disuse induced changes may be predicted for tissue quantity but not micro-mechanical parameters. Also, it was possible to identify morphological indicators for stress adaptations to altered weight-bearing at baseline, but lack of correlations suggests that those indicators may be indirect effects of mechanosensitivity regulation on morphology.

INTRODUCTION

Formation and maintenance of the bone structure in skeletal extremities relies on the mechanical forces applied to it [10, 177, 178]. Habitual loading profile on skeletal extremities consists of forces formed by weight-bearing and muscle contractions and temporary interruptions in weight-bearing, as experienced during bedrest or spaceflight, results in deterioration of bone structure especially targeting trabecular compartment [179-181]. Also, once the individuals return to regular weight bearing, lost bone tissue may never be recovered or even continue to deteriorate [148, 182]. Sensitivity of bone to the changes in mechanical environment also has a large genetic component as suggested by large variations in bone loss observed in spaceship crew [30]. Differential modulation of bone's mechanosensitivity was previously shown in the studies using inbred mice with distinct genetic backgrounds [65, 70, 71]. On the other hand, studies on the role of genome are yet to produce specific genetic markers that may predict mechanosensitivity of bone.

In the absence of such genetic determinants, quantity and quality of the healthy bone tissue may serve as an indicator of tissue level adaptations to loss and recovery of functional weight-bearing. During catabolic stimulus that attract rapid response from trabecular bone, baseline bone volume was shown to be negatively (disuse [183]) or positively (OVX [184]) correlated with longitudinal tissue loss using inbred mouse strains. However, it is not entirely clear how strong this relationship would be in a genetically heterogeneous population, given that not only mechanosensitivity but also baseline trabecular morphology is largely affected from individual genetic background [77].

Furthermore, information on interaction of baseline properties with the longitudinal changes during recovery after disuse is currently lacking.

Given that there is an intricate relationship between trabecular structure and its micro-mechanical properties, deterioration of the structure (e.g. trabecular thinning or resorption of an entire strut) increases mechanical risk of failure [167, 185]. Measurements in apparent trabecular bone mineral density [151, 186] or volume [153, 166] was found to be well correlated to peak stress, strain and elastic modulus of bone. However, if there are morphological parameters at baseline that may determine bone's micro-mechanical response to altered weight bearing, they are yet to be determined. Here, using female adult mice from a genetically heterogeneous population, we asked following research questions: (1) Are bone morphology and micro-mechanical properties at baseline correlated with longitudinal changes during disuse and reambulation? (2) Do the most- and least-susceptible sub-populations to disuse differ in morphology at baseline? (3) Do the sub-populations that show most- and least-recovery during reambulation differ in morphology at baseline?

MATERIALS AND METHODS

Experimental design

All procedures were reviewed and approved by the Institutional Animal Care and Use Committee (IACUC). Female adult (16wks old) mice selected from a second generation cross of BALB/cByJ (BALB) and C3H/HeJ (C3H) strains were used for all experiments (n=359). Catabolic stimulus to long bones was introduced by hindlimb

unloading (disuse) for 3wks by tail suspension method [154] followed by releasing them to 3 more weeks of habitual cage activity (reambulation). Trabecular and cortical bone morphology of distal femoral metaphysis was quantified using in vivo micro-computed tomography (vivaCT40, Scanco Medical, Switzerland). Scans were performed at baseline as well as immediately after disuse and reambulation. Reconstructed 3D images from the scans were translated to finite element (FE) models and simulated under uniaxial compression for the evaluation of micro-mechanical properties of trabecular and the cortical bone.

Micro-computed tomography

Trabecular and cortical bone morphology of the tibia was assessed from the in vivo microCT scans using an isometric voxel size of 17.5 µm for distal femoral metaphysis. Region of interests were defined as 600µm (35 slices) proximal from growth plate and spanned 1500 µm (85 slices) [65, 71]. Trabecular bone was separated from cortical bone using an image processing language algorithm [155] followed by a noise suppression using a 3D Gaussian filter which "sigma" and "support" values were set at 0.3 and 1. Threshold value that was used to contrast calcified tissue from background was set at 29.5% of the maximum voxel intensity and strictly controlled for all subjects. For trabecular bone, bone volume (BV), bone volume fraction (BV/TV), trabecular connectedness (Conn.D), structural model index (SMI), number (Tb.N), thickness (Tb.Th) and degree of anisotropy (DA) were determined. Cortical bone that surrounds trabecular bone was represented with cortical (Ct.Ar) and endocortical envelope (Ec.En)

areas. Also, tissue mineral density as a function of linear attenuation was assessed for trabecular bone (TMD).

Finite element modeling

Micro-mechanical properties were evaluated by the simulation of uniaxial compression that was applied to the metaphyseal segments consisting both of cortical and trabecular bone. Proximal and distal surfaces of the samples that were transverse to longitudinal loading, were subjected to 1 N of a uniformly distributed force to simulate a frictionless compression test [153]. All voxels were assigned with elastic modulus (E) of 25 GPa and Poisson's ratio (υ) of 0.3 [156-158]. FE solutions were completed via an iterative FE-solver [159] with a force (N) and displacement (mm) tolerance of 1×10^{-4} (ScancoFE, Scanco Medical, SUI). For post-processing, voxels pertaining to trabecular and cortical bone were analyzed separately. Apparent stiffness values (Tb.Stiff) for trabecular bone were calculated as the ratio of input force to resultant displacement. Von-Mises (VM) stresses were calculated for all elements and represented with either 95^{th}% for peak stresses or skewness of VM stresses for general distribution [153, 160].

Statistics

All data were presented as mean (± standard deviation) and statistical significance was set at 5%. Based on the longitudinal (percent) changes in peak VM stresses during disuse or upon reambulation, sub-populations were selected from the entire F2 population based on the percentiles within the population. For a given time point or the longitudinal changes in between, morphological and micro-mechanical results from different sub-populations were compared by unpaired t-tests.

RESULTS

Differences induced by altered weight-bearing in the entire population

The morphological and micro-mechanical response of the F2 population to 3wks of disuse followed by 3wks of reambulation was presented elsewhere (Chapter 2). Briefly, experimental mice lost 41% of their trabecular BV/TV during disuse, while Ct.Ar was unresponsive. In parallel, trabecular stiffness reduced 42% while peak VM stresses (PVM) in trabecular bone increased 21% and skewness of VM stresses (SVM) increased 104%. Upon reambulation, there was a limited regain in BV/TV (10%) and Ct.Ar was increased 3%. Also, during reambulation trabecular stiffness increased 13% while PVM reduced 10% and SVM reduced 22%.

Correlations between baseline parameters and longitudinal changes

Linear regressions that were attempted to link baseline morphology (BV/TV) or micro-mechanical parameters (Stiffness, PVM or SVM) to their longitudinal (%) changes during disuse and reambulation showed poor associations (Fig.3.1a-d). Out of these parameters baseline BV/TV and SVM were moderately correlated (R^2=0.27 and 0.22, $p<0.05$) to disuse induced changes (Fig.3.1a and 3.1d), while the others were not correlated ($R^2<0.10$). Baseline values were also poor predictors of longitudinal changes upon reambulation for any given parameter (Fig.3.1a-d).

Categorization based on stress response during disuse

Two sub-groups within the entire population were selected based on the disuse induced increase (Fig.3.2a) in PVM as an indicator of mechanical failure risk, as high risk (H.Ris, peak VM change 66^{th}-100^{th}%, n=120) and low risk (L.Ris peak VM change 0^{th}-33^{th}%, n=120). H.Ris group had 14% (p=0.003) less BV/TV at baseline compared to L.Ris, and this difference increased to 44% (p<0.001) after disuse and 43% (p<0.001) upon reambulation (Fig.3.3a). The longitudinal decrease in BV/TV was 86% (p<0.001) larger in H.Ris group, while reambulation induced similar (p=0.35) longitudinal change in this trait between groups (Fig.3.3c). In contrast, trabecular PVM was only 4% (p=0.08) greater in H.Ris than in L.Ris mice at baseline but this difference became 33% (p<0.001) after disuse and 23% (p<0.001) after reambulation (Fig.3.3b). Longitudinal change in PVM was 250% larger and 49% smaller (both p<0.001) for H.Ris group compared to L.Ris during disuse and upon reambulation (Fig.3.3d).

Baseline properties of mice grouped based on risk of failure

Other trabecular morphology (Table 3.1) at baseline showed H.Ris mice had a poorer trabecular structure as indicated by 15% larger SMI (p=0.01), 6% smaller Tb.N (p=0.001), 5% smaller Tb.Th (p=0.001) and 1% smaller TMD (p=0.001) compared to L.Ris. However, L.Ris and H.Ris groups had similar trabecular BV (p=0.11) and Conn.D (p=0.58), leading to similar trabecular stiffness (p=0.1) and SVM (p=0.91). Parameters that depict cortical bone were also 3% (p=0.04) smaller for Ct.Ar and 6% (p=0.001) larger in Ec.En for H.Ris mice at baseline (Table 3.1).

Categorization based on stress response during reambulation

Entire F2 population was also stratified based on the recovery of disuse induced increase in peak VM stress values during reambulation, as high recovery (H.Rec, PVM recovery 66^{th}-100^{th}%, n=115) and low recovery (L.Rec, PVM recovery 0^{th}-33^{th}%, n=115) mice (Fig.3.1b). H.Rec group had similar BV/TV at baseline (p=0.30) and after disuse (p=0.30) compared to L.Rec mice (Fig.3.4a). Upon reambulation, H.Rec mice had 32% larger BV/TV compared to L.Rec mice. The longitudinal decrease in BV/TV was 19% (p<0.001) smaller in H.Rec mice during disuse and upon reambulation BV/TV of H.Rec mice increased 21% while L.Rec mice lost 1% BV/TV (Fig.3.4c). Trabecular PVM for H.Rec mice was 5% (p=0.05) greater in H.Rec than in L.Rec mice at baseline but this difference was reduced to 1% (p=0.80) after disuse and upon reambulation H.Rec mice had 14% (p<0.001) smaller PVM compared to L.Rec mice (Fig.3.4b). Longitudinal change in PVM was 18% (p=0.004) smaller in H.Rec mice during disuse and 6-fold (p<0.001) greater upon reambulation compared to L.Rec mice (Fig.3.4d).

Baseline properties of mice grouped based on recovery

Other trabecular morphology (Table 3.2) at baseline showed H.Rec mice had similar trabecular structure to L.Rec mice indicated by non-significant differences in Conn.D (p=0.07), SMI (p=0.21), Tb.N (p=0.42), Tb.Th (p=0.31). However, H.Rec mice had 12% (p=0.01) smaller BV than L.Rec mice, leading to an 11% (p=0.02) smaller trabecular stiffness. Also H.Rec and L.Rec mice had similar skewness of VM stress distribution

(p=0.36). Parameters that depict cortical bone were 3% (p=0.06) and 7% (p<0.001) smaller for Ct.Ar and Ec.En in H.Rec mice compared to L.Rec mice (Table 3.2).

DISCUSSION

Baseline morphology and micro-mechanical properties were used to determine trabecular response to 3wks of disuse and 3wks of subsequent reambulation in female adult mice belonging to a genetically F2 heterogeneous population. Progenitor strains were selected from two inbred mice (BALB and C3H) based on their distinct response to disuse (high and low mechanosensitivity). Moderate correlations were found between baseline BV/TV and longitudinal (%) BV/TV change during disuse but not reambulation. Also, trabecular peak Von-Mises (PVM) stresses at baseline were neither correlated to changes during disuse nor reambulation. Once mice were stratified based on disuse induced increase in PVM, it was found that high risk (H.Ris) mice had poorer trabecular structure but similar stresses at baseline, and similar changes in PVM upon reambulation compared to low risk (L.Res) mice. Once the mice were stratified based on recovery of disuse induced increase in PVM, high recovery (H.Rec) mice were found to have similar trabecular structure at baseline compared to low recovery mice (L.Rec) but higher PVM stresses. Overall, results indicate that poor bone quality, even though sufficiently protective against high stress levels at baseline, may be a risk factor for disuse induced increase in peak stresses. Further, trabecular structures that experience higher stresses at baseline showed higher recovery of stress levels upon reambulation.

Consistent with the previous evidence, disuse induced changes in trabecular BV/TV were moderately and positively correlated to baseline BV/TV [183]. It implies that having greater trabecular bone mass at baseline may be protective to a degree against tissue losses during disuse. It also corroborates well with the understanding that increased peak bone mass is protective against aging related bone loss in humans [187]. Remaining variability in disuse induced change in BV/TV (~70%) that was not explained by baseline morphology should be largely affected by differences in individual genetic backgrounds [65]. On the other hand, baseline BV/TV was not correlated to changes in BV/TV upon reambulation suggesting a different regulation of these mechanisms. For example, BALB mice, one of the progenitor strains that was used here, is extremely sensitive to disuse [65], however they only show limited response to signals that induce anabolism in trabecular bone [110]. In that sense, perhaps trabecular adaptation to disuse and reambulation are regulated differently as well.

Trabecular BV/TV is strongly coupled with peak stresses experienced within trabecular bone during weight-bearing [166, 188]. However, stress response of trabecular bone to disuse, unlike tissue response, was completely unpredictable in this study by baseline values. Earlier studies showed that the presence of strong associations between baseline BV/TV and micro-mechanical properties may be weakened once the trabecular bone turnover is disturbed as in disuse [153] or during bisphosphanate treatment [189]. In any event, changes in peak stresses during disuse were harder to predict based on the baseline values.

In an attempt to reduce the effect of genetic variability in the population, mice that showed similar stress response to disuse were sub-grouped. Indicators of this differential response at baseline supported the premise that poor bone quality in healthy individuals would make them more susceptible to bone loss [190]. It was surprising however, that both H.Ris and L.Ris mice showed similar PVM at baseline. Perhaps baseline trabecular bone volume (BV) and connectedness (Conn.D) in healthy bones were dominant factors in determination of the stress levels and compensated for differences in other indices of bone quality such as BV/TV, SMI, Tb.Th or Tb.N. Even though adapted to carry similar peak loads and load distributions at baseline while they are healthy, trabecular bone of the H.Ris group showed higher deterioration during disuse and L.Ris mice were unresponsive. Other than the difference in TMD, BV/TV and accompanying parameters depicting the bone quality, no difference was observed at baseline between H.Ris mice and L.Ris mice. This parallels with the evidence that differences in trabecular bone mineral density and morphology across different inbred strains of mice [77, 191] can cause differential response to bone loss induced by either disuse or estrogen deficiency [65, 110, 184]. Different responder sub-populations may be representing a similar scenario here, albeit in a different level (micro-mechanical rather than tissue level). If so, observed differences in baseline becomes indicators of upcoming response rather than the determinants of it. Most probably, those baseline indicators are byproducts of indirect and/or partial contributions of genes that are responsible for mechanosensitivity, or their interactions with genes that are responsible for determining trabecular morphology.

Recovery of bone tissue in bedrest patients and astronauts following disuse is known to be variable and smaller in magnitude compared to amount that was lost during disuse in an equal time frame [148, 182]. However, within the entire F2 population, there was a sub-population of mice with the potential of recovering most of their tissue and micro-mechanical level losses, indicating that it is possible for some organisms to regain their disuse induced losses. Previously it was shown in outbreed rats that, a strenuous jumping exercise that hypothetically induces a high stress environment in trabecular bone may improve recovery of trabecular bone tissue after disuse [149]. Nevertheless, it would be more advantageous for recovery to be facilitated by regular weight-bearing rather than the superposition of a strenuous exercise regimen given the poor quality of trabecular structure that may be more prone to mechanical failure.

If H.Rec mice were still responsive to stress after catabolic stimulus and increased trabecular bone quantity in order to reduce peak stresses, that means perhaps somehow bone cells in H.Rec mice were still responsive to alterations in mechanical environment [2]. This was unexpected given that as disuse deteriorates the morphology, it also reduces the osteogenic potential of bone marrow cells [55, 68]. Since both L.Rec and H.Rec mice are moderately prone to disuse induced deterioration, perhaps the mechanism that regulates tissue recovery is completely different than the mechanism that regulates tissue losses. Complimentary evidence was also found in the sub-groups that were stratified based on stress response during disuse, in which recovery during reambulation was similar between groups.

Contrary to what was observed in the F2 subpopulations based on their stress response to disuse, in the subgroups based on stress response to reambulation had similar trabecular bone micro-architectural parameters at baseline, except trabecular BV. That difference in trabecular bone mass resulted in a stress environment that H.Rec mice carried significantly higher stresses compared to L.Rec mice at baseline. However, it is not entirely clear how more stressed trabecular bones at baseline were to recover disuse induced deterioration more readily. On the other hand, reduced trabecular bone volume and more stressed structure at baseline may be another example of indirect effect of genes that regulate mechanosensitivity on baseline morphology.

A diagnostic criterion based on baseline bone mass may be applicable for detection of an individual's risk of mechanical failure before or in the early stages of non- or reduced-weight bearing (bedrest patients, spaceship crew, etc.). Therefore, customized prophylactic measures can be employed to protect those individuals from deleterious effects of disuse. However, it is not clear what would be the most effective method for protecting those high risk individuals from bone loss. Given that responsiveness to disuse and exercise may be regulated similarly in different genetic strains [110] it may be likely that, individuals at high risk of bone loss may benefit more from exercise regimens superimposed to their daily routines. Unfortunately, such a loading condition on bone may not be practical, since they rely on weight-bearing to begin with. Alternatively, pharmaceutical interventions that retard bone resorption may be beneficial [192], but they are not as efficient in preventing disuse induced bone loss [57] and may cause long-term complications in skeletal matrix [94]. Perhaps molecular

regulation on mechanosensitivity, once elucidated with QTL or microarray studies, will lead to small molecule drugs that can suppress bone mechanosensitivity transiently.

Overall, it was observed that healthy mice with poor bone quality may be compensated for micro-mechanical parameters at baseline. However, those mice with low trabecular bone quality show larger predisposition to increased risk of mechanical failure once subjected to disuse. On the other hand, mice that have less trabecular bone volume that is more stressed at baseline indicated a better recovery of disuse induced deterioration upon reambulation. In any case, data here demonstrated the importance of the tissue phenotype as an indicator on the mechanosensitivity of trabecular bone. Potential combination of the variations in baseline phenotype with the effects from the individual genomes (QTLs) may lead to the identification of individuals that are at greater risk of bone loss or impaired bone recovery.

ACKNOWLEDGEMENTS

Financial support by NASA NAG 9-1499 is gratefully acknowledged.

Tables

Table 3.1. Representative values from bone morphology and trabecular Von-Mises stress distributions at baseline (16wks) from F2 mice that were sub-grouped based on increase in peak VM during disuse as high responsive (H.Ris) or low responsive (L.Ris). *: significant differences between H.Res and L.Res sub-groups ($p<0.05$).

	BV [mm^3]		**Conn.D [1/mm^3]**		**SMI [-]**		**Tb.N [1/mm]**	
	L.Res	H.Res	L.Res	H.Res	L.Res	H.Res	L.Res	H.Res
Mean	**0.38**	**0.36**	**87.6**	**85.7**	**1.47***	**1.64***	**4.47***	**4.25***
SD	0.13	0.14	30.7	34.2	0.73	0.72	0.85	0.82
	Tb.Th [μm]		**TMD [mgHA/ccm]**		**Tb.BS/BV [1/mm]**		**DA [-]**	
	L.Res	H.Res	L.Res	H.Res	L.Res	H.Res	L.Res	H.Res
Mean	**66.6***	**63.8***	**850***	**842***	**34.1***	**35.8***	**1.68**	**1.66**
SD	8.3	7.4	21	23	5.6	5.6	0.10	0.12
	Ct.Ar [mm^2]		**Ec.En [mm^2]**		**Tb. Stiff [N/mm]**		**VM Skewness [-]**	
	L.Res	H.Res	L.Res	H.Res	L.Res	H.Res	L.Res	H.Res
Mean	**1.03**	**1.00**	**1.16***	**1.22***	**2454**	**2313**	**0.53**	**0.53**
SD	0.14	0.12	0.16	0.17	920	916	0.21	0.21

Table 3.2. Representative values from bone morphology and trabecular Von-Mises stress distributions at baseline (16wks) from F2 mice that were sub-grouped based on decrease in peak VM upon reambulation as high recovery (H.Rec) or low recovery (L.Rec).*: significant differences between H.Rec and L.Rec sub-groups ($p<0.05$).

	BV [mm^3]		**Conn.D [1/mm^3]**		**SMI [-]**		**Tb.N [1/mm]**	
	H.Rec	L.Rec	H.Rec	L.Rec	H.Rec	L.Rec	H.Rec	L.Rec
Mean	**0.34***	**0.39***	**84.7**	**92.7**	**1.62**	**1.49**	**4.34**	**4.43**
SD	0.11	0.16	28.3	38.9	0.62	0.83	0.73	0.99
	Tb.Th [µm]		**TMD [mgHA/ccm]**		**Tb.BS/BV [1/mm]**		**DA [-]**	
	H.Rec	L.Rec	H.Rec	L.Rec	H.Rec	L.Rec	H.Rec	L.Rec
Mean	**65.2**	**64.8**	**845**	**842**	**35.1**	**35.1**	**1.66**	**1.66**
SD	7.3	9.0	24	23	5.2	6.4	0.10	0.11
	Ct.Ar [mm^2]		**Ec.En [mm^2]**		**Tb. Stiff [N/mm]**		**VM Skewness [-]**	
	H.Rec	L.Rec	H.Rec	L.Rec	H.Rec	L.Rec	H.Rec	L.Rec
Mean	**0.99**	**1.03**	**1.15***	**1.24***	**2222***	**2499***	**0.56**	**0.53**
SD	0.13	0.14	0.17	0.17	709	1035	0.18	0.23

Figures

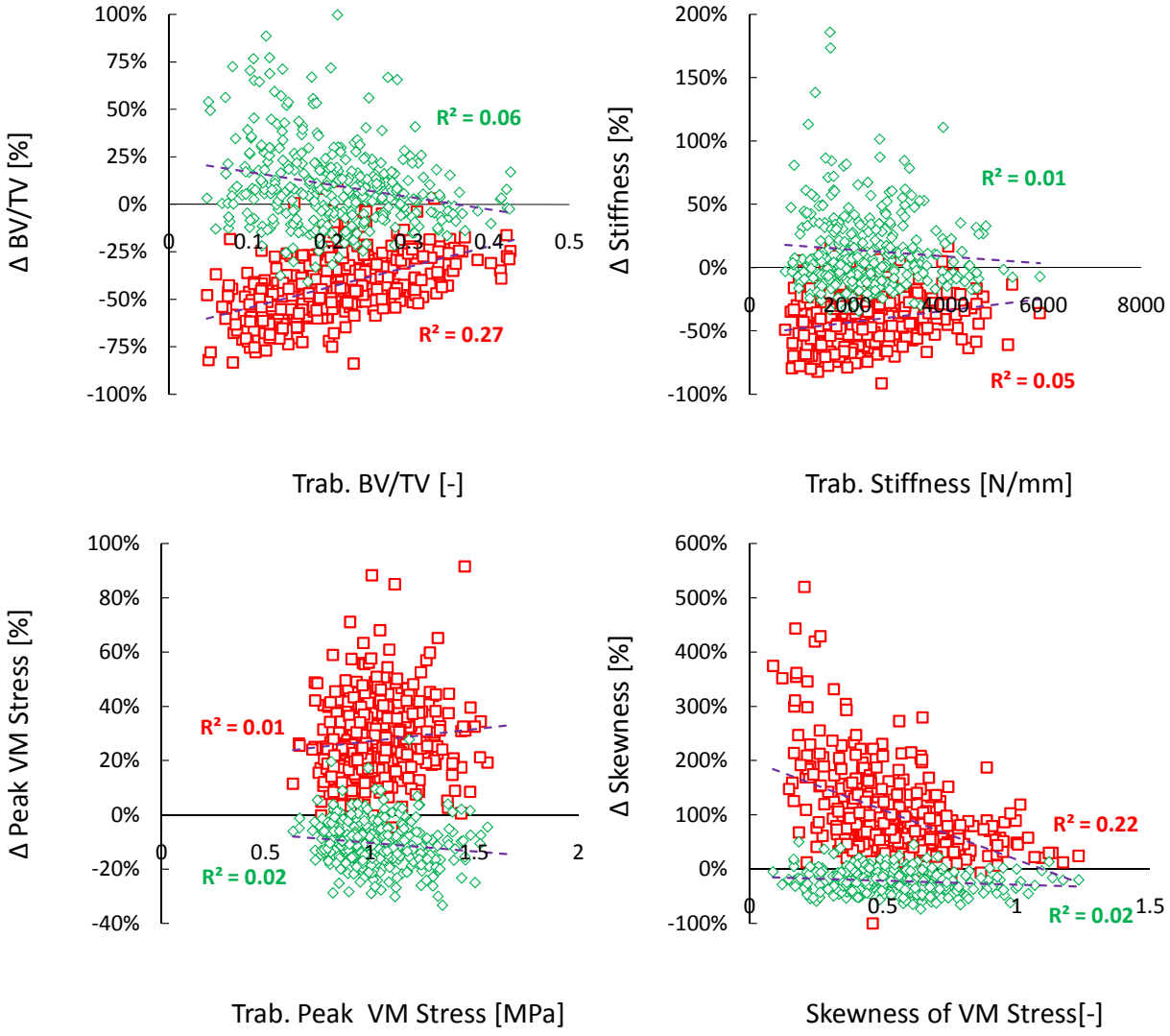

Figure 3.1. Linear regressions of baseline morphological and micro-mechanical properties to disuse (red) or reambulation (green) induced longitudinal changes. **a.** Trabecular bone volume fraction **b.** Trabecular stiffness **c.** Trabecular peak VM stresses, **d.** Skewness of trabecular VM stress distribution.

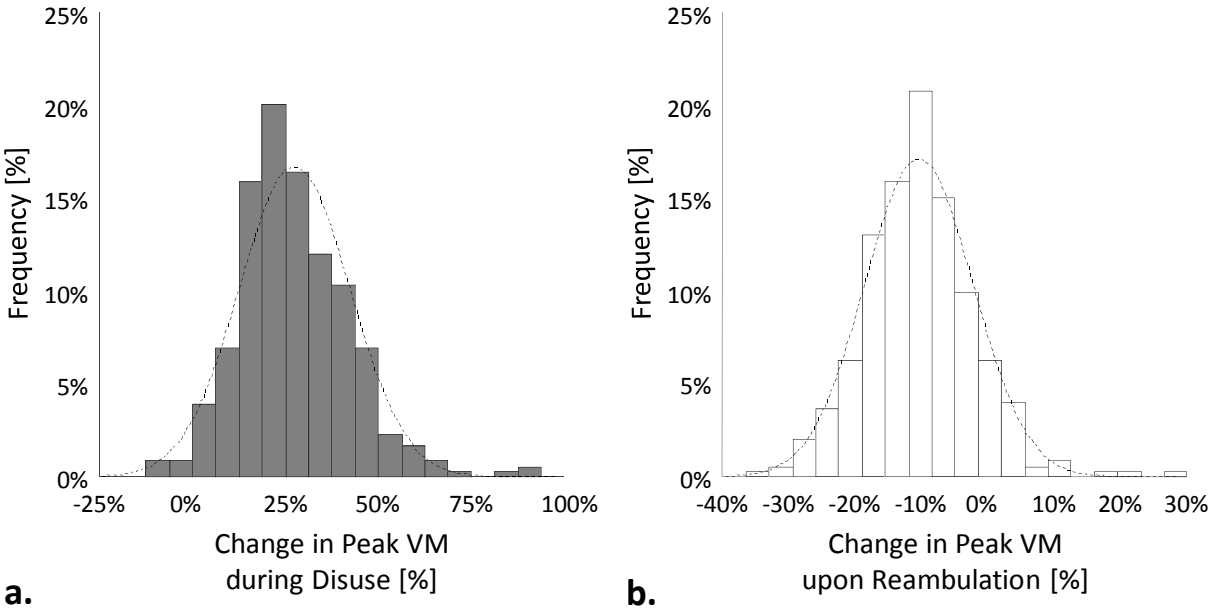

Figure 3.2. Histograms of longitudinal changes in trabecular peak Von-Mises stresses of F2 mice **a)** during disuse; **b)** upon reambulation.

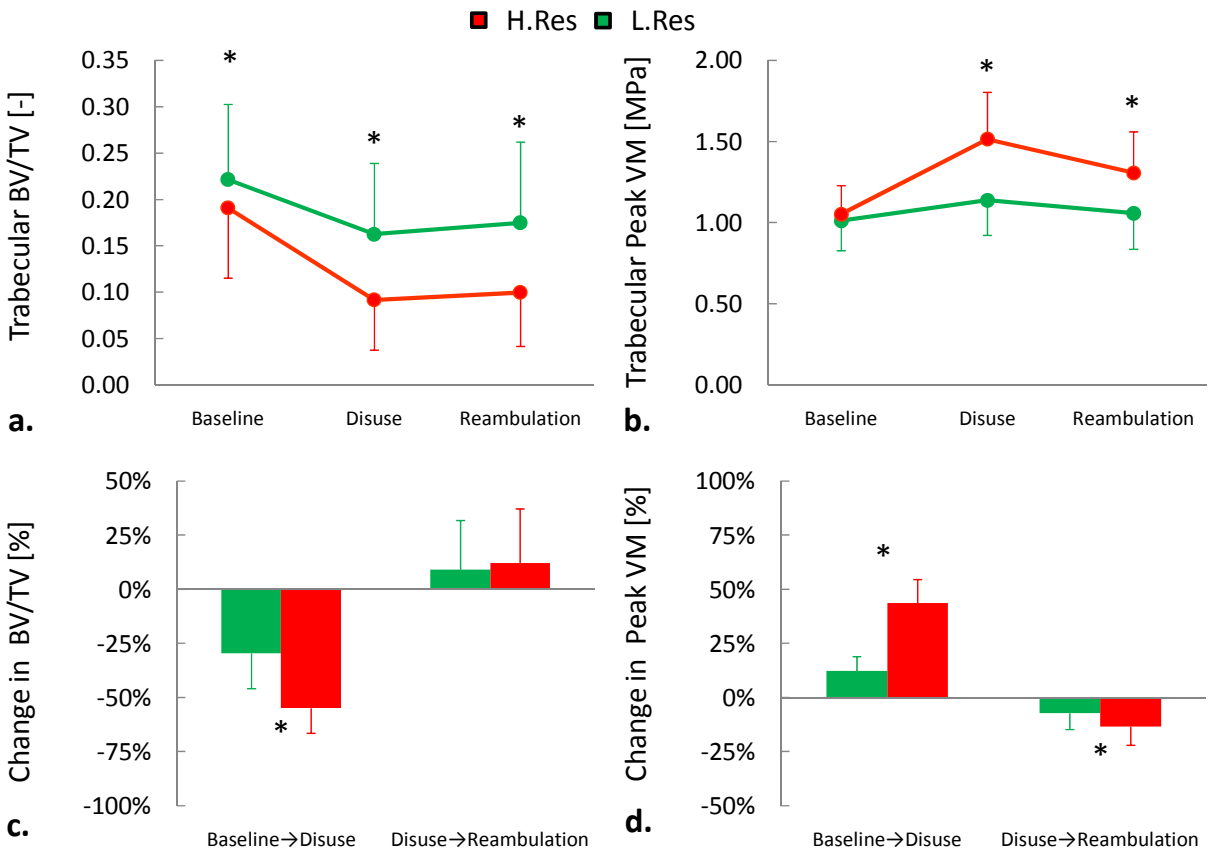

Figure 3.3. Morphology and micro-mechanical properties from F2 mice that were stratified based on increase in peak VM during disuse as high responsive (H.Ris, n=120) and low responsive (L.Ris, n=120) at baseline, disuse and reambulation time points. **a)** Trabecular bone volume fraction (BV/TV); **b)** Trabecular peak VM stresses; **c)** Longitudinal (%) change in BV/TV during disuse and reambulation; **d)** Longitudinal (%) change in peak VM during disuse and reambulation. ***:p<0.05 between H.Ris and L.Ris for a given time point.

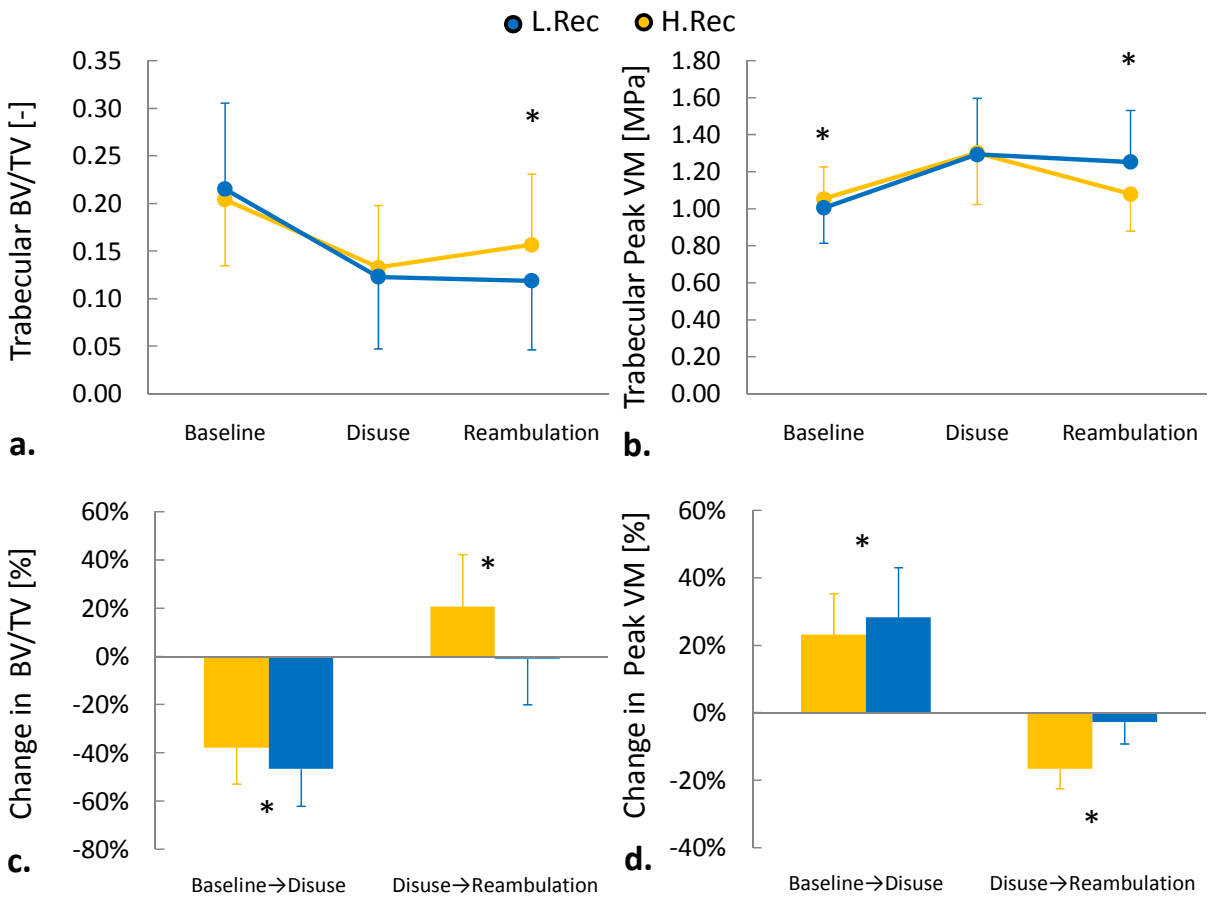

Figure 3.4. Morphology and micro-mechanical properties from F2 mice that were stratified based on changes in peak VM during reambulation as high recovery (H.Rec, n=120) and low recovery (L.Rec, n=120) at baseline, disuse and reambulation time points. **a)** Trabecular bone volume fraction (BV/TV); **b)** Trabecular peak VM stresses; **c)** Longitudinal (%) change in BV/TV during disuse and reambulation; **d)** Longitudinal (%) change in peak VM during disuse and reambulation. ***:p<0.05 between H.Rec and L.Rec for a given time point.

Chapter 4

HIGH FREQUENCY, LOW MAGNITUDE MECHANICAL SIGNALS PROTECT AGAINST A DISUSE INDUCED DECLINE IN BONE MARROW OSTEOROGENITORS AND AUGMENT BONE RECOVERY DURING REAMBULATION

ABSTRACT

Loss of functional weight-bearing will bias bone marrow stromal cells towards adipogenesis, ultimately compromising the regenerative capacity of the stem cell pool and impeding the rapid and full recovery of bone mass and architecture. Here, it was tested whether brief daily exposure to high-frequency, low-magnitude vibrations can stem deterioration of marrow cells during disuse and thereby accelerate the regeneration of tissue upon reambulation. Male C57BL/6J mice were subjected to hindlimb unloading (HLU, n=24), HLU interrupted by weight-bearing for 15min/d (SHAM, n=24), HLU interrupted by low-level, 90Hz whole body vibrations for 15min/d (VIB, n=24), or served as age-matched controls (AC, n=24). Following 3w of disuse, half of the mice in each group were sacrificed. The remaining mice were released for 3w of reambulation (normal cage activity). VIB mice continued to receive the mechanical signal for 15min/d. After disuse, vibrated mice had a 91% greater osteogenic bone marrow stromal cell population, but similar trabecular bone volume fraction compared to disuse controls. After 3w of reambulation, trabecular bone of vibrated mice had a 30% greater bone volume fraction, 98% greater marrow osteoprogenitor population, 83% greater osteoblast surfaces, 59% greater bone formation rates, and a 235% greater ratio of bone lining osteoblasts to marrow adipocytes, than disuse plus reambulation mice. A subsequent experiment demonstrated that receiving the mechanical intervention only during disuse, rather than only during reambulation, was more influential in maintaining tissue viability. These data indicate that the osteogenic potential of bone marrow cells is retained by low magnitude mechanical signals despite

disuse, an attribute which contributed to the rapid restoration of bone mass and morphology on reambulation.

Keywords: bone morphology, disuse, reambulation, stromal cells, osteoblasts, osteogenesis, bone formation, biomechanics

INTRODUCTION

The removal of weight-bearing from the skeleton as a consequence of spaceflight, bedrest, paraplegia, or aging adversely affects the quality and quantity of trabecular bone [30, 36]. Unfortunately, full recovery of skeletal tissues upon reambulation may not be possible [148], increasing the risk of traumatic and atraumatic fractures and, ultimately, compromising quality of life [79]. Failure of the bone structure to recover on reambulation may in part be caused by the collapse of the osteogenic potential of bone marrow cell populations during disuse. Without relevant mechanical signals, mesenchymal stem cells with the potential to become bone cells may instead die or commit to other cell lineages such as adipocytes [55, 56, 193]. As a consequence, a reduced or distracted pool of cells may not be capable to effectively rebuild the intricate skeletal architecture upon the reintroduction of load-bearing regulatory signals [194].

Consistent with the importance of mechanical signals to maintain the osteogenic potential of bone marrow cells, superposition of exogenous mechanical signals onto normal daily activities can enhance bone at the both the cellular and tissue levels [195] with exercise promoting osteoblastogenesis and inhibiting adipogenesis [119, 196]. Despite the various benefits that exercise provides, many exercise-based interventions have been ineffective in stemming tissue deterioration during disuse [30, 197, 198] or to fully recapture bone mass upon reambulation [30].

Exercise typically imposes a limited number of loading cycles at relatively high magnitudes (>1500 microstrain) and low (<10Hz) loading frequencies [199, 200]. Functional daily activities, however, subject the skeleton to a much greater spectrum of loading

magnitudes, frequencies and cycles, including high-frequency signals induced by quasi-isometric muscle activity [16, 201]. As bone is responsive to high-frequency mechanical signals, even if applied at extremely low magnitudes [106, 107], it is conceivable that that these mechanical signal components are critical to the retention of cellular and tissue homeostasis. Consistent with this hypothesis, the decline in trabecular bone formation rates during disuse can be rescued by brief applications of high-frequency mechanical signals induced via whole body vibration, but not by similar periods of normal weight bearing [66]. As these physical signals retain their osteogenic influence even when the mode of application virtually eliminates matrix deformations [112, 153], it is possible that these stimuli are sensed directly by cells within the bone marrow to initiate a cascade of events promoting the population of mesenchymal cells and biasing their differentiation towards osteoblastogenesis.

In the healthy, physically active skeleton, high-frequency, low-magnitude mechanical signals can potentiate bone's anabolic responsiveness by biasing the differentiation and proliferation of mesenchymal stem cells in the marrow towards a musculoskeletal lineage [202]. The criticality of these mechanical signals in preserving the viability of stromal cells in the bone marrow environment during disuse is unknown. Here, we tested if brief, daily exposure to high-frequency, low magnitude mechanical signals during disuse can inhibit the decline in the number of osteoprogenitor cells, and thus enhance recovery of bone tissue upon reambulation. In the second phase of this study, it was investigated whether trabecular bone recovery during reambulation can be

augmented more effectively by applying mechanical signals during disuse or during reambulation.

MATERIALS AND METHODS

Experimental design

All procedures were reviewed and approved by the Institutional Animal Care and Use Committee (IACUC). Seven-week old male C57BL/6J (B6) mice were used for all phases of the study (n=108 total), an age at which trabecular bone mass peaks in this specific inbred mouse strain [203]. Three groups of mice (n=24 each) were subjected to hindlimb unloading (HLU) for 3w, depriving the hindlimbs of gravitational loading for the entire period. In VIB mice, HLU was interrupted for 15min/d, 7d/w by the application of high-frequency (90Hz), low-magnitude (0.2g, where 1g = earth's gravitational field = 9.8m/s^2) whole body vibrations. During this 15min period, mice were allowed to roam freely on the vertically oscillating plate. SHAM mice were treated identically to VIB mice except that the vibrating plate on which they ambulated for 15min/d was inactive. A group of age-matched controls (AC, n=24) were individually housed in normal cages for the duration of the study.

At the end of 3w, half of the mice from each group (n=12/group) were euthanized, and the remaining mice (n=12/group) were placed in standard mouse cages and allowed full, free ambulation. During the 3w of reambulation, VIB and SHAM groups continued to receive the daily vibratory or sham loading. Body mass of all mice was monitored daily for the duration of the experiment. Mice were injected with calcein

(15mg/kg, i.p.) 12 and 2 days prior to sacrifice. After overnight fasting, mice were sacrificed and serum was collected by cardiac puncture. Left tibiae were stored in 10% formalin for micro-computed tomography (μCT) and histomorphometry. Right tibiae and femurs were stored in cold DPBS for flow cytometry.

In an attempt to identify whether application of the low-magnitude mechanical signals were more influential during the disuse or reambulation period, two additional groups of male C57BL/6J mice were subjected to 3w of hind-limb unloading followed by 3w of reambulation. In VIB-D mice (n=6), the daily vibratory stimulus described above was applied only during disuse but not during reambulation. VIB-R mice received the mechanical intervention only during reambulation, but not during disuse. Tibiae of mice in these two groups were μCT-scanned *in vivo* at baseline, after the 3w of disuse period and after the 3w reambulation period.

Micro Computed Tomography

Extracted tibiae were fixed in 10% formalin at 4°C [112] and transferred to a 70% ethanol solution in which they were scanned by μCT at a 12μm isotropic resolution (MicroCT40, Scanco AG, Switzerland). *In vivo* scans of phase II mice were acquired at the same resolution (VivaCT40, Scanco AG). For both ex-vivo and in-vivo scans, the metaphysis was defined as a 600μm long region extending from the proximal tibial-fibular junction. Trabecular bone was separated from the surrounding cortex by an automated algorithm [155]. Indices of trabecular bone morphology and density – bone volume (Tb.BV), bone volume fraction (BV/TV), connectedness (Conn.D), thickness (Tb.Th), number (Tb.N),

tissue mineral density (Tb.TMD) – and of the surrounding cortical bone – area (Ct.Ar), endocortical envelope area (Ec.En) – were quantified for each bone.

Histomorphometry

After μCT scanning, tibiae were dehydrated and embedded in PMMA. Coronal, 4 μm thick sections (8 per bone) of the proximal tibia were cut (n=3/6 bones per 3w/6w groups). Two non-consecutive slices were analyzed for dynamic indices of bone formation, including mineralizing surface (MS/BS), mineral apposition rate (MAR), and bone formation rate (BFR/BS). The remaining slices were decalcified and either stained with 1% toluidine blue (TB, 2 per bone) to determine osteoblast number (N.Ob) and surface (Ob.S), or stained for tartrate resistant acid phosphatase (TRAP, 2 per bone) activity to quantify osteoclast surface (Oc.S). All the measurements were performed using Osteomeasure software (Osteomeasure, OsteoMetrics Inc., Atlanta, GA). Furthermore, adipocyte number (N.Adi) and surface (Adi.S) embedded in the marrow of the region of interest were measured based on the easily identifiable size and geometry of fat droplets without any specific stain [204].

Flow Cytometry

Flow cytometry measurements were acquired as detailed elsewhere [202]. Briefly, bone marrow was flushed from the right tibia and femur, strained in cold PBS and subjected to 1% Pharmlyse (BD Bioscience, San Diego, CA) to remove red blood cell contamination. Cells were then immediately were stained with PE conjugated Sca-1 and FITC conjugated CD90.2 antigens (BD Bioscience) to detect marrow cell populations with osteogenic potential [205, 206]. Flow cytometry (FACScan, Becton Dickinson, San Jose, CA) counted the

stained cells and quantified their size (forward scatter or FSC) and granularity (side scatter or SSC). Cells were stratified based on their FSC and SSC into separate regions, including small and less mature cells (R2) and large and granulated cells (R3). Proportions of Sca-1 and CD90.2 positive cells to total marrow cells were reported for any given region (n=6 per group and time point).

ELISA

Collected blood volumes were centrifuged (4°C, 5000rpm, 10 minutes) and serum was separated from blood cells. ELISA kits were used to measure serum concentrations of osteocalcin (Biomedical Technologies, Stoughton, MA) and osteopontin (R&D Systems, Minneapolis, MN) were evaluated in serum (n=6 per group and per time point).

Statistics

All data were presented as mean ± SD. Paired t-tests were used to compare the longitudinal changes in body mass within each group. Group means of cross-sectional data were compared by ANOVA and, if significant, a SNK post-hoc test was applied. Analyses were performed with and without adjusting for differences in body mass as a covariate. Statistical significance was set at 5% and p-values between 5% and 10% were presented to indicate statistical trends.

RESULTS

Longitudinal changes in body mass

During the first 3w, body mass of AC mice increased continuously, while the body mass of the other three groups of mice (HLU, SHAM and VIB) increased following a 1w delay.

At the end of the first 3w experimental phase, AC, HLU, SHAM and VIB mice had increased their body mass by 15%, 4%, 5% and 5% (all $p<0.001$) compared to baseline (Fig.4.1). During reambulation, all groups continued to gain body mass, with HLU mice showing the greatest increase resulting in a significantly greater body mass of HLU mice (5-6%, $p<0.05$) than of VIB mice during the last 2w of the reambulation period (Fig 4.1). At the end of reambulation, AC, HLU, SHAM and VIB mice had increased body mass 23%, 21%, 16% and 15% (all $p<0.001$) compared to baseline (Fig.4.1). Body mass at the end of 3w and 6w periods was used as a covariate for the analysis of group contrasts, but post-hoc contrasts did not deviate from the original outcome, hence the presentation of adjusted means are not discussed.

Bone morphology after disuse and reambulation

After 3w of disuse, mice that received the vibratory stimulus (VIB) had an 18% ($p=0.08$) greater trabecular BV/TV than mice that were unloaded (HLU), a difference similar to the 24% difference ($p=0.06$) between SHAM and HLU groups (Fig.4.2). All disuse groups (HLU, SHAM and VIB) had smaller (-55%, -45% and -47%, all $p<0.001$) BV/TV compared to age-matched controls (AC). The group differences in BV/TV were accompanied by similar differences in other micro-architectural parameters (Table 4.1). Tissue mineral density (Tb.TMD) of trabecular bone was similar between all groups.

Mice that received the mechanical stimulus during the 3w disuse and 3w reambulation period, had 22% ($p=0.003$) and 30% ($p=0.01$) greater BV/TV than HLU and SHAM groups at the end of the reambulation phase. However, the vibratory stimulus failed to fully restore trabecular bone within the 3w reloading period, as indicated by

the 20% difference ($p<0.001$) in BV/TV between VIB and AC mice (Fig.4.2). Parameters describing trabecular architecture displayed group differences that were similar to those reported for BV/TV except Tb.Th which, upon reambulation, fully recovered in all disuse groups (Table 4.1). At the end of the reambulation period, trabecular bone of the disuse groups had a greater tissue density than that of age-matched controls, a difference that reached 5% in HLU and SHAM mice and 3% VIB mice (all $p<0.001$).

Trabecular bone formation and resorption

Compared to toluidine blue stained sections of age matched controls, disuse without intervention reduced Ob.S/BS and N.Ob/BS in trabecular bone by 67% and 73% ($p<0.001$) (Fig.4.3, Table 4.2). Disuse combined with 15min/d of normal activities (SHAM) caused 75% greater Ob.S/BS and 136% greater N.Ob/BS ($p=0.01$ and $p=0.02$) as compared to HLU mice. Compared to HLU, VIB mice also showed 83% greater Ob.S/BS and 156% greater N.Ob/BS (83%, $p=0.02$ and 156%, $p=0.03$). Differences in dynamic indexes of bone formation were evident between AC and DIS mice even though only the 50% difference in MAR ($p=0.03$) was significant. Values of SHAM and VIB mice were not significantly different from AC and HLU mice (Fig.4.3).

As compared to AC, disuse followed by 3w of ambulation resulted in HLU mice with 34% smaller Ob.S/BS ($p<0.001$) and 31% smaller N.Ob/BS ($p=0.07$; Fig. 4.3, Table 4.2). There were no significant differences in Ob.S/BS and N.Ob/BS between SHAM and HLU mice (Fig.4.3, Table 4.2). In contrast, VIB mice had 83% greater Ob.S/BS and 62% greater N.Ob/BS (83%, $p<0.001$ and 62%, $p=0.02$) than HLU mice. Compared to AC mice, VIB mice allowed to reambulate had 21% ($p=0.01$) greater Ob.S/BS but not a greater

N.Ob/BS. After 3w of reambulation, smaller MS/BS (33%, p<0.001) and BFR/BS (24%, p=0.08) were found in HLU mice compared to AC (Fig.4.3, Table 4.2). On the other hand, VIB mice showed 59% (p<0.01) greater MS/BS and BFR/BS than HLU mice with reambulation (Fig.4.3, Table 4.2). Bone resorption, as measured by osteoclast surface relative to trabecular bone surface (Oc.S/BS) did not show any significant difference between groups after disuse (Table 4.2) nor disuse plus reambulation (Table 4.2).

Number of bone lining osteoblasts and adipocytes

After the disuse phase, the total number of bone lining osteoblasts (N.Ob) was 80%, 69% and 64% (all p<0.001) smaller in HLU, SHAM and VIB mice than in AC mice (Fig.4.4). However, VIB had 74% (p=0.03) greater N.Ob compared to HLU mice (Fig.4.4). After reambulation, N.Ob in AC mice was 63% (p=0.003) and 55% (p=0.003) greater than HLU and SHAM, but 15% (p=0.08) smaller than VIB mice (Fig.4.4)

After the disuse phase, the total number of bone lining osteoblasts (N.Ob) was 80%, 69% and 64% (all p<0.001) smaller in HLU, SHAM and VIB mice than in AC mice (Fig.4.4). However, VIB had 74% (p=0.03) greater N.Ob compared to HLU mice (Fig.4.4). After reambulation, N.Ob in AC mice was 63% (p=0.003) and 55% (p=0.003) greater than HLU and SHAM, but 15% (p=0.08) smaller than VIB mice (Fig.4.4)

After 3w, the number of adipocytes (N.Adi) was 102% greater in the pooled disuse groups than in AC mice (p=0.01) but individual groups were not significantly different from each other (Fig.4) except SHAM controls in which N.Adi was significantly greater than in the other groups. Upon reambulation, there were no significant differences in N.Adi (Fig.4.4). For the proportion of osteoblasts to adipocytes

(N.Ob/N.Adi), HLU, SHAM and VIB levels were 89% (p=0.002), 89% (p=0.004) and 66% (p=0.005) smaller than those in AC mice (Fig.4.4). Upon reambulation, N.Ob/N.Adi was 235% (p=0.04) greater in VIB than in HLU (Fig.4.4).

Osteogenic marrow cells

Flow cytometry measurements were assessed based on the scatter profile of total marrow cells (Fig.4.5). For regions R2 and R3, cells that showed positive SCA-1 and CD90.2 expression were calculated as a fraction of total events (Fig.4.5). The quantification of bone marrow stromal cells that were extracted after disuse showed that the total number of stem cells of mesenchymal origin (SCA-1+, CD90.2+, small and non-granulated cells), was 46% (p=0.04), 91% (p=0.002) and 41% (p=0.03) greater in VIB mice than in AC, HLU and SHAM mice, respectively (Fig.4.5). Also, HLU mice showed a 23% (p=0.04) diminished marrow osteoprogenitor population (SCA-1+, CD90.2+, large and granulated cells) compared to AC mice (Fig.4.5). Unloaded mice that were subjected to 15min/d, of ambulation or ambulation plus vibration (SHAM and VIB), had 43% (p=0.01) and 23% (p=0.07) greater osteoprogenitor populations than HLU mice.

With disuse followed by 3w of ambulation, the vibration group had a (non-significant) greater proportion of stem cells to the total number of marrow cells than the AC, SHAM and HLU groups (4%, 27% and 45%, respectively; Fig.4.5). With reambulation, the number of osteoprogenitor cells was 2-fold greater in the vibration group than in the HLU and SHAM groups ($p<0.01$) and not significantly different from AC mice (Fig.4.5).

Systemic factors of bone metabolism

Serum concentration of osteocalcin, a marker of bone formation, was smaller in HLU, SHAM and VIB mice than in AC mice (44%, 60% and 54%, all $p<0.001$) after disuse (Table 4.2). No significant differences were detected between groups in osteocalcin levels upon reambulation (Table 4.2). Osteopontin concentration, a marker of bone turnover was 68% ($p=0.04$) and 73% ($p=0.04$) greater in SHAM and VIB mice than in AC mice with no significant differences between VIB and AC mice (Table 4.2). Upon reambulation, similar to osteocalcin, osteopontin levels did not show any significant differences between groups (Table 4.2).

Comparing the influence of vibration during disuse versus recovery

In a follow-on study, to determine the relative contributions of the vibratory stimulus to bone morphology during disuse vs. reambulation, vibrations were applied *only* during the 3w disuse period (VIB-D), or *only* during the 3w reambulation period (VIB-R). Morphological evaluations were performed longitudinally at 3w and 6w. Compared to mice that received vibrations only during reambulation (VIB-R), mice that had received vibrations only during disuse (VIB-D) had similar Ec.En, BV and BV/TV at baseline and after disuse (Fig.4.6). Upon 3w of reambulation, VIB-D mice had 9% greater ($p=0.03$) Ec.En, 30% ($p=0.04$) greater trabecular bone volume, and 19% ($p=0.09$) greater BV/TV than VIB-R mice (Fig.4.6).

DISCUSSION

The ability of high-frequency, low-magnitude mechanical signals to protect and augment indices of bone cell and tissue quantity and quality was investigated during disuse and

reambulation. Disuse for 3w significantly eroded trabecular bone morphology in the proximal tibia, and neither 15min/d of weight-bearing nor the application of the low-magnitude mechanical signals were able to prevent this loss. In contrast to the lack of a response at the level of the tissue, mice subjected to the mechanical loading during disuse preserved, at least in part, their bone marrow based osteoprogenitor cells, as well as promote the relative number of uncommitted stem cells.

Following the disuse period with three weeks of reambulation, the enhanced population of osteoprogenitor cells in the bone marrow of the mechanically stimulated mice coincided with a greater degree of recovery of trabecular bone in the tibia. Supporting the hypothesis that the ability of bone to recover will correlate to the status of the bone marrow cell population, subsequent experiments indicated that reestablishment of bone morphology upon reambulation was best defined by the mechanical protection of the progenitor pool during disuse; mechanical stimulation introduced at reambulation failed to restore bone morphology. Combined, these data indicate that the application of high-frequency, low-magnitude mechanical signals during disuse provides a long-term benefit towards the ultimate recovery of the musculoskeletal system, a critical achievement despite their inability to retain bone tissue challenged with disuse.

As apparent from the minimal changes which occurred in the tibia over the course of the protocol in the age-matched controls, the male C57BL/6J mice used in this study had reached peak trabecular bone mass. While the lack of regional *trabecular* bone growth eliminated the effect of growth as a potentially confounding factor [203],

mice were still adding body mass and cortical bone. Hence, extrapolations to a primarily quiescent skeleton can only be made with great care. Further, the interpretation of results from flow cytometry measurements was based on only two surface markers expressed by stem cells, and as such this population is enriched and not exclusive for MSCs. For instance, Sca-1 is known to be a marker of hematopoietic and mesenchymal stem cells. As in previous studies, bone marrow cells positive for Sca-1 and CD90.2 expression were presumed to be osteogenic stem cells, and their size and granularity served as an estimate for their degree of commitment and maturity towards osteogenesis [205, 206]. Nevertheless, flow cytometry data should be considered preliminary and eventually confirmed by bone marrow cells cultures.

In addition to the crippling of the stem cell population, disuse reduced the quantity of surface osteoblasts, mineralizing surfaces and mineral apposition rates. This suppression of bone formation, in conjunction with unperturbed osteoclast activity, conspired towards an overall net loss of bone [55, 207, 208]. Simultaneously, the number of fat cells within the bone marrow increased with disuse, suggesting that the absence of mechanical loading is permissive towards marrow stem cells differentiating along adipogenesis pathways, and ultimately compromising their ability to recover the bone phenotype [56]. Interrupting disuse by 15 minutes of weight-bearing activities contributed to the preservation of the marrow osteoprogenitors, as well as promoted osteoblast activity. That brief ambulatory periods proved insufficient to attenuate the bone loss is consistent with the failure of weight-bearing [66] or rigorous exercise [30, 209] to stem the

osteopenia caused by extended bedrest or weightlessness, and further indicates the dominant nature of disuse in suppressing any, if not all, anabolic actions in bone.

During disuse, a daily superposition of low-magnitude vibrations upon the 15 minutes of weight-bearing stimulated protected the cellular status such that they remained similar to those measured in the weight-bearing control cohort. Importantly, these low-magnitude mechanical signals also increased the uncommitted stem cell pool in the marrow, and protected the proportion of bone cells to fat cells within bone marrow, avoiding the bias towards adipogenesis. This result is similar to the benefits of low-level, high-frequency signals measured in the marrow stem cell population of normally ambulating mice, in which these signals preferentially drove mesenchymal stem cell differentiation toward osteogenesis and away from adipogenesis [202], ultimately increasing bone mass while suppressing adiposity [210, 211].

The importance of protecting the regenerative potential of the bone marrow cell population during the challenge of disuse becomes most clear upon reambulation. Similar to humans recovering from spaceflight [181], chronic debilitating injury [212] or bedrest [36], disuse and sham control mice showed only hampered recovery of trabecular bone morphology upon reambulation, a consequence of non-weight bearing that we conclude is directly associated with the compromised osteoprogenitor pool. Cultured bone marrow cells from rats subject to disuse and then allowed to ambulate showed that the inability to reestablish bone formation rates was defined by impaired osteoblast recruitment [194]. Here, we support the conclusion that disuse causes a suppressed osteoprogenitor cell population, as well as a diminution of osteoblast

recruitment during reambulation. Superimposing the mechanical signal upon 15min/d of habitual loading activities prior to full reambulation protected from this cellular impairment by increasing both the osteoprogenitor populations and mature osteoblasts, such that when weight-bearing was restored, the animals were able to quickly increase mineralization, bone formation rates, and bone tissue quality and quantity. These data suggest that protecting the osteogenic potential of bone marrow cells from the devastation of disuse is critical for tissue recovery. In support of this hypothesis, restricting the application of the mechanical signal to the reambulation period failed to enhance trabecular recovery, while applying the vibration signal only during disuse gave rise to increased trabecular bone mass during reambulation. While pharmaceutical interventions may or may not serve to preserve bone structure during disuse [57, 192, 213], if the osteoprogenitor pool collapses, the ability to regenerate bone may ultimately fail. Whether there is a balance between pharmaceutical preservation of bone structure, and physical protection of the osteoprogenitor pool, has yet to be determined.

The reambulation period in this study was relatively short and at its completion, trabecular bone quantity of the mechanically stimulated mice was still lower compared to age-matched controls. However, greater indices of bone formation in the mechanically stimulated mice suggest a persistent regeneration, a trend towards full recover that was seen in neither disuse nor sham control mice. This greater potential for restoration of bone quantity and quality is supported by the shift in the preference of bone marrow stem cells towards osteoblastogenesis over adipogenesis [202]. In support of this conclusion, those mice that did not receive any mechanical signals during disuse

showed a disproportional increase in body mass during reambulation. While this may indicate that brief periods of either weight bearing or low magnitude mechanical signals during disuse decreased the likelihood of stem cells to steer towards adipogenesis, the combination of increased body mass and decreased bone quantity/quality would inevitably compound the risk of fracture in bone [214].

In summary, brief daily periods of mechanical signals delivered at high frequency and extremely low-magnitudes did not prevent the deterioration in bone morphology caused by disuse, yet significantly improved the osteogenic potential of bone marrow cells, the population ultimately responsible for recovery of bone structure. It appears that the augmented regenerative response of trabecular bone during reambulation in the mechanically stimulated mice resulted from a more viable, osteogenic stem cell population, as these mechanical signals, by themselves, did not enhance trabecular bone recovery during reambulation. If it is true that preserving or increasing the osteogenic potential of bone marrow cells is critical for bone regeneration, one could speculate that the mechanical signal could also serve as prophylactic treatment which, if applied during periods of disuse (e.g., space flight, bedrest, immobilization), could serve to accelerate recovery upon restoration of weight bearing.

ACKNOWLEDGEMENTS

This research was kindly funded by NASA and NIAMS. Expert technical help from Benjamin Adler, Svetlana Lublinsky and Adiba M. Ali was greatly appreciated.

TABLES

TABLE 4.1. Trabecular and cortical bone morphology at the tibial proximal metaphysis in age-matched controls (AC), disuse controls (HLU), sham controls (SHAM) and vibrated mice (VIB) after the 3w disuse period as well as at the end of the 6w disuse and remabulation period.

		AC	HLU	SHAM	VIB
3W	**Tb.BV[mm^3]**	0.14±0.03^{a}	0.05±0.01^{b}	0.07±0.01^{b}	0.06±0.01^{b}
	Conn.D[1/mm^3]	120±41^{a}	14±11^{b}	29±16^{b}	23±12^{b}
	Tb.N[1/mm]	6.08±0.35^{a}	4.58±0.44^{b}	4.79±0.37^{b}	4.80±0.20^{b}
	Tb.Th[µm]	36.7±1.3^{a}	33.9±2.7^{b}	34.9±2.2^{b}	34.9±1.8^{a,b}
	Tb.TMD[mgHA/ccm]	793±26	798±23	803±17	808±19
	Ct.Ar[mm^2]	0.59±0.07^{a}	0.51±0.04^{b}	0.54±0.04^{b}	0.53±0.04^{b}
	Ec.En[mm^2]	1.75±0.15^{a}	1.50±0.12^{b}	1.55±0.11^{b}	1.56±0.08^{b}
6W	**Tb.BV[mm^3]**	0.12±0.02^{a}	0.07±0.02^{b}	0.08±0.02^{b}	0.10±0.02^{c}
	Conn.D[1/mm^3]	109±25^{a}	30±14^{b}	35±20^{b}	56±20^{c}
	Tb.N[1/mm]	5.73±0.25^{a}	4.54±0.39^{b}	4.70±0.53^{b}	5.03±0.36^{c}
	Tb.Th[µm]	39.0±3.0	39.5±2.5	39.3±2.9	40.2±3.3
	Tb.TMD[mgHA/ccm]	795±12^{a}	838±17^{b}	835±13^{b}	822±17^{c}
	Ct.Ar[mm^2]	0.66±0.06^{a}	0.61±0.07^{a,b}	0.62±0.05^{a,b}	0.62±0.06^{b}
	Ec.En[mm^2]	1.52±0.12^{a,b}	1.47±0.10^{a}	1.45±0.13^{a}	1.60±0.14^{b}

Data are mean ± sd. Difference in letters denominate significant ($p<0.05$) differences between groups (ANOVA and SNK).

TABLE 2. Indices of bone formation, marrow adipocity, and bone resorption measured in the proximal tibia or the serum in age-matched controls (AC), disuse controls (HLU), sham controls (SHAM) and vibrated mice (VIB) after the 3w disuse period as well as at the end of the 6w disuse and remabulation period.

		AC	HLU	SHAM	VIB
3W	**N.Ob/BS[1/mm]**	61.64±3.03^{a}	16.48±1.90^{b}	38.88±18.74^{c}	42.27±4.30^{c}
	MAR[µm/d]	1.57±0.06^{a}	0.78±0.13^{b}	0.97±0.42^{b}	1.07±0.29^{b}
	BFR/BS[µm^3/ µm^2/d]	0.29±0.10	0.10±0.05	0.25±0.17	0.27±0.11
	N.Adi/BS[1/mm]	4.99±1.64^{a}	15.09±4.87^{a}	28.34±14.68^{b}	11.64±6.80^{a}
	Oc.S/BS[%]	14.31±1.56	15.13±1.58	13.79±0.93	11.50±3.73
	Serum OC[ng/ml]	36±5^{a}	20±7^{b}	14±4^{b}	16±4^{b}
	Serum OPN[ng/ml]	216±73^{a}	276±54^{a,b}	364±110^{b}	373±131^{b}
6W	**N.Ob/BS[1/mm]**	57.00±18.47^{a,b}	39.28±8.15^{b,c}	40.27±6.13^{c}	63.81±9.26^{a}
	MAR[µm/d]	1.26±0.13	1.44±0.23	1.16±0.18	1.45±0.18
	BFR/BS[µm^3/ µm^2/d]	0.28±0.06^{a}	0.21±0.04^{b}	0.19±0.06^{b}	0.34±0.06^{a}
	N.Adi/BS[1/mm]	6.56±2.28^{a}	17.41±9.62^{b}	12.61±6.93^{a,b}	5.86±2.24^{a}
	Oc.S/BS[%]	11.59±1.66	12.19±1.27	11.36±1.46	10.20±3.28
	Serum OC[ng/ml]	21±10	20±11	15±5	18±4
	Serum OPN[ng/ml]	219±51	233±123	303±86	186±68

Data are mean ± sd. Difference in letters denominate significant ($p<0.05$) differences between groups (ANOVA and SNK).

FIGURES

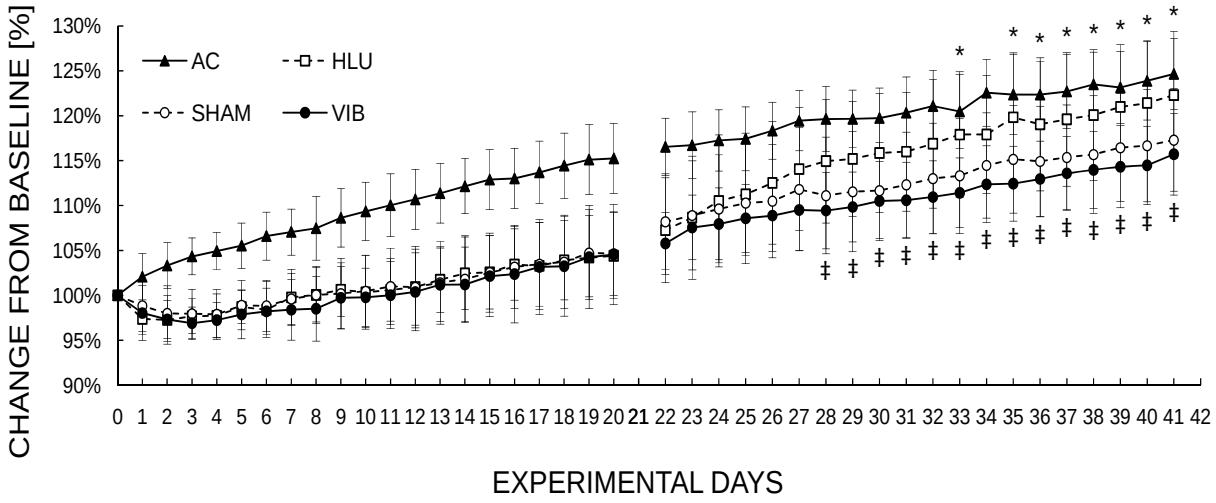

Figure 4.1. Longitudinal changes in body mass relative to baseline values during the experiment of age-matched controls (AC, solid triangles), hindlimb unloaded (HLU, empty squares), sham loaded (SHAM, empty circles) and vibrated mice (VIB, solid circles). For all disuse groups, the first 21 days mark hindlimb unloading while the last 21 days mark reambulation. ‡: $p<0.05$ between VIB and HLU mice. *: $p>0.05$ between AC and HLU mice (ANOVA and SNK).

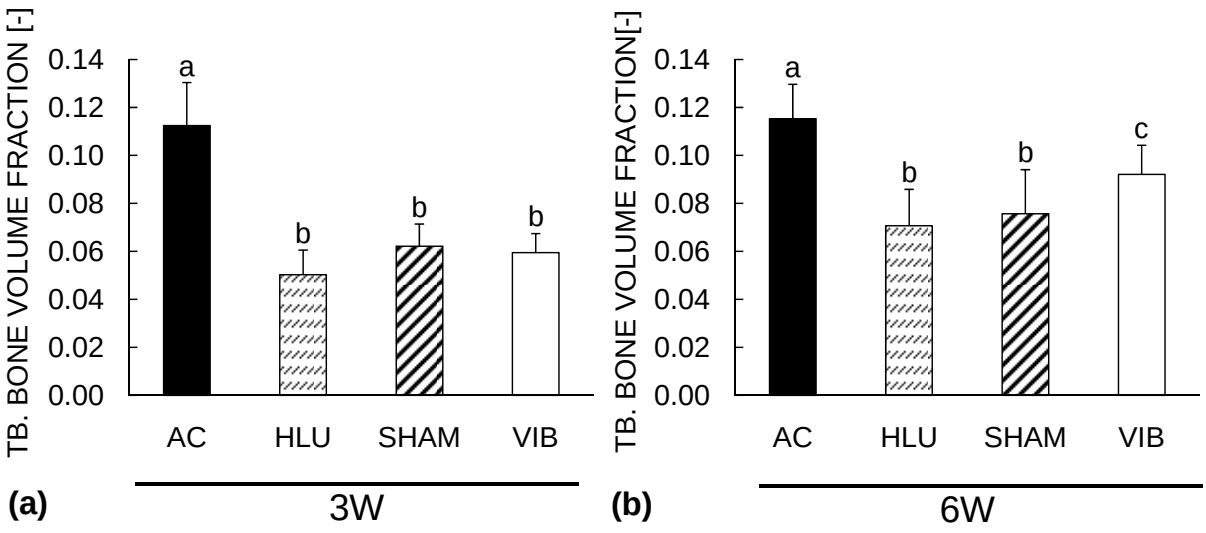

Figure 4.2. Trabecular bone volume fraction in the metaphysis of the proximal tibia of age-matched controls (AC), hindlimb unloaded (HLU), sham loaded (SHAM) and vibrated mice (VIB); **(a)** after 3w of disuse and **(b)** after 3w of disuse followed by 3w of reambulation. Difference in letters denominate significant ($p<0.05$) differences between groups (ANOVA and SNK).

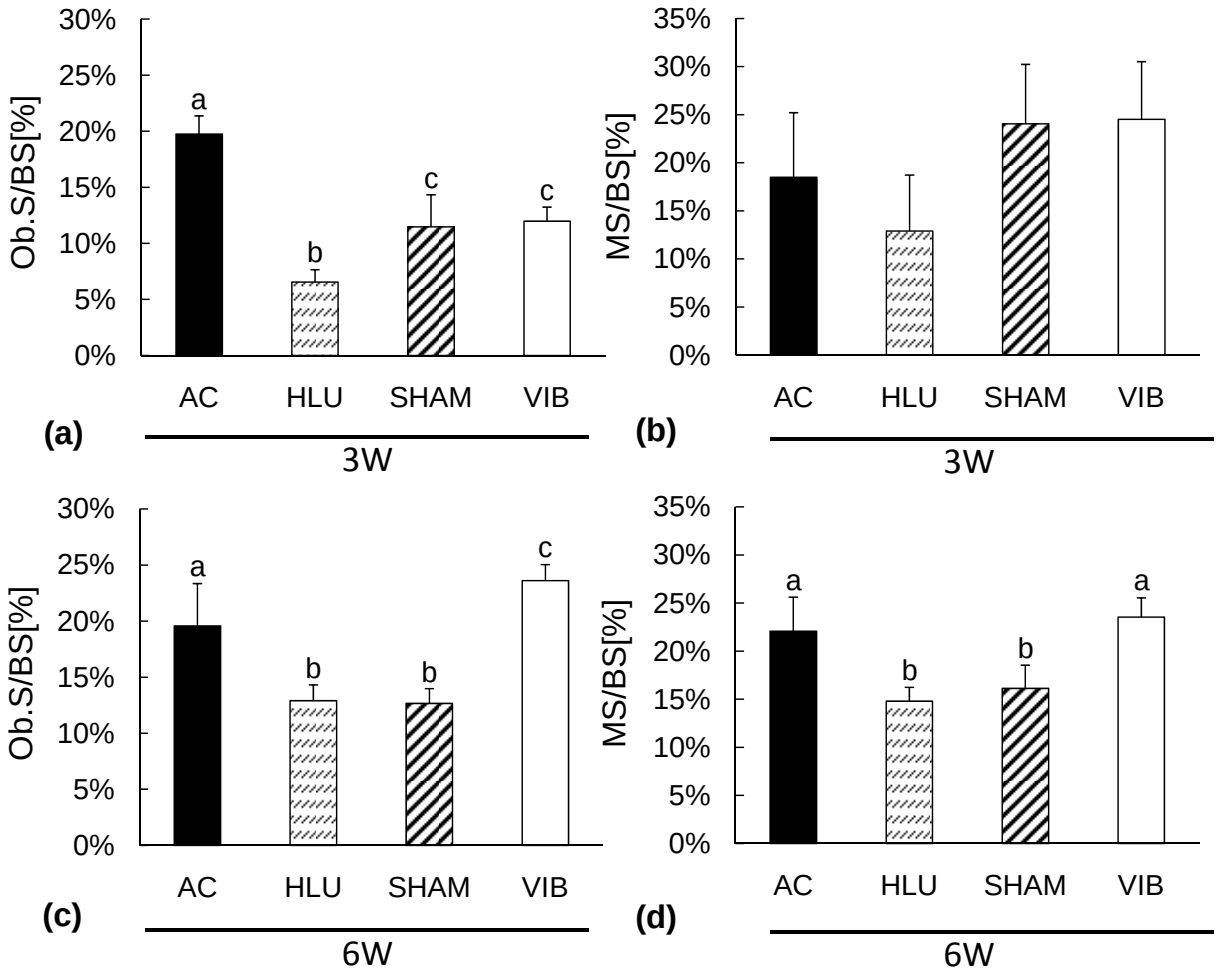

Figure 4.3. Bone lining osteoblasts and mineralizing surfaces in metaphyseal trabecular bone surfaces of age-matched controls (AC), hindlimb unloaded (HLU), sham loaded (SHAM) and vibrated mice (VIB) **(a,b)** after the initial 3w phase or **(c,d)** at completion of the 6w of experimental phase. Difference in letters denominate significant ($p<0.05$) differences between groups (ANOVA and SNK).

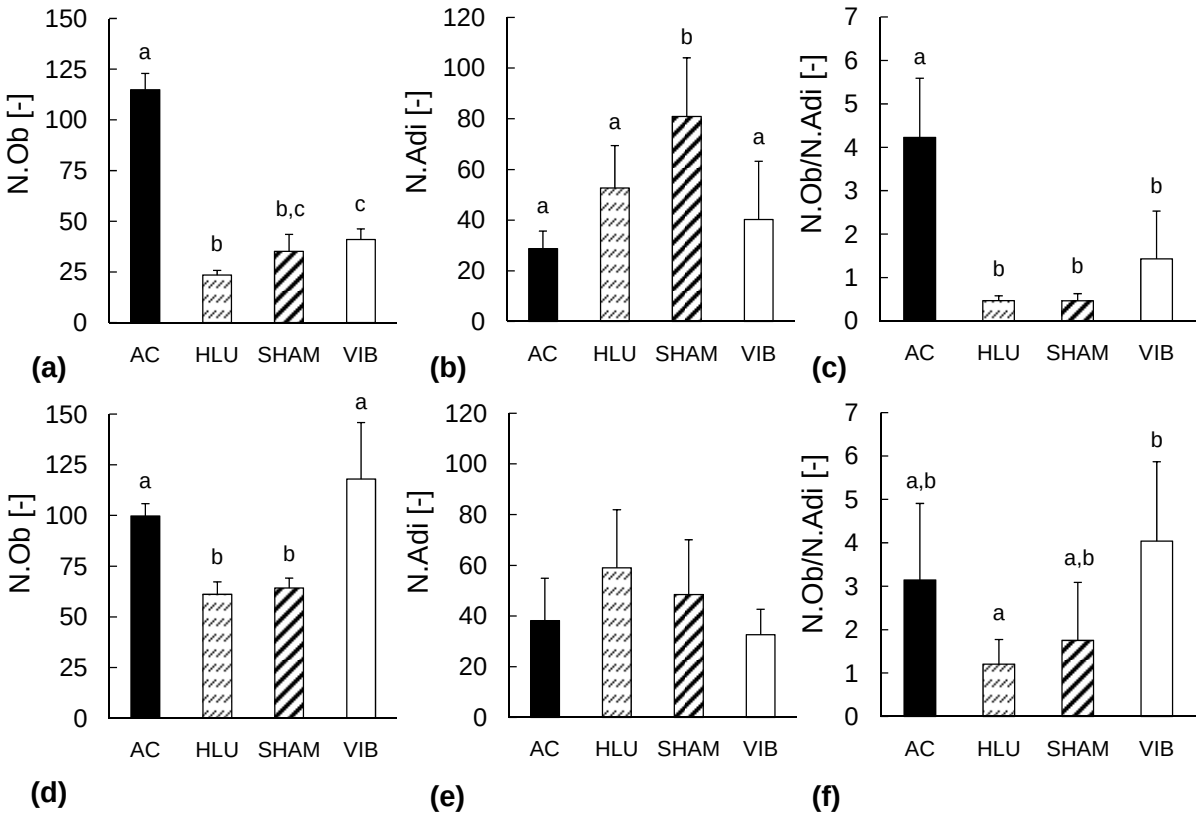

Figure 4.4. Number of trabecular bone lining osteoblasts, marrow adipocytes, and the ratio of osteoblasts to adipocytes in the proximal tibial metaphysis of age-matched controls (AC), hindlimb unloaded (HLU), sham loaded (SHAM) and vibrated mice (VIB) after**(a-c)** 3w of disuse or **(d-f)** 3w of disuse followed by 3w of reambulation. Difference in letters denominate significant ($p<0.05$) differences between groups (ANOVA and SNK).

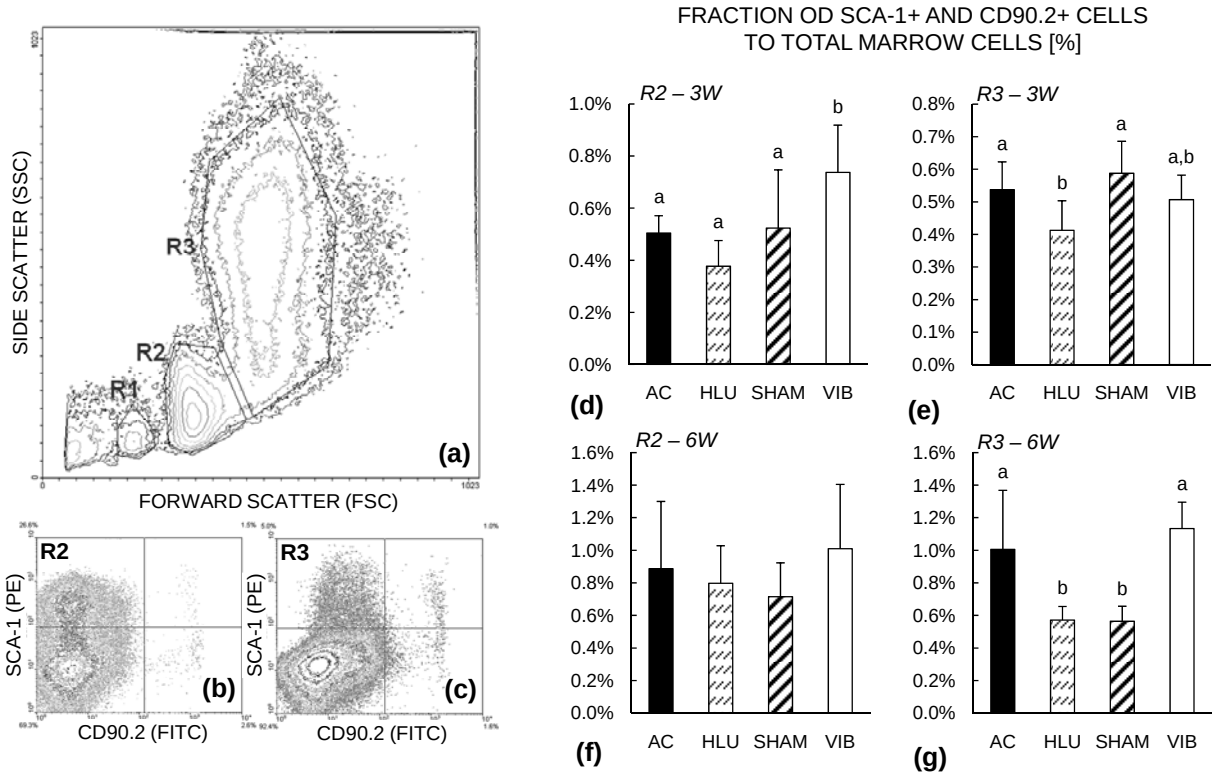

Figure 4.5. **(a)** Cell size (FSC) and complexity (SSC) of bone marrow cells subjected to flow cytometry. Regions in which cells accumulated are denoted by R1, R2, and R3. Fluorescence of cells that were positive for SCA-1 and CD90.2 surface antigens resided **(b)** in R2 or **(c)** R3. Ratio of SCA-1 and CD90.2 positive cells to total marrow cells **(d)** in R2 after 3w, **(e)** in R3 after 3w, **(d)** in R2 after 6w, **(g)** in R3 after 6w. Difference in letters denominate significant ($p<0.05$) differences between groups (ANOVA and SNK).

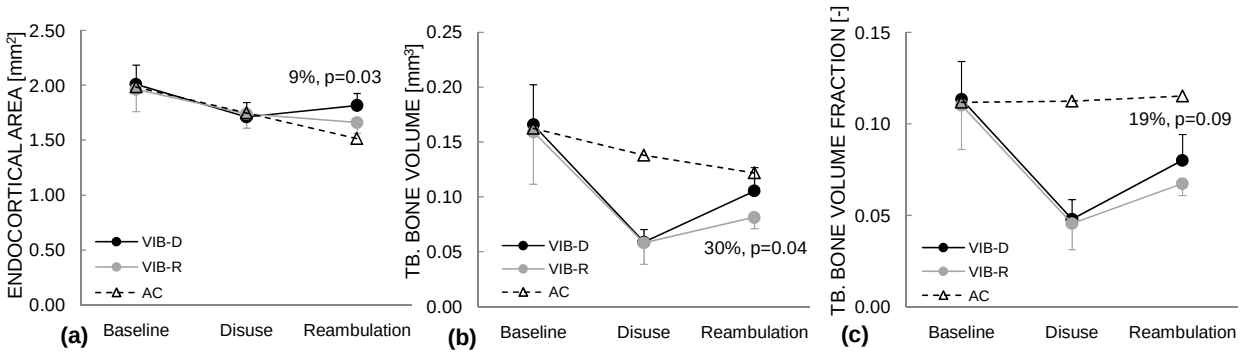

Figure 4.6. Longitudinal changes in (a) endocortical envelope area, (b) trabecular bone volume, and (c) trabecular bone volume fraction of the tibial metaphysis in mice that either received vibrations only during the disuse period (VIB-D, n=6) or during reambulation (VIB-R, n=6). Open triangles correspond to-cross-sectional data of age-matched control mice (n=12).

Chapter 5

CONCLUSIONS

SUMMARY

Mechanical unloading (disuse), is a strong catabolic signal for bone marrow cells, bone quantity, bone microarchitecture and bone micro-mechanical properties. Other physiological systems (e.g. blood cells, muscle volume) are also affected severely from disuse but they reach a state of homeostasis during disuse. However no plateau was yet observed in bone loss during disuse [215]. Moreover, unlike other physiological systems, effects of disuse on bone tissue are not completely reversible, increasing the mechanical risk of failure for individuals after returning to regular weight bearing activities. Studies in this dissertation examined micro-mechanical, microarchitectural and cellular level effects of disuse and subsequent recovery. Furthermore, the premise of a mechanical based exogenous stimulation that would alleviate catabolic effects of disuse was also tested.

Results from the **second chapter** showed the importance of genetic background on disuse induced bone loss and subsequent reambulation. Also, results indicated that deterioration in micro-architecture is paralleled by the deterioration in micro-mechanical properties. In return, during reambulation mice showed a preferential recovery in micro-mechanical properties in the direction of loading axis rather than the micro-architecture.

In the **third chapter**, disuse induced deterioration and reambulation induced recovery were attempted to be predicted using baseline morphology. It was found that disuse induced loss in trabecular bone volume fraction was moderately correlated to baseline values, however micro-mechanical properties at baseline were not correlated

with longitudinal changes during disuse. Further, baseline properties were not correlated with the changes upon reambulation either. In an effort to determine individual mice at more risk in mechanical failure, mice were stratified based on their disuse induced increase in peak stresses. It was found that mice with the higher risk had lower baseline trabecular bone volume fraction and other indices of bone quality. However, even with the differences in trabecular bone volume fraction, mice had similar micro-mechanical properties at baseline.

Fourth chapter tested the hypothesis that exogenous mechanical stimulation (high-frequency low-magnitude vibrations) would prevent disuse induced deterioration in bone's osteogenic potential. It was found that vibrations increased the number of osteogenic marrow stromal cells in disuse mice; however they had no immediate tissue level effects. Upon reambulation mice that were exposed to vibrations had higher number and surface of osteoblasts, greater bone formation rates, lower bone marrow adiposity and higher bone mass compared to the mice that were deprived of mechanical signals during disuse or sham controls.

LIMITATIONS OF THE ANIMAL MODEL

Studies in this dissertation utilized hindlimb unloading model in mice to simulate disuse in weight-bearing skeleton. In this model, weightlessness only affects hindlimbs, while forelimbs are loaded and functional for mice to feed, groom and ambulate itself [61]. Although not addressed in this dissertation, it is known that systemic stress may be

experienced when the experimental setup is not ideal [216]. Systemic stress (e.g. as indicated by levels of Corticosterone hormone) may cause catabolism in muscle, cartilage and bone accretion [217]. Levels of corticosterone hormone was found to be elevated in urine of rats exposed to hindlimb unloading for the first 3 days of the experiment in the following days rats adapted to the experiment [218]. Reductions in the body mass was also used as an indicator of systemic stress in growing rats, which corresponds to the first few days of the hindlimb unloading experiment [219]. Mice in our study also showed a short adaptive period to hindlimb unloading protocol, indicating the observed bone losses were mainly caused by the loss of weight-bearing rather than systemic stress.

CELLULAR, TISSUE LEVEL AND MICRO-MECHANICAL EFFECTS OF DISUSE AND REAMBULATION

Results in this dissertation demonstrated that disuse induced by loss of mechanical loading, resulted in loss of trabecular bone in skeletal extremities. Structural deterioration also affected micro-mechanical properties, by making trabecular bone to experience higher stress values and less efficient stress distributions. On the level of the cell, mechanical disuse caused a decline in osteoblast recruitment and mineralization of bone tissue. Disuse induced effects were also sustained upon returning to regular weight-bearing, indicated by sustained reduction in osteoblasts and mineralization after equal period of reambulation. Therefore, recovery of the tissue quantity and quality was

limited. Data also suggested that recovery of tissue during reambulation was not motivated by returning to its healthy levels, but rather to reduce the deterioration in micro-mechanical properties in principal loading direction. These results corroborate well with the literature on disuse induced: **a)** Reduction in the osteogenic potential of stem cells [56] and osteoprogenitor population size [55]; **b)** Decrease in trabecular bone mineralization and bone formation rates [66]; **c)** Decrease in quality and quantity of trabecular bone [30, 181]; **d)** Lack of complete recovery in osteoprogenitor population [194] and tissue quantity [148] upon reambulation. Results from this dissertation also indicated that recovery during reambulation focused primarily in the micro-mechanical properties in the loading direction rather than trabecular bone quantity. This indicates the importance of tracking the micro-mechanical properties for each individual that was exposed to disuse [151] rather than simply relying on the tissue quantity.

EFFECT OF INDIVIDUAL GENETIC BACKGROUND ON MECHANOSENSITIVITY

Magnitude of the trabecular bone loss during disuse was moderately correlated to the baseline morphology in a genetically heterogeneous population, indicating increased bone mass of a healthy individual may be protective against disuse induced bone loss [71]. Rest of the variation may be explained by the individual differences in genetic background, perhaps even to a single gene as seen in some other phenotypes [220]. Although this aspect of the study needs further investigation, it is not clear which component of bone remodeling would be affected from variations in genetic background. As any other cell in the bone marrow environment, maintenance and

function of bone resorpting osteoclasts are also affected from the variations in their mechanical environment in vitro [221, 222]. However, osteoclast population and function is known to be strictly regulated by osteoblast and osteocyte signaling in vivo [223, 224]. Therefore osteoclastic activity may not differ during disuse as observed in this study (Chapter 4) and shown by the others [54]. On the other hand, recruitment and maturation of the osteoblasts may vary based on genetic variability. For example mineralization of osteoblasts is regulated in part by the vitamin D [225] and any polymorphism in vitamin D receptor [226] would affect new bone formation. Furthermore, recruitment of osteoblasts may be affected from the variations in sensing of disuse by osteocytes. For example integrins are important determining cellular signaling from osteocytes to osteoblasts [227], and polymorphisms in integrins may affect bone's mechanotransduction and thereby osteoblast recruitment [228, 229]. It is also highly possible that instead of a single gene, a variety of genes are orchestrating mechanosensitivity of bone, each having some level of contribution.

MECHANICAL BASED COUNTERMEASURE FOR DISUSE INDUCED BONE LOSS

High frequency low magnitude exogenous mechanical vibrations increase bone mass in osteopenic young females, female adults after menopause and children with neurodegenerative conditions [106, 107, 230]. Vibrations were also shown to increase muscle and bone quantity in growing mice [231]. Furthermore, the anabolic potential of mechanical vibrations were found to be effective in restoring disuse induced reduction in bone formation rates in female rats [66]. In this study, vibrations were only effective in

increasing marrow stromal cells with osteogenic potential but the tissue level effects of vibrations were not significantly different than controls. Similar trends were also found in the bedrest studies where subjects were exposed to daily vibrations with a harnessing system that induces 60% of their body weight [232]. Perhaps lack of regular weight-bearing is the key factor for cells in marrow stroma to be recruited as bone lining cells and mineralize into new bone. Rapid increase in trabecular bone quantity and mineralization of vibrated mice during reambulation also supports the observation that regular weight-bearing may be an important aspect of anabolism induced by vibrations.

Regardless, in order to respond to the high frequency vibrations, bone marrow cells are required to be able to sense the presence of that mechanical signal. Lack of response in the skeletal tissue after disuse suggests that bone matrix (and its deformations) may not be an important factor in sensing the vibratory stimulus. This hypothesis is supported by other hindlimb unloading experiments that introduce high frequency oscillations in the complete absence of any matrix strains and observed a response in the system [112, 153]. However, these observations do not exclude potential functioning of osteocytes in sensing mechanical signals even in the absence of matrix deformations. Osteocytes, as being the most abundant cell type in the bone matrix combined with their enmeshed architecture to each other [233] were shown to be able to sense and amplify received mechanical signals in theoretical and experimental studies [234]. Being able to regulate both bone formation [235] and bone resorption [224], osteocyte signaling may be important for other cells in bone marrow environment, including stem cells. Whether with direct mechanosensitivity or via osteocye signaling, factors that

trigger preservation of phenotype in bone marrow environment during disuse may be used to improve regenerative potential in skeletal tissue not just against disuse (Chapter 4) but also other detrimental factors for bone such as aging [203] or obesity [236].

CONCLUSIONS

In conclusion, this dissertation indicated the importance of genetic background for determination of trabecular bone's architectural and micro-mechanical response to disuse and subsequent reambulation. Perhaps morphological indicators of tissue response to altered weight-bearing can be used in parallel with genomic variations (QTL) to identify individuals that are in greater risk of tissue loss during disuse. Furthermore, given that natural regeneration upon reambulation is limited and favors improving micro-mechanical parameters only in the direction of weight-bearing, perhaps prophylactic measures (e.g. mechanical vibrations) to prevent bone loss or improve bone regeneration can be optimized to protect individuals that are exposed to short or long-term disuse.

BIBLIOGRAPHY

Reference List

1. Martini,F. & Ober,W.C. *Fundamentals of anatomy & physiology*(Pearson Benjamin Cummings, San Francisco, CA, 2006).

2. Robling,A.G., Castillo,A.B., & Turner,C.H. Biomechanical and molecular regulation of bone remodeling. *Annu. Rev. Biomed. Eng* **8**, 455-498 (2006).

3. Lian,J.B. & Stein,G.S. Development of the osteoblast phenotype: molecular mechanisms mediating osteoblast growth and differentiation. *Iowa Orthop. J.* **15**, 118-140 (1995).

4. Roodman,G.D. Advances in bone biology: the osteoclast. *Endocr. Rev.* **17**, 308-332 (1996).

5. Turner,C.H. & Pavalko,F.M. Mechanotransduction and functional response of the skeleton to physical stress: the mechanisms and mechanics of bone adaptation. *J. Orthop. Sci.* **3**, 346-355 (1998).

6. Kodama,Y. *et al.* Cortical tibial bone volume in two strains of mice: effects of sciatic neurectomy and genetic regulation of bone response to mechanical loading. *Bone* **25**, 183-190 (1999).

7. Lanyon,L.E. & Rubin,C.T. Static vs dynamic loads as an influence on bone remodelling. *J. Biomech.* **17**, 897-905 (1984).

8. Rubin,C.T. & Lanyon,L.E. Regulation of bone mass by mechanical strain magnitude. *Calcif. Tissue Int.* **37**, 411-417 (1985).

9. Gross,T.S., Edwards,J.L., McLeod,K.J., & Rubin,C.T. Strain gradients correlate with sites of periosteal bone formation. *J. Bone Miner. Res.* **12**, 982-988 (1997).

10. Judex,S., Gross,T.S., & Zernicke,R.F. Strain gradients correlate with sites of exercise-induced bone-forming surfaces in the adult skeleton. *J Bone Miner Res* **12**, 1737-1745 (1997).

11. Judex,S. & Zernicke,R.F. High-impact exercise and growing bone: relation between high strain rates and enhanced bone formation. *J. Appl. Physiol* **88**, 2183-2191 (2000).

12. Mosley,J.R., March,B.M., Lynch,J., & Lanyon,L.E. Strain magnitude related changes in whole bone architecture in growing rats. *Bone* **20**, 191-198 (1997).

13. Turner,C.H. Three rules for bone adaptation to mechanical stimuli. *Bone* **23**, 399-407 (1998).

14. Qin,Y.X., Rubin,C.T., & McLeod,K.J. Nonlinear dependence of loading intensity and cycle number in the maintenance of bone mass and morphology. *J. Orthop. Res.* **16**, 482-489 (1998).

15. Cullen,D.M., Smith,R.T., & Akhter,M.P. Bone-loading response varies with strain magnitude and cycle number. *J. Appl. Physiol* **91**, 1971-1976 (2001).

16. Fritton,S.P., McLeod,K.J., & Rubin,C.T. Quantifying the strain history of bone: spatial uniformity and self- similarity of low-magnitude strains. *J. Biomech.* **33**, 317-325 (2000).

17. Tate,M.L. & Knothe,U. An ex vivo model to study transport processes and fluid flow in loaded bone. *J. Biomech.* **33**, 247-254 (2000).

18. Weinbaum,S., Cowin,S.C., & Zeng,Y. A model for the excitation of osteocytes by mechanical loading-induced bone fluid shear stresses. *J. Biomech.* **27**, 339-360 (1994).

19. Rubin,C. *et al.* Differentiation of the bone-tissue remodeling response to axial and torsional loading in the turkey ulna. *J. Bone Joint Surg. Am.* **78**, 1523-1533 (1996).

20. Qin,Y.X., Kaplan,T., Saldanha,A., & Rubin,C. Fluid pressure gradients, arising from oscillations in intramedullary pressure, is correlated with the formation of bone and inhibition of intracortical porosity. *J Biomech.* **36**, 1427-1437 (2003).

21. Datta,N. *et al.* In vitro generated extracellular matrix and fluid shear stress synergistically enhance 3D osteoblastic differentiation. *Proc. Natl. Acad. Sci. U. S. A* **103**, 2488-2493 (2006).

22. Cherian,P.P. *et al.* Effects of mechanical strain on the function of Gap junctions in osteocytes are mediated through the prostaglandin EP2 receptor. *J. Biol. Chem.* **278**, 43146-43156 (2003).

23. Sen,B. *et al.* Mechanical strain inhibits adipogenesis in mesenchymal stem cells by stimulating a durable beta-catenin signal. *Endocrinology* **149**, 6065-6075 (2008).

24. Jones,H.H., Priest,J.D., Hayes,W.C., Tichenor,C.C., & Nagel,D.A. Humeral hypertrophy in response to exercise. *J. Bone Joint Surg. Am.* **59**, 204-208 (1977).

25. Snow-Harter,C., Bouxsein,M.L., Lewis,B.T., Carter,D.R., & Marcus,R. Effects of resistance and endurance exercise on bone mineral status of young women: a randomized exercise intervention trial. *J Bone Miner Res* **7**, 761-769 (1992).

26. Bailey,D.A., Faulkner,R.A., & McKay,H.A. Growth, physical activity, and bone mineral acquisition. *Exerc Sport Sci Rev* **24**, 233-266 (1996).

27. Notomi,T. *et al.* Effects of resistance exercise training on mass, strength, and turnover of bone in growing rats. *Eur. J. Appl. Physiol* **82**, 268-274 (2000).

28. Hart,K.J., Shaw,J.M., Vajda,E., Hegsted,M., & Miller,S.C. Swim-trained rats have greater bone mass, density, strength, and dynamics. *J. Appl. Physiol* **91**, 1663-1668 (2001).

29. Fyhrie,D.P. & Carter,D.R. A unifying principle relating stress to trabecular bone morphology. *J. Orthop. Res.* **4**, 304-317 (1986).

30. Vico,L. *et al.* Effects of long-term microgravity exposure on cancellous and cortical weight-bearing bones of cosmonauts. *Lancet* **355**, 1607-1611 (2000).

31. Pruitt,L.A., Taaffe,D.R., & Marcus,R. Effects of a one-year high-intensity versus low-intensity resistance training program on bone mineral density in older women. *J Bone Miner Res* **10**, 1788-1795 (1995).

32. Shackelford,L.C. *et al.* Resistance exercise as a countermeasure to disuse-induced bone loss. *J Appl. Physiol* **97**, 119-129 (2004).

33. Bikle,D.D., Sakata,T., & Halloran,B.P. The impact of skeletal unloading on bone formation. *Gravit. Space Biol. Bull.* **16**, 45-54 (2003).

34. Ohira,Y. *et al.* Gravitational unloading effects on muscle fiber size, phenotype and myonuclear number. *Adv. Space Res.* **30**, 777-781 (2002).

35. Ortega,F.B., Ruiz,J.R., Castillo,M.J., & Sjostrom,M. Physical fitness in childhood and adolescence: a powerful marker of health. *Int. J. Obes. (Lond)* **32**, 1-11 (2008).

36. LeBlanc,A.D., Schneider,V.S., Evans,H.J., Engelbretson,D.A., & Krebs,J.M. Bone mineral loss and recovery after 17 weeks of bed rest. *J Bone Miner Res* **5**, 843-850 (1990).

37. LeBlanc,A., Shackelford,L., & Schneider,V. Future human bone research in space. *Bone* **22**, 113S-116S (1998).

38. Shackelford,L., LeBlanc,A., Feiveson,A., & Oganov,V. Bone loss in space: Shuttle/Mir experience and bed rest countermeasure program. *1st Biennial Space Biomed. Inv. Workshop* **1**, 17 (1999).

39. LeBlanc,A. & Schneider,V. Can the adult skeleton recover lost bone? *Exp Gerontol* **26**, 189-201 (1991).

40. Collet,P. *et al.* Effects of 1- and 6-month spaceflight on bone mass and biochemistry in two humans. *Bone* **20**, 547-551 (1997).

41. Caillot-Augusseau,A. *et al.* Bone formation and resorption biological markers in cosmonauts during and after a 180-day space flight (Euromir 95). *Clin. Chem.* **44**, 578-585 (1998).

42. Smith,S.M. *et al.* Bone markers, calcium metabolism, and calcium kinetics during extended-duration space flight on the mir space station. *J. Bone Miner. Res.* **20**, 208-218 (2005).

43. Smith,S.M. *et al.* Calcium metabolism before, during, and after a 3-mo spaceflight: kinetic and biochemical changes. *Am. J. Physiol* **277**, R1-10 (1999).

44. Ontiveros,C. & McCabe,L.R. Simulated microgravity suppresses osteoblast phenotype, Runx2 levels and AP-1 transactivation. *J. Cell Biochem.* **88**, 427-437 (2003).

45. Carmeliet,G., Nys,G., & Bouillon,R. Microgravity reduces the differentiation of human osteoblastic MG-63 cells. *J. Bone Miner. Res.* **12**, 786-794 (1997).

46. Nakamura,H. *et al.* Suppression of osteoblastic phenotypes and modulation of pro- and anti-apoptotic features in normal human osteoblastic cells under a vector-averaged gravity condition. *J. Med. Dent. Sci.* **50**, 167-176 (2003).

47. Sarkar,D. *et al.* Culture in vector-averaged gravity under clinostat rotation results in apoptosis of osteoblastic ROS 17/2.8 cells. *J. Bone Miner. Res.* **15**, 489-498 (2000).

48. Burger,E.H. & Klein-Nulend,J. Mechanotransduction in bone--role of the lacuno-canalicular network. *FASEB J.* **13 Suppl**, S101-S112 (1999).

49. Aguirre,J.I. *et al.* Osteocyte apoptosis is induced by weightlessness in mice and precedes osteoclast recruitment and bone loss. *J. Bone Miner. Res.* **21**, 605-615 (2006).

50. Kumei,Y. *et al.* Microgravity induces prostaglandin E2 and interleukin-6 production in normal rat osteoblasts: role in bone demineralization. *J. Biotechnol.* **47**, 313-324 (1996).

51. Sakai,A. & Nakamura,T. Changes in trabecular bone turnover and bone marrow cell development in tail-suspended mice. *J. Musculoskelet. Neuronal. Interact.* **1**, 387-392 (2001).

52. David,V. *et al.* Two-week longitudinal survey of bone architecture alteration in the hindlimb-unloaded rat model of bone loss: sex differences. *Am. J. Physiol Endocrinol. Metab* **290**, E440-E447 (2006).

53. Hefferan,T.E. *et al.* Effect of gender on bone turnover in adult rats during simulated weightlessness. *J. Appl. Physiol* **95**, 1775-1780 (2003).

54. Dehority,W. *et al.* Bone and hormonal changes induced by skeletal unloading in the mature male rat. *Am J Physiol* **276**, E62-E69 (1999).

55. Basso,N., Bellows,C.G., & Heersche,J.N. Effect of simulated weightlessness on osteoprogenitor cell number and proliferation in young and adult rats. *Bone* **36**, 173-183 (2005).

56. Zayzafoon,M., Gathings,W.E., & McDonald,J.M. Modeled microgravity inhibits osteogenic differentiation of human mesenchymal stem cells and increases adipogenesis. *Endocrinology* **145**, 2421-2432 (2004).

57. Li,C.Y. *et al.* Long-term disuse osteoporosis seems less sensitive to bisphosphonate treatment than other osteoporosis. *J. Bone Miner. Res.* **20**, 117-124 (2005).

58. Warner,S.E. *et al.* Botox induced muscle paralysis rapidly degrades bone. *Bone*(2005).

59. Jiang,S.D., Jiang,L.S., & Dai,L.Y. Spinal cord injury causes more damage to bone mass, bone structure, biomechanical properties and bone metabolism than sciatic neurectomy in young rats. *Osteoporos. Int.* **17**, 1552-1561 (2006).

60. Iwamoto,J., Seki,A., Takeda,T., Sato,Y., & Yamada,H. Effects of risedronate on femoral bone mineral density and bone strength in sciatic neurectomized young rats. *J. Bone Miner. Metab* **23**, 456-462 (2005).

61. Morey-Holton,E.R. & Globus,R.K. Hindlimb unloading rodent model: technical aspects. *J. Appl. Physiol* **92**, 1367-1377 (2002).

62. Judex,S. *et al.* Mechanical modulation of molecular signals which regulate anabolic and catabolic activity in bone tissue. *J. Cell Biochem.* **94**, 982-994 (2005).

63. Bikle,D.D. & Halloran,B.P. The response of bone to unloading. *J Bone Miner Metab* **17**, 233-244 (1999).

64. Martin,R.B. Effects of simulated weightlessness on bone properties in rats. *J Biomech* **23**, 1021-1029 (1990).

65. Judex,S. *et al.* Genetically linked site-specificity of disuse osteoporosis. *J. Bone Miner. Res.* **19**, 607-613 (2004).

66. Rubin,C., Xu,G., & Judex,S. The anabolic activity of bone tissue, suppressed by disuse, is normalized by brief exposure to extremely low-magnitude mechanical stimuli. *FASEB J.* **15**, 2225-2229 (2001).

67. Turner,R.T. *et al.* Dose-response effects of intermittent PTH on cancellous bone in hindlimb unloaded rats. *J. Bone Miner. Res.* **22**, 64-71 (2007).

68. Grano,M. *et al.* Rat hindlimb unloading by tail suspension reduces osteoblast differentiation, induces IL-6 secretion, and increases bone resorption in ex vivo cultures. *Calcif. Tissue Int.* **70**, 176-185 (2002).

69. Sakata,T. *et al.* Trabecular bone turnover and bone marrow cell development in tail-suspended mice. *J. Bone Miner. Res.* **14**, 1596-1604 (1999).

70. Amblard,D. *et al.* Tail suspension induces bone loss in skeletally mature mice in the C57BL/6J strain but not in the C3H/HeJ strain. *J Bone Miner Res* **18**, 561-569 (2003).

71. Squire,M., Donahue,L.R., Rubin,C., & Judex,S. Genetic variations that regulate bone morphology in the male mouse skeleton do not define its susceptibility to mechanical unloading. *Bone* **35**, 1353-1360 (2004).

72. Eisman,J.A. Genetics of osteoporosis. *Endocr. Rev.* **20**, 788-804 (1999).

73. Heaney,R.P. *et al.* Peak bone mass. *Osteoporos. Int.* **11**, 985-1009 (2000).

74. Videman,T. *et al.* Determinants of Changes in Bone Density: A 5-Year Follow-Up Study of Adult Male Monozygotic Twins. *J. Clin. Densitom.*(2007).

75. Jones,G. & Nguyen,T.V. Associations between maternal peak bone mass and bone mass in prepubertal male and female children. *J. Bone Miner. Res.* **15**, 1998-2004 (2000).

76. Duncan,E.L., Cardon,L.R., Sinsheimer,J.S., Wass,J.A., & Brown,M.A. Site and gender specificity of inheritance of bone mineral density. *J Bone Miner Res* **18**, 1531-1538 (2003).

77. Judex,S., Garman,R., Squire,M., Donahue,L.R., & Rubin,C. Genetically based influences on the site-specific regulation of trabecular and cortical bone morphology. *J. Bone Miner. Res.* **19**, 600-606 (2004).

78. Peacock,M. *et al.* Sex-specific and non-sex-specific quantitative trait loci contribute to normal variation in bone mineral density in men. *J. Clin. Endocrinol. Metab* **90**, 3060-3066 (2005).

79. Marwick,C. Consensus panel considers osteoporosis. *JAMA* **283**, 2093-2095 (2000).

80. Qiu,S., Rao,D.S., Palnitkar,S., & Parfitt,A.M. Differences in osteocyte and lacunar density between Black and White American women. *Bone* **38**, 130-135 (2006).

81. Devoto,M. *et al.* First-stage autosomal genome screen in extended pedigrees suggests genes predisposing to low bone mineral density on chromosomes 1p, 2p and 4q. *Eur. J. Hum. Genet.* **6**, 151-157 (1998).

82. Wilson,S.G. *et al.* Comparison of genome screens for two independent cohorts provides replication of suggestive linkage of bone mineral density to 3p21 and 1p36. *Am. J. Hum. Genet.* **72**, 144-155 (2003).

83. Carn,G. *et al.* Sibling pair linkage and association studies between peak bone mineral density and the gene locus for the osteoclast-specific subunit (OC116) of the vacuolar proton pump on chromosome 11p12-13. *J. Clin. Endocrinol. Metab* **87**, 3819-3824 (2002).

84. Styrkarsdottir,U. *et al.* Linkage of osteoporosis to chromosome 20p12 and association to BMP2. *PLoS. Biol.* **1**, E69 (2003).

85. Korstanje,R. & Paigen,B. From QTL to gene: the harvest begins. *Nat. Genet.* **31**, 235-236 (2002).

86. Beamer,W.G. *et al.* Quantitative trait loci for femoral and lumbar vertebral bone mineral density in C57BL/6J and C3H/HeJ inbred strains of mice. *J. Bone Miner. Res.* **16**, 1195-1206 (2001).

87. Robling,A.G. & Turner,C.H. Mechanotransduction in bone: genetic effects on mechanosensitivity in mice. *Bone* **31**, 562-569 (2002).

88. Bouxsein,M.L. *et al.* Mapping quantitative trait Loci for vertebral trabecular bone volume fraction and microarchitecture in mice. *J Bone Miner. Res.* **19**, 587-599 (2004).

89. Wergedal,J.E. *et al.* Femur mechanical properties in the F2 progeny of an NZB/B1NJ x RF/J cross are regulated predominantly by genetic loci that regulate bone geometry. *J. Bone Miner. Res.* **21**, 1256-1266 (2006).

90. Jiao,Y. *et al.* Quantitative trait loci that determine mouse tibial nanoindentation properties in an F2 population derived from C57BL/6J x C3H/HeJ. *Calcif. Tissue Int.* **80**, 383-390 (2007).

91. Boonen,S. *et al.* Recent developments in the management of postmenopausal osteoporosis with bisphosphonates: enhanced efficacy by enhanced compliance. *J. Intern. Med.* **264**, 315-332 (2008).

92. Rittweger,J. *et al.* Muscle atrophy and bone loss after 90 days' bed rest and the effects of flywheel resistive exercise and pamidronate: results from the LTBR study. *Bone* **36**, 1019-1029 (2005).

93. Mashiba,T. *et al.* Suppressed bone turnover by bisphosphonates increases microdamage accumulation and reduces some biomechanical properties in dog rib. *J Bone Miner. Res.* **15**, 613-620 (2000).

94. Mashiba,T. *et al.* Effects of suppressed bone turnover by bisphosphonates on microdamage accumulation and biomechanical properties in clinically relevant skeletal sites in beagles. *Bone* **28**, 524-531 (2001).

95. Woo,S.B., Hellstein,J.W., & Kalmar,J.R. Systematic review: bisphosphonates and osteonecrosis of the jaws. *Ann. Intern. Med.* **144**, 753-761 (2006).

96. Lloyd,S.A., Travis,N.D., Lu,T., & Bateman,T.A. Development of a low-dose anti-resorptive drug regimen reveals synergistic suppression of bone formation when coupled with disuse. *J. Appl. Physiol* **104**, 729-738 (2008).

97. Kidder,L.S. *et al.* Skeletal effects of sodium fluoride during hypokinesia. *Bone Miner.* **11**, 305-318 (1990).

98. Hott,M., Deloffre,P., Tsouderos,Y., & Marie,P.J. S12911-2 reduces bone loss induced by short-term immobilization in rats. *Bone* **33**, 115-123 (2003).

99. Meunier,P.J. *et al.* The effects of strontium ranelate on the risk of vertebral fracture in women with postmenopausal osteoporosis. *N. Engl. J. Med.* **350**, 459-468 (2004).

100. Reginster,J.Y. *et al.* Strontium ranelate reduces the risk of nonvertebral fractures in postmenopausal women with osteoporosis: Treatment of Peripheral Osteoporosis (TROPOS) study. *J. Clin. Endocrinol. Metab* **90**, 2816-2822 (2005).

101. Reid,I.R. Pharmacotherapy of osteoporosis in postmenopausal women: focus on safety. *Expert. Opin. Drug Saf* **1**, 93-107 (2002).

102. Haguenauer,D., Welch,V., Shea,B., Tugwell,P., & Wells,G. Fluoride for treating postmenopausal osteoporosis. *Cochrane. Database. Syst. Rev.*CD002825 (2000).

103. Rubin,C., Turner,A.S., Bain,S., Mallinckrodt,C., & McLeod,K. Anabolism: Low mechanical signals strengthen long bones. *Nature* **412**, 603-604 (2001).

104. Rubin,C. *et al.* Quantity and quality of trabecular bone in the femur are enhanced by a strongly anabolic, noninvasive mechanical intervention. *J. Bone Miner. Res.* **17**, 349-357 (2002).

105. Rubin,C. *et al.* Mechanical strain, induced noninvasively in the high-frequency domain, is anabolic to cancellous bone, but not cortical bone. *Bone* **30**, 445-452 (2002).

106. Gilsanz,V. *et al.* Low-Level, High-Frequency Mechanical Signals Enhance Musculoskeletal Development of Young Women With Low BMD. *J. Bone Miner. Res.* **21**, 1464-1474 (2006).

107. Rubin,C. *et al.* Prevention of postmenopausal bone loss by a low-magnitude, high-frequency mechanical stimuli: a clinical trial assessing compliance, efficacy, and safety. *J Bone Miner. Res.* **19**, 343-351 (2004).

108. Ward,K. *et al.* Low magnitude mechanical loading is osteogenic in children with disabling conditions. *J. Bone Miner. Res.* **19**, 360-369 (2004).

109. Xie,L. *et al.* Low-level mechanical vibrations can influence bone resorption and bone formation in the growing skeleton. *Bone* **39**, 1059-1066 (2006).

110. Judex,S., Donahue,L.R., & Rubin,C. Genetic predisposition to low bone mass is paralleled by an enhanced sensitivity to signals anabolic to the skeleton. *FASEB J.* **16**, 1280-1282 (2002).

111. Judex,S., Lei,X., Han,D., & Rubin,C. Low-magnitude mechanical signals that stimulate bone formation in the ovariectomized rat are dependent on the applied frequency but not on the strain magnitude. *J. Biomech.* **40**, 1333-1339 (2007).

112. Garman,R., Rubin,C., & Judex,S. Small oscillatory accelerations, independent of matrix deformations, increase osteoblast activity and enhance bone morphology. *PLoS. ONE.* **2**, e653 (2007).

113. Christiansen,B.A. & Silva,M.J. The effect of varying magnitudes of whole-body vibration on several skeletal sites in mice. *Ann. Biomed. Eng* **34**, 1149-1156 (2006).

114. Judex,S. *et al.* Adaptations of trabecular bone to low magnitude vibrations result in more uniform stress and strain under load. *Ann Biomed Eng* **31**, 12-20 (2003).

115. Han,Y., Cowin,S.C., Schaffler,M.B., & Weinbaum,S. Mechanotransduction and strain amplification in osteocyte cell processes. *Proc. Natl. Acad. Sci. U. S. A* **101**, 16689-16694 (2004).

116. Satija,N.K. *et al.* Mesenchymal stem cells: molecular targets for tissue engineering. *Stem Cells Dev.* **16**, 7-23 (2007).

117. Fan,X. *et al.* Response to mechanical strain in an immortalized pre-osteoblast cell is dependent on ERK1/2. *J. Cell Physiol* **207**, 454-460 (2006).

118. Rubin,J., Murphy,T.C., Fan,X., Goldschmidt,M., & Taylor,W.R. Activation of extracellular signal-regulated kinase is involved in mechanical strain inhibition of RANKL expression in bone stromal cells. *J. Bone Miner. Res.* **17**, 1452-1460 (2002).

119. David,V. *et al.* Mechanical loading down-regulates peroxisome proliferator-activated receptor gamma in bone marrow stromal cells and favors osteoblastogenesis at the expense of adipogenesis. *Endocrinology* **148**, 2553-2562 (2007).

120. Cooper,L.F., Harris,C.T., Bruder,S.P., Kowalski,R., & Kadiyala,S. Incipient analysis of mesenchymal stem-cell-derived osteogenesis. *J. Dent. Res.* **80**, 314-320 (2001).

121. Bruder,S.P. *et al.* Mesenchymal stem cells in osteobiology and applied bone regeneration. *Clin. Orthop. Relat Res.*S247-S256 (1998).

122. Grompe,M. Bone marrow-derived hepatocytes. *Novartis. Found. Symp.* **265**, 20-27 (2005).

123. Okada,H. & Kalluri,R. Cellular and molecular pathways that lead to progression and regression of renal fibrogenesis. *Curr. Mol. Med.* **5**, 467-474 (2005).

124. Natsu,K. *et al.* Allogeneic bone marrow-derived mesenchymal stromal cells promote the regeneration of injured skeletal muscle without differentiation into myofibers. *Tissue Eng* **10**, 1093-1112 (2004).

125. Mashiba,T. *et al.* The effects of suppressed bone remodeling by bisphosphonates on microdamage accumulation and degree of mineralization in the cortical bone of dog rib. *J. Bone Miner. Metab* **23 Suppl**, 36-42 (2005).

126. Mauney,J.R., Volloch,V., & Kaplan,D.L. Role of adult mesenchymal stem cells in bone tissue engineering applications: current status and future prospects. *Tissue Eng* **11**, 787-802 (2005).

127. Kopen,G.C., Prockop,D.J., & Phinney,D.G. Marrow stromal cells migrate throughout forebrain and cerebellum, and they differentiate into astrocytes after injection into neonatal mouse brains. *Proc. Natl. Acad. Sci. U. S. A* **96**, 10711-10716 (1999).

128. Bianco,P. & Robey,P.G. Stem cells in tissue engineering. *Nature* **414**, 118-121 (2001).

129. Pittenger,M.F. *et al.* Multilineage potential of adult human mesenchymal stem cells. *Science* **284**, 143-147 (1999).

130. Arthur,A., Zannettino,A., & Gronthos,S. The therapeutic applications of multipotential mesenchymal/stromal stem cells in skeletal tissue repair. *J. Cell Physiol* **218**, 237-245 (2009).

131. Yamahara,K. & Nagaya,N. Stem cell implantation for myocardial disorders. *Curr. Drug Deliv.* **5**, 224-229 (2008).

132. Heino,T.J. & Hentunen,T.A. Differentiation of osteoblasts and osteocytes from mesenchymal stem cells. *Curr. Stem Cell Res. Ther.* **3**, 131-145 (2008).

133. Kemp,K.C., Hows,J., & Donaldson,C. Bone marrow-derived mesenchymal stem cells. *Leuk. Lymphoma* **46**, 1531-1544 (2005).

134. Bruder,S.P., Kraus,K.H., Goldberg,V.M., & Kadiyala,S. The effect of implants loaded with autologous mesenchymal stem cells on the healing of canine segmental bone defects. *J. Bone Joint Surg. Am.* **80**, 985-996 (1998).

135. Zhu,L., Liu,W., Cui,L., & Cao,Y. Tissue-engineered bone repair of goat-femur defects with osteogenically induced bone marrow stromal cells. *Tissue Eng* **12**, 423-433 (2006).

136. Meinel,L. *et al.* Silk based biomaterials to heal critical sized femur defects. *Bone*(2006).

137. Petite,H. *et al.* Tissue-engineered bone regeneration. *Nat. Biotechnol.* **18**, 959-963 (2000).

138. Prockop,D.J., Gregory,C.A., & Spees,J.L. One strategy for cell and gene therapy: harnessing the power of adult stem cells to repair tissues. *Proc. Natl. Acad. Sci. U. S. A* **100 Suppl 1**, 11917-11923 (2003).

139. Ichioka,N. *et al.* Prevention of senile osteoporosis in SAMP6 mice by intrabone marrow injection of allogeneic bone marrow cells. *Stem Cells* **20**, 542-551 (2002).

140. Fehrer,C. & Lepperdinger,G. Mesenchymal stem cell aging. *Exp. Gerontol.* **40**, 926-930 (2005).

141. Rodriguez,J.P., Rios,S., Fernandez,M., & Santibanez,J.F. Differential activation of ERK1,2 MAP kinase signaling pathway in mesenchymal stem cell from control and osteoporotic postmenopausal women. *J. Cell Biochem.* **92**, 745-754 (2004).

142. Chamberlain,J.R. *et al.* Gene Targeting of Mutant COL1A2 Alleles in Mesenchymal Stem Cells From Individuals With Osteogenesis Imperfecta. *Mol. Ther.*(2007).

143. Takada,K. *et al.* Treatment of senile osteoporosis in SAMP6 mice by intra-bone marrow injection of allogeneic bone marrow cells. *Stem Cells* **24**, 399-405 (2006).

144. Shaw,S.R. *et al.* Mechanical, morphological and biochemical adaptations of bone and muscle to hindlimb suspension and exercise. *J Biomech* **20**, 225-234 (1987).

145. Berg,H.E., Eiken,O., Miklavcic,L., & Mekjavic,I.B. Hip, thigh and calf muscle atrophy and bone loss after 5-week bedrest inactivity. *Eur. J. Appl. Physiol* **99**, 283-289 (2007).

146. Hui,S.L., Slemenda,C.W., & Johnston,C.C., Jr. Age and bone mass as predictors of fracture in a prospective study. *J Clin. Invest* **81**, 1804-1809 (1988).

147. Cummings,S.R. *et al.* Appendicular bone density and age predict hip fracture in women. The Study of Osteoporotic Fractures Research Group. *JAMA* **263**, 665-668 (1990).

148. Lang,T.F., LeBlanc,A.D., Evans,H.J., & Lu,Y. Adaptation of the proximal femur to skeletal reloading after long-duration spaceflight. *J. Bone Miner. Res.* **21**, 1224-1230 (2006).

149. Ju,Y.I., Sone,T., Okamoto,T., & Fukunaga,M. Jump exercise during remobilization restores integrity of the trabecular architecture after tail suspension in young rats. *J. Appl. Physiol* **104**, 1594-1600 (2008).

150. Yeh,O.C. & Keaveny,T.M. Biomechanical effects of intraspecimen variations in trabecular architecture: a three-dimensional finite element study. *Bone* **25**, 223-228 (1999).

151. Keyak,J.H., Koyama,A.K., LeBlanc,A., Lu,Y., & Lang,T.F. Reduction in proximal femoral strength due to long-duration spaceflight. *Bone*(2008).

152. Judex,S. *et al.* Combining high-resolution microct with material composition to define the quality of bone tissue. *Current Osteoporosis Reports* **1**, 11-19 (2003).

153. Ozcivici,E., Garman,R., & Judex,S. High-frequency oscillatory motions enhance the simulated mechanical properties of non-weight bearing trabecular bone. *J. Biomech.* **40**, 3404-3411 (2007).

154. Morey-Holton,E. & Wronski,T.J. Animal models for simulating weightlessness. *Physiologist* **24**, 545-548 (1981).

155. Lublinsky,S., Ozcivici,E., & Judex,S. An automated algorithm to detect the trabecular-cortical bone interface in micro-computed tomographic images. *Calcif. Tissue Int.* **81**, 285-293 (2007).

156. Busa,B., Miller,L.M., Rubin,C.T., Qin,Y.X., & Judex,S. Rapid establishment of chemical and mechanical properties during lamellar bone formation. *Calcif. Tissue Int.* **77**, 386-394 (2005).

157. Rho,J.Y., Tsui,T.Y., & Pharr,G.M. Elastic properties of human cortical and trabecular lamellar bone measured by nanoindentation. *Biomaterials* **18**, 1325-1330 (1997).

158. Bayraktar,H.H. *et al.* Comparison of the elastic and yield properties of human femoral trabecular and cortical bone tissue. *J. Biomech.* **37**, 27-35 (2004).

159. Van Rietbergen,B., Weinans,H., Huiskes,R., & Odgaard,A. A new method to determine trabecular bone elastic properties and loading using micromechanical finite-element models. *J Biomech* **28**, 69-81 (1995).

160. Van,R.B., Huiskes,R., Eckstein,F., & Ruegsegger,P. Trabecular bone tissue strains in the healthy and osteoporotic human femur. *J. Bone Miner. Res.* **18**, 1781-1788 (2003).

161. Yeni,Y.N., Hou,F.J., Vashishth,D., & Fyhrie,D.P. Trabecular shear stress in human vertebral cancellous bone: intra- and inter-individual variations. *J. Biomech.* **34**, 1341-1346 (2001).

162. Bozic,K.J., Keyak,J.H., Skinner,H.B., Bueff,H.U., & Bradford,D.S. Three-dimensional finite element modeling of a cervical vertebra: an investigation of burst fracture mechanism. *J. Spinal Disord.* **7**, 102-110 (1994).

163. Niebur,G.L., Feldstein,M.J., Yuen,J.C., Chen,T.J., & Keaveny,T.M. High-resolution finite element models with tissue strength asymmetry accurately predict failure of trabecular bone. *J. Biomech.* **33**, 1575-1583 (2000).

164. Morgan,E.F. *et al.* Contribution of inter-site variations in architecture to trabecular bone apparent yield strains. *J. Biomech.* **37**, 1413-1420 (2004).

165. Bevill,G., Eswaran,S.K., Gupta,A., Papadopoulos,P., & Keaveny,T.M. Influence of bone volume fraction and architecture on computed large-deformation failure mechanisms in human trabecular bone. *Bone* **39**, 1218-1225 (2006).

166. Van Der Linden,J.C., Birkenhager-Frenkel,D.H., Verhaar,J.A., & Weinans,H. Trabecular bone's mechanical properties are affected by its non-uniform mineral distribution. *J. Biomech.* **34**, 1573-1580 (2001).

167. Silva,M.J., Keaveny,T.M., & Hayes,W.C. Computed tomography-based finite element analysis predicts failure loads and fracture patterns for vertebral sections. *J. Orthop. Res.* **16**, 300-308 (1998).

168. Nagaraja,S., Couse,T.L., & Guldberg,R.E. Trabecular bone microdamage and microstructural stresses under uniaxial compression. *J. Biomech.* **38**, 707-716 (2005).

169. Huiskes,R., Ruimerman,R., van Lenthe,G.H., & Janssen,J.D. Effects of mechanical forces on maintenance and adaptation of form in trabecular bone. *Nature* **405**, 704-706 (2000).

170. Mori,S. & Burr,D.B. Increased intracortical remodeling following fatigue damage. *Bone* **14**, 103-109 (1993).

171. Turner,C.H. *et al.* High fluoride intakes cause osteomalacia and diminished bone strength in rats with renal deficiency. *Bone* **19**, 595-601 (1996).

172. Klinck,J. & Boyd,S.K. The magnitude and rate of bone loss in ovariectomized mice differs among inbred strains as determined by longitudinal in vivo micro-computed tomography. *Calcif. Tissue Int.* **83**, 70-79 (2008).

173. Waarsing,J.H., Day,J.S., Verhaar,J.A., Ederveen,A.G., & Weinans,H. Bone loss dynamics result in trabecular alignment in aging and ovariectomized rats. *J. Orthop. Res.* **24**, 926-935 (2006).

174. Homminga,J. *et al.* Cancellous bone mechanical properties from normals and patients with hip fractures differ on the structure level, not on the bone hard tissue level. *Bone* **30**, 759-764 (2002).

175. Homminga,J. *et al.* The osteoporotic vertebral structure is well adapted to the loads of daily life, but not to infrequent "error" loads. *Bone* **34**, 510-516 (2004).

176. Sibonga,J.D. *et al.* Recovery of spaceflight-induced bone loss: bone mineral density after long-duration missions as fitted with an exponential function. *Bone* **41**, 973-978 (2007).

177. Klein-Nulend,J., Bacabac,R.G., & Mullender,M.G. Mechanobiology of bone tissue. *Pathol. Biol. (Paris)* **53**, 576-580 (2005).

178. Loomer,P.M. The impact of microgravity on bone metabolism in vitro and in vivo. *Crit Rev. Oral Biol. Med.* **12**, 252-261 (2001).

179. Thomsen,J.S. *et al.* Cancellous bone structure of iliac crest biopsies following 370 days of head-down bed rest. *Aviat. Space Environ. Med.* **76**, 915-922 (2005).

180. Takata,S. & Yasui,N. Disuse osteoporosis. *J. Med. Invest* **48**, 147-156 (2001).

181. Lang,T. *et al.* Cortical and trabecular bone mineral loss from the spine and hip in long-duration spaceflight. *J Bone Miner. Res.* **19**, 1006-1012 (2004).

182. Rittweger,J. & Felsenberg,D. Recovery of muscle atrophy and bone loss from 90 days bed rest: Results from a one-year follow-up. *Bone*(2008).

183. Squire,M., Brazin,A., Keng,Y., & Judex,S. Baseline bone morphometry and cellular activity modulate the degree of bone loss in the appendicular skeleton during disuse. *Bone* **42**, 341-349 (2008).

184. Bouxsein,M.L. *et al.* Ovariectomy-induced bone loss varies among inbred strains of mice. *J. Bone Miner. Res.* **20**, 1085-1092 (2005).

185. Iwamoto,J., Yeh,J.K., & Aloia,J.F. Differential effect of treadmill exercise on three cancellous bone sites in the young growing rat. *Bone* **24**, 163-169 (1999).

186. Keaveny,T.M., Morgan,E.F., Niebur,G.L., & Yeh,O.C. Biomechanics of trabecular bone. *Annu. Rev. Biomed Eng* **3**, 307-333 (2001).

187. Chen,Y. *et al.* Conservation of early odontogenic signaling pathways in Aves. *Proc. Natl. Acad. Sci. U. S. A* **97**, 10044-10049 (2000).

188. Ulrich,D., Van Rietbergen,B., Laib,A., & Ruegsegger,P. Load transfer analysis of the distal radius from in-vivo high-resolution CT-imaging. *J Biomech.* **32**, 821-828 (1999).

189. Eswaran,S.K., Allen,M.R., Burr,D.B., & Keaveny,T.M. A computational assessment of the independent contribution of changes in canine trabecular bone volume fraction and microarchitecture to increased bone strength with suppression of bone turnover. *J. Biomech.* **40**, 3424-3431 (2007).

190. Matkovic,V. *et al.* Timing of peak bone mass in Caucasian females and its implication for the prevention of osteoporosis. Inference from a cross-sectional model. *J. Clin. Invest* **93**, 799-808 (1994).

191. Beamer,W.G., Donahue,L.R., Rosen,C.J., & Baylink,D.J. Genetic variability in adult bone density among inbred strains of mice. *Bone* **18**, 397-403 (1996).

192. LeBlanc,A.D. *et al.* Alendronate as an effective countermeasure to disuse induced bone loss. *J Musculo Neuron Interact* **2**, 235-243 (2002).

193. Ahdjoudj,S., Lasmoles,F., Holy,X., Zerath,E., & Marie,P.J. Transforming growth factor beta2 inhibits adipocyte differentiation induced by skeletal unloading in rat bone marrow stroma. *J Bone Miner Res* **17**, 668-677 (2002).

194. Basso,N., Jia,Y., Bellows,C.G., & Heersche,J.N. The effect of reloading on bone volume, osteoblast number, and osteoprogenitor characteristics: studies in hind limb unloaded rats. *Bone* **37**, 370-378 (2005).

195. Kim,C.H. *et al.* Trabecular bone response to mechanical and parathyroid hormone stimulation: the role of mechanical microenvironment. *J Bone Miner. Res.* **18**, 2116-2125 (2003).

196. Karinkanta,S. *et al.* Maintenance of exercise-induced benefits in physical functioning and bone among elderly women. *Osteoporos. Int.* **20**, 665-674 (2009).

197. Smith,S.M. *et al.* WISE-2005: supine treadmill exercise within lower body negative pressure and flywheel resistive exercise as a countermeasure to bed rest-induced bone loss in women during 60-day simulated microgravity. *Bone* **42**, 572-581 (2008).

198. Smith,S.M. *et al.* Effects of artificial gravity during bed rest on bone metabolism in humans. *J. Appl. Physiol*(2008).

199. Zernicke,R., MacKay,C., & Lorincz,C. Mechanisms of bone remodeling during weight-bearing exercise. *Appl. Physiol Nutr. Metab* **31**, 655-660 (2006).

200. Rittweger,J. & Felsenberg,D. Recovery of muscle atrophy and bone loss from 90 days bed rest: results from a one-year follow-up. *Bone* **44**, 214-224 (2009).

201. Huang,R.P., Rubin,C.T., & McLeod,K.J. Changes in postural muscle dynamics as a function of age. *J Gerontol A Biol Sci Med Sci* **54**, B352-B357 (1999).

202. Luu,Y.K. *et al.* Mechanical stimulation of mesenchymal stem cell proliferation and differentiation promotes osteogenesis while preventing dietary-induced obesity. *J. Bone Miner. Res.* **24**, 50-61 (2009).

203. Glatt,V., Canalis,E., Stadmeyer,L., & Bouxsein,M.L. Age-related changes in trabecular architecture differ in female and male C57BL/6J mice. *J. Bone Miner. Res.* **22**, 1197-1207 (2007).

204. Travlos,G.S. Normal structure, function, and histology of the bone marrow. *Toxicol. Pathol.* **34**, 548-565 (2006).

205. Chen,X.D., Qian,H.Y., Neff,L., Satomura,K., & Horowitz,M.C. Thy-1 antigen expression by cells in the osteoblast lineage. *J. Bone Miner. Res.* **14**, 362-375 (1999).

206. Van,V.P., Falla,N., Snoeck,H., & Mathieu,E. Characterization and purification of osteogenic cells from murine bone marrow by two-color cell sorting using anti-Sca-1 monoclonal antibody and wheat germ agglutinin. *Blood* **84**, 753-763 (1994).

207. Keila,S., Pitaru,S., Grosskopf,A., & Weinreb,M. Bone marrow from mechanically unloaded rat bones expresses reduced osteogenic capacity in vitro. *J. Bone Miner. Res.* **9**, 321-327 (1994).

208. Wozniak,M., Fausto,A., Carron,C.P., Meyer,D.M., & Hruska,K.A. Mechanically strained cells of the osteoblast lineage organize their extracellular matrix through unique sites of alphavbeta3-integrin expression. *J. Bone Miner. Res.* **15**, 1731-1745 (2000).

209. Baldwin,K.M. *et al.* Musculoskeletal adaptations to weightlessness and development of effective countermeasures. *Med Sci Sports Exerc* **28**, 1247-1253 (1996).

210. Maddalozzo,G.F., Iwaniec,U.T., Turner,R.T., Rosen,C.J., & Widrick,J.J. Whole-body vibration slows the acquisition of fat in mature female rats. *Int. J. Obes. (Lond)* **32**, 1348-1354 (2008).

211. Rubin,C.T. *et al.* Adipogenesis is inhibited by brief, daily exposure to high-frequency, extremely low-magnitude mechanical signals. *Proc. Natl. Acad. Sci. U. S. A* **104**, 17879-17884 (2007).

212. Yavuzer,G., Ataman,S., Suldur,N., & Atay,M. Bone mineral density in patients with stroke. *Int. J. Rehabil. Res.* **25**, 235-239 (2002).

213. Yang,L.C., Majeska,R.J., Laudier,D.M., Mann,R., & Schaffler,M.B. High-dose risedronate treatment partially preserves cancellous bone mass and microarchitecture during long-term disuse. *Bone* **37**, 287-295 (2005).

214. Goulding,A., Grant,A.M., & Williams,S.M. Bone and body composition of children and adolescents with repeated forearm fractures. *J. Bone Miner. Res.* **20**, 2090-2096 (2005).

215. *Space medicine, space life science, aerospace biomedicine*(World spaceflight news, United States, 2003).

216. Wronski,T.J. & Morey-Holton,E.R. Skeletal response to simulated weightlessness: a comparison of suspension techniques. *Aviat. Space Environ. Med.* **58**, 63-68 (1987).

217. Klasing,K.C. & Johnstone,B.J. Monokines in growth and development. *Poult. Sci.* **70**, 1781-1789 (1991).

218. Kanda,K. *et al.* Urinary excretion of stress hormones of rats in tail-suspension. *Environ. Med.* **37**, 39-41 (1993).

219. Morey-Holton,E.R. & Globus,R.K. Hindlimb unloading of growing rats: a model for predicting skeletal changes during space flight. *Bone* **22**, 83S-88S (1998).

220. Sutter,N.B. *et al.* A single IGF1 allele is a major determinant of small size in dogs. *Science* **316**, 112-115 (2007).

221. Rubin,J., Fan,X., Biskobing,D.M., Taylor,W.R., & Rubin,C.T. Osteoclastogenesis is repressed by mechanical strain in an in vitro model. *J. Orthop. Res.* **17**, 639-645 (1999).

222. Klein-Nulend,J., Veldhuijzen,J.P., van Strien,M.E., de Jong,M., & Burger,E.H. Inhibition of osteoclastic bone resorption by mechanical stimulation in vitro. *Arthritis Rheum.* **33**, 66-72 (1990).

223. Zaidi,M. Skeletal remodeling in health and disease. *Nat. Med.* **13**, 791-801 (2007).

224. You,L. *et al.* Osteocytes as mechanosensors in the inhibition of bone resorption due to mechanical loading. *Bone* **42**, 172-179 (2008).

225. Suda,T., Ueno,Y., Fujii,K., & Shinki,T. Vitamin D and bone. *J. Cell Biochem.* **88**, 259-266 (2003).

226. Liu,Y.Z., Liu,Y.J., Recker,R.R., & Deng,H.W. Molecular studies of identification of genes for osteoporosis: the 2002 update. *J. Endocrinol.* **177**, 147-196 (2003).

227. Iqbal,J. & Zaidi,M. Molecular regulation of mechanotransduction. *Biochem. Biophys. Res. Commun.* **328**, 751-755 (2005).

228. Lee,H.J. *et al.* Polymorphisms and haplotypes of integrinalpha1 (ITGA1) are associated with bone mineral density and fracture risk in postmenopausal Koreans. *Bone* **41**, 979-986 (2007).

229. Tofteng,C.L. *et al.* Integrin beta3 Leu33Pro polymorphism and risk of hip fracture: 25 years follow-up of 9233 adults from the general population. *Pharmacogenet. Genomics* **17**, 85-91 (2007).

230. Ward,K. *et al.* Low magnitude mechanical loading is osteogenic in children with disabling conditions. *J Bone Miner. Res.* **19**, 360-369 (2004).

231. Xie,L., Rubin,C., & Judex,S. Enhancement of the adolescent murine musculoskeletal system using low-level mechanical vibrations. *J. Appl. Physiol* **104**, 1056-1062 (2008).

232. Muir,J.W. *et al.* Low magnitude mechanical signals reduce risk-factors for fracture during 90-day bed rest. *J Bone Miner Res* **22**, S338 (2007).

233. Bonewald,L.F. & Johnson,M.L. Osteocytes, mechanosensing and Wnt signaling. *Bone* **42**, 606-615 (2008).

234. Weinbaum,S., Guo,P., & You,L. A new view of mechanotransduction and strain amplification in cells with microvilli and cell processes. *Biorheology* **38**, 119-142 (2001).

235. Tatsumi,S. *et al.* Targeted ablation of osteocytes induces osteoporosis with defective mechanotransduction. *Cell Metab* **5**, 464-475 (2007).

236. Cao,J.J., Gregoire,B.R., & Gao,H. High-fat diet decreases cancellous bone mass but has no effect on cortical bone mass in the tibia in mice. *Bone*(2009).